The recombination landscape of fission yeast: Natural variation and the effects of direct selection and inversions on the evolution of recombination

Dissertation der Fakultät für Biologie
der Ludwig-Maximilians-Universität München

Cristina Berenguer Millanes
Aus Olot, Spanien

München, 2024

The recombination landscape of fission yeast: natural variation and the effects of direct selection and inversions on the evolution of recombination

Dissertation zur Erlangung des narurwissenschaftlichen Doktorgrades
„Doctor rerum naturalium“ (Dr. rer. nat)
an der Fakultät für Biologie
der Ludwig-Maximilians-Universität München

GRADUATE SCHOOL
LIFE SCIENCE MUNICH

Cristina Berenguer Millanes

Aus Olot, Spanien

München, 2024

Diese Dissertation wurde angefertigt
unter der Leitung von **PD Dr. Bart Nieuwenhuis**
im Bereich von **Evolutionary Biology**
an der Ludwig-Maximilians-Universität München

Erstgutachter/in:	PD Dr. Bart Nieuwenhuis
Zweitgutachter/in:	Prof. Dr. Jochen Wolf
Tag der Abgabe:	8. November, 2024
Tag der mündlichen Prüfung:	9. Mai, 2025

EIDESSTATTLICHE ERKLÄRUNG

Ich versichere hier mit an Eides statt, dass meine Dissertation selbständig und ohne unerlaubte Hilfsmittel angefertigt worden ist.
Die vorliegende Dissertation wurde weder ganz, noch teilweise bei einer anderen Prüfungs kommission vorgelegt.
Ich habe noch zu keinem früheren Zeitpunkt versucht, eine Dissertation einzureichen oder an einer Doktorprüfung teilzunehmen.

München, den **16.05.2025**

Cristina Berenguer Millanes

1 ABSTRACT

Sex, and therefore meiotic recombination, are almost ubiquitous in the eukaryotic world. Recombination involves the shuffling of genes during meiosis, generating new combination of alleles in the offspring. This process is widely believed to be beneficial for adaptation, as it creates new variation for evolution to act on, and it separates deleterious mutations from beneficial alleles. Recombination comes, however, with costs, such as breaking up combinations that are already beneficial in a certain environment, or possible mechanistic mistakes.

Recombination variation in nature – from higher taxonomic clades, to changes in recombination rates within the same chromosome –is influenced by a complex interplay of genetic and environmental factors. Concretely, the discovered genetic factors that control recombination rate variation show that recombination rates not only affect evolution, but are affected by evolution too.

Despite decades of research, the mechanisms which regulate recombination rates are still unknown. Using the fission yeast *Schizosaccharomyces pombe* as a model organism, I elucidate some of the previously unanswered questions about the current variation of recombination rates, and what mechanisms affect them. In the first part of the results, it is shown that recombination rates significantly vary among strains, and within the strains when comparing the three chromosomes. The data indicates that recombination rates in fission yeast could be locally regulated, within distances of few kilobases.

To elucidate how this current variation came to be, in my second part of the results I performed an evolutionary experiment where the effect of direct selection in recombination rate changes is proved. Here, recombination rates in two intervals were changed, both increased and decreased, after 36 generations.

Finally, the effect of the presence of inversions in heterozygosis, as well as the effect of their size, is tested. These show an effect on recombination both inside and on the flanks of the inverted segment, as well as demonstrating that inversions affect cell viability. These effects depend on size.

This work provides a framework for understanding the role that direct selection and genomic rearrangements have on the evolution of recombination rates, and they shed light on how the current variation we observe has been achieved.

Table of contents

2 INTRODUCTION

Sex is almost ubiquitous across eukaryotic life, and it is thought to have arised already in the Last Eukaryotic Common Ancestor (LECA) (Bernstein and Bernstein 2010; Goodenough and Heitman 2014). From single-celled organisms to complex multicellular life forms, sex plays a crucial role in the generation of genetic diversity and evolution. However, the reproduction landscape is far from uniform, showing a remarkable spectrum of strategies ranging from exclusively asexual organisms to exclusively sexual organisms. While the most commonly known form of sexuality involves males and females (Yadav et al. 2023), eukaryotic microorganisms, fungi and plants show a wide array of sexualities, such as multiple mating types; and some prefer to grow clonally and undergo infrequent facultative sexual reproduction (Yadav et al. 2023).

This diversity in reproductive strategies raises intriguing questions about the evolutionary forces at play, and it is widely accepted that sexual reproduction confers both costs and benefits (Butlin 2002). However, the benefits seem to outweigh the costs. Sexual reproduction, has the benefits of filtering out deleterious mutations and generating novel genotypes through meiotic recombination. The shuffling of genes can, on the contrary, break apart well-adapted gene combinations and genomic configurations, and it allows only half of the parental genome to pass on to an individual offspring (Butlin 2002; Yadav et al. 2023).

While sexual reproduction has been widely studied, not all processes are well understood, concretely the ones concerning the evolution, maintenance and variation of recombination. This dissertation characterizes the variation in recombination rates in a wide array of natural fission yeast strains. In addition, it studies in detail de effects of direct selection on recombination rates, through an evolutionary experiment where I selected for increased and decreased recombination rates in a locus. It also studies how the presence of chromosomal rearrangements affect recombination rates in fission yeast. Finally, the new information regarding variation and evolution of recombination rates are summarized.

2.1 MEIOTIC RECOMBINATION

Meiotic recombination is ubiquitous in eukaryotic organisms (Stapley et al. 2017b), and it plays a fundamental role in sexual reproduction. Sexual reproduction involves the shuffling of genes during meiosis, which generates new combinations of alleles in the offspring, known as recombination. This shuffling of genes can be beneficial for adaptation, uniting beneficial alleles that work together. Recombination is, moreover, crucial for proper chromosome segregation and the generation of genetic

variation in the offspring (Davis and Smith 2001). It can prevent the accumulation of deleterious mutations by separating them from beneficial alleles (Fisher, R. 1930; Muller 1932; Hill and Robertson 1966; Peck 1994; Johnston et al. 2016), and lead to an increase in genetic variance, allowing populations to respond to selection at a faster rate (Weismann 1891; Hill and Robertson 1966; Felsenstein 1974). However, while sexual reproduction most likely evolved to allow recombination, which generates novel variation for selection to act on, paradoxically it can break apart favourable combinations of alleles that have already survived in that certain environment (Otto and Barton 2001; Stapley et al. 2017b). Recombination comes also with mechanistic costs. For example, mistakes during chromosome segregation can result in improper distribution of chromosomes, as seen in several early experiments on fitness components in *Drosophila* that suggest that genetic recombination could cause an immediate reduction in fitness. This fitness reduction can be due to both the mechanistic effects, or to breaking up beneficial mutations and generating unfavourable combinations (Spassky et al. 1958; Spiess 1958, 1959), a phenomena later named *recombination load* by Charlesworth and Charlesworth, 1975. High recombination also has been shown to increase deleterious mutations and chromosomal rearrangements, due to the disruption of chromosomal integrity, leading to fewer viable gametes (Inoue and Lupski 2002). This variety in the effects that recombination has in different populations leads to the wide variation in recombination rates in different organisms (Johnston et al. 2016), but it does not explain the predominance of sexual species among eukaryotes, or the maintenance of genetic recombination (Charlesworth 1989; Otto 2009; Hartfield 2016).

Among the many hypotheses written and tested along the years of research on the evolution of recombination rates and the maintenance of recombination, the main conclusions so far have been that recombination is maintained for three reasons. First, (1) The long-term fitness of asexual populations is lower than that of the related sexual populations. In some sexual populations, there is the emergence of an asexual parthenogenic female line; in almost all cases, these populations are evolutionarily young, which suggests these go extinct with a higher probability than their obligate sexual counterparts (Stebbins 1957; Smith and Maynard-Smith 1978). However, while this might explain why sexual reproduction and recombination are maintained, it cannot explain why sex evolved in the first place, as selection acts on short term fitness benefits, which generally favour asexual reproduction (Otto 2009). Second, (2) There are individual level advantages to sex. The asexual individuals might end up with a lower net fitness than the sexual individuals with which it competes, and cannot even establish itself as a population (Charlesworth 1989). Lastly, (3) meiosis is needed for proper development. Mammals, for example, require crossovers for the correct development of the embryo (Dumont 2017). In a lot of fungal species, sexuality – and therefore meiosis and recombination - is activated in stressful environments, such as lack of nitrogen presence in *Schizosaccharomyces pombe* (Asakawa et al. 2007; Hoffman et al. 2015; Vyas et al. 2021), and spores act as survival structures. Moreover, deleterious variants are introduced in a population each generation by

mutations at a large number of different loci, which generates a perpetual pressure against asexual individuals, which are not able to purge these novel mutations (Muller 1964; Felsenstein 1974; Charlesworth 1989). In evolutionary terms, recombination generates a wider variety of genotypes, which will give an advantage when the population is exposed to a changing environment, as it gives a greater ability to sexual populations to respond to selection.

While a certain consensus has been reached about the reasons for the maintenance of meiosis and recombination, their origins are still unknown and strongly debated. Traditionally, meiosis was believed to have evolved directly from mitosis, but more recent research has opened the door to alternative perspectives (e. g. Lane and Martin, 2012; Speijer, Lukeš and Eliáš, 2015; Garg and Martin, 2016). Some scientists propose that meiosis arose as a response to oxidative stress in early eukaryotes (Lane and Martin 2012) while others suggest that it evolved as a repair mechanism in response to reactive oxygen species (ROS) produced by the proto-mitochondrion during the early stages of eukaryotic evolution (Speijer et al. 2015). A more radical theory posits that meiosis originated in a syncytial eukaryote common ancestor, which was a multinucleated cell (Garg and Martin 2016). Despite these differing views, it is widely accepted that the Last Eukaryotic Common Ancestor (LECA) was sexual, and that sex provided significant evolutionary advantages during the rise of eukaryotes. Even though much has been learned through the years about the importance of recombination rates, still much more is left to discover.

2.2 RECOMBINATION RATES VARY

Due to its ubiquity and its importance for reproduction, recombination is an evolutionarily conserved process (Peñalba and Wolf 2020). Despite this conservation, the recombination rate varies across multiple biological levels (Johnston et al. 2016; Ritz et al. 2017; Peñalba and Wolf 2020). Crossovers can differ in the total number per genome, or in the distribution of recombination along the genome. Variation in recombination rates can be found in all classifications, starting from basal eukaryotic clades, such as animals, fungi and plants (Lian *et al.*, 2023, see figure 3). Recombination rates also differ between species, with some species having much higher rates than others (Smukowski and Noor 2011). Within species, differences can be found among subspecies, and even among different populations of the same species (Peñalba and Wolf 2020). Another layer of variation that has been described in many species is between the sexes, a phenomenon known as heterochiasmy. Variation ranges from equal rates of recombination between the two sexes, to no recombination at all in one of the sexes, the latter known as achiasmy (Lenormand and Dutheil 2005; Ritz et al. 2017; Peñalba and Wolf 2020). The most common pattern is that females exhibit higher recombination rates than males. Surprisingly, in heterochiasmate species, there is no

relation between which sex has higher recombination rate, and which is the heterogametic one (Ritz et al. 2017).

Recombination rates also vary among chromosomes, caused by the effect of size where smaller chromosomes often have higher recombination rates per unit length compared to larger chromosomes (Liu et al. 2019; Lian et al. 2023). The evolutionary history of each chromosome, such as those resulting from ancient chromosome fusions or fissions, may lead to differences in recombination rate patterns (Farré et al. 2012). Along each chromosome recombination is not uniform, generally with higher recombination towards the telomeres, and lower to non-recombination around the centromeres. Furthermore, there are the so-called recombination hotspots: highly localized, short regions (1-2kb) where most recombination events occur (Lichten and Goldman 1995; Boulton et al. 1997; Pryce and McFarlane 2009). Recombination hotspots are interspaced with coldspots: regions where recombination is much lower than the genomic average. Structural variants can also profoundly affect recombination rates. Particularly, inversions have been extensively studied for their role in limiting recombination and maintaining specific combinations of alleles (Hoffmann and Rieseberg 2008; Stevison et al. 2011; Berdan et al. 2023; Hu et al. 2024). These topics will be further explained in the following sections.

Even though we know that recombination rates vary, it is neither clear how recombination rates evolve, nor what the general mechanisms that allow for this variation are. Most research has studied how recombination coevolves under selection at other traits. Due to the multiple studied characteristics, the mechanisms behind these changes might be obscured. In this study, I use the fission yeast *S. pombe* to analyse how recombination might evolve under direct selection. To study this, I performed experimental evolution during 36 sexual generations, selecting either for an increase or a decrease of recombination in a chromosomal region. Furthermore, I studied the effect of inversions and their size on recombination rate, as they are a specific known trait that has an effect on the recombination landscape. Finally, I analysed the occurrence of natural variation in recombination rates, utilising a large number of available natural isolates with varying genetic variation. Together, these three studies give a new general perspective on recombination rate variation and its evolution to the current recombination landscapes.

2.2.1 Variation in the fission yeast genome

The genomes of the individuals in natural populations are mosaics reflecting different evolutionary histories, and fission yeast is no exception. Tusso et al. (2019) studied 57 fission yeast strains found globally (Jeffares et al. 2015a) by dividing each of the genotypes in about 2000 genomic overlapping windows of ~13kb length average, and inferring their ancestry. A PCA analysing the genetic variance of each window suggested that the strains grouped into two discrete groups, suggesting that the genomic diversity in this

collection was derived from two distinct ancestral populations, from now on called Sp and Sk. The reference strain (EBC70) derives almost 100% from the ancestral Sp. The variation between the groups is associated with reproductive incompatibility. For example, EBC134 was initially considered to be a different species, called *Schizosaccharomyces kambucha,* here Sk (Singh and Klar 2002), due to the strong inviability of spores in crosses. However, more recent population genetic studies concluded that the different strains belong to the same species and that incompatibility is mostly, though not completely, driven by selfish genetic killer elements (Jeffares et al. 2015; Hu et al. 2017; Tusso et al. 2019). The most likely evolutionary scenario that described the current fission yeast population structure is that two populations diverged in isolation for ~2500 years, followed by a more recent pulse of hybridization and gene flow. This scenario explains both the ancestral divergence and the observed introgression landscape due to hybridization in the last 20-60 sexual generations (Tusso et al. 2019). While the biology of fission yeast makes estimation of the time in years nearly impossible, the hybridization events are placed around the 14th century, when the intercontinental trade between Europe and Asia and Africa were established, and around the 16th century with the Americas. The fact that this species is human related and that all pure strains were found in Europe, Africa and Asia, and all strains found in the Americas were hybrids, supports this hypothesis.

Hybridization between these strains has been shown to bring an array of phenotypic variation in the available hybrids that exceeds the variation of the pure strains (Jeffares et al. 2015). If recombination rates are genetically influenced, variation in recombination rates might be included in this phenotypic variation. Selection can work on this variation, and therefore, recombination rates might be able evolve. I will analyse recombination rate variation among these strains, which is expected to give different results depending on each strain's ancestry.

2.2.2 The evolvability of recombination rates

Recombination rates affect evolution by generating new allele combinations, therefore influencing genetic diversity, the efficacy of selection and genome structure, where selection can act. These recombination rates vary, although the causes for this variation of recombination rates are still largely unknown. Recombination rate in an individual can be affected by environmental cues such as temperature (Plough 1917), stress (Parsons 1988; Zhong and Priest 2011), age of the individual (Hussin et al. 2011), or parasite load (Camacho et al. 2002; Kerstes et al. 2012). However, recombination rates have also been shown to be heritable, and therefore can be targets for natural selection. Recombination rate is subject to long-term selection (Stapley et al. 2017b), and therefore it can be treated both like a process that affects evolution, but that is itself a product of evolution (Stapley et al. 2017b). Population level variation that has become available over the last few decades, have shown the heritability of recombination rates in a range of organisms (Kong et al. 2004; Johnston et al. 2016; Kawakami et al. 2019; Weng et al. 2019). These studies have attributed some

heritable variation to specific genetic variants of certain genes, including *ring finger protein 202 (RNF202), complexin 1 (CPLX1), meiotic recombination protein REC8 (REC8),* and *PR domain zinc finger protein 9 (PRDM9)* (Baudat et al. 2010; Parvanov et al. 2010; Johnston et al. 2016). Most of these loci appear to influence crossover frequency, and these studies suggest that recombination rate has the potential to respond rapidly to selection over short evolutionary periods (Johnston et al. 2016). However, recombination in itself is not likely to have an effect on fitness. While higher recombination rates might be associated with reduction in fitness due to chromosome segregation errors, the effect recombination has on fitness is mostly indirect. Most theory on the evolution of recombination rates assume that a heritable variant that affects recombination rate – a so called modifier – becomes associated with allele combinations that are under selection.

Box 1. Hill-Robertson interference, the Fisher-Müller model, and the importance of recombination in finite populations

The **Hill-Robertson effect** describes how genetic linkage between alleles under selection can reduce the efficiency of natural selection in finite populations. When beneficial mutations at different loci arise in different individuals, the lack of recombination can hinder the process of natural selection because such beneficial mutations will never be able to be combined in the same individual if they are on the same chromosome. This effect leads to an overall reduction in the efficiency of selection, as linked alleles can interfere with each other's fixation in the population.

The **Fisher-Müller model** highlights the benefits of sexual reproduction and recombination in accelerating the process of evolution. According to this model, recombination allows beneficial mutations to combine in the same genetic background more quickly than they would in asexual populations, where beneficial mutations arising in separate lineages would be in competition with each other. Recombination leads to faster adaptation because it can bring together the most advantageous alleles.

These two effects were proven to be mathematically identical by Felsenstein (1974), although the verbal arguments for each of them are substantially different (Fisher, R. 1930; Muller 1932; Hill and Robertson 1966; Mooney 1995).

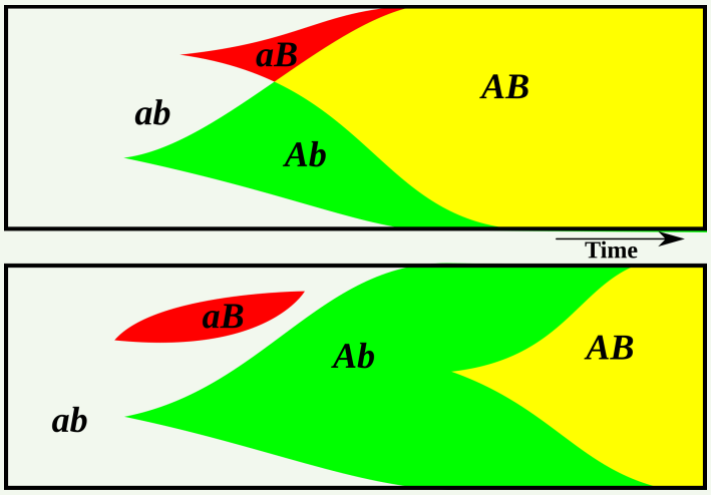

There is evidence of novel environments favouring changes in recombination rates, corresponding for example to periods of artificial selection such as domestication (Otto and Barton 2001). Domestication's strong directional selection towards certain characteristics, will favour alleles in the before mentioned genes that increase recombination rate to overcome Hill-Robertson interference (**Box 1**) (Hill and Robertson 1966; Otto and Barton 2001; Comeron et al. 2008). Next to competition between favourable alleles, additionally, deleterious alleles will hitchhike with the selected variants, lowering the fitness of the individual. Some experimental systems show increased recombination rates after strong selection on unrelated characters (Otto and Lenormand 2002), and recombination rates tend to be higher in domesticated plants and animals

than in their known ancestors (Burt and Bell 1987; Ross-Ibarra 2004; Schwarzkopf et al. 2020). It is unclear how general this hypothesis can be applied, a study in 2015 showed that in domesticated sheep, goats and dogs no different recombination rates were observed relative to their wild relatives (Muñoz-Fuentes et al. 2015). While the genes described above alter recombination rates at a global, recombination rates are not homogeneously distributed. Recombination along the genome does not happen uniformly, but instead are predominantly targeted to specific chromosomal regions called recombination hotspots. In contrast, there are recombination coldspots, where recombination happens very rarely. The differences in these areas are influenced by factors such as chromatin accessibility and the binding of specific proteins like PRDM9 in mammals (Ségurel et al. 2011). Local genomic context, such as the presence of repetitive elements or the proximity of telomeres or centromeres, can also affect recombination events. Next to environment factors, recombination rates are thus defined by a combination of global regulators – such as allelic variants of PRDM9 and REC8 – local sequence variation – such as sequence motifs – and chromatin structure. Each of these elements can be a target for selection allowing recombination rates to evolve.

2.2.3 Hotspots and the heritability of recombination rates

As mentioned above, meiotic recombination occurs more frequently at hotspots, which are regions of the eukaryotic genome, usually around 1 to 2kb long (Lichten and Goldman 1995; Pryce and McFarlane 2009). The importance of recombination hotspots lies in the possibility of shuffling genetic variation at higher rates in certain parts of the genome, increasing the variability in those regions. By increasing genetic variation in specific genomic regions, hotspots can enhance adaptation potential and evolutionary flexibility (Charlesworth and Jensen 2021). This increased recombination breaks down LD, allowing alleles to be inherited more independently (Wahls 1998).

Recombination hotspots have been linked to regions that are frequently near, but not within, coding regions (Schwarzkopf et al. 2020), leading the crossover events away from essential genes that need to be conserved, while shuffling the alleles. They also tend to be located in regions of the genome that are relatively open and accessible to the recombination machinery, as processes that are only mechanistically related to meiotic recombination can also play an important role in determining the shape of the meiotic landscape (Lichten and Goldman 1995; Tock and Henderson 2018). In baker's yeast and *Arabidopsis thaliana* for example, recombination is targeted around promoters, which has a more open chromatin structure (Choi et al. 2013) but not in fission yeast (Zanders et al. 2014). Sequence variation in the genome also plays a crucial role, with certain DNA motifs being more prone to recombination (Ségurel et al. 2011; Paigen and Petkov 2018). In many mammals, including humans and mice, the zinc-finger protein PRDM9 acts as a key mediator of DSB formation, determining hotspot locations by binding to specific DNA sequences, called motifs (Ségurel et al. 2011; Paigen and Petkov 2018; Schwarzkopf and Cornejo 2021).

Recombination coldspots, on the other hand, tend to be located in regions that are more compact and less accessible to the recombination machinery, as well as regions that are evolutionarily conserved. Double-strand breaks can lead to an increased mutation rate, which are likely costly in coding regions that tend to be evolutionarily conserved, especially in essential genes. Therefore, these areas will be protected from recombination (Lam et al. 2013). Differences between the sequences of homologous chromosomes can also affect recombination, with some studies suggesting that sequence mismatches can inhibit recombination (Wahls 1998; Opperman et al. 2004). Recombination coldspots and hotspots might evolve for several reasons. Hotspots could be positioned where recombination is least harmful to essential genetic functions or where it is particularly beneficial, such as in major histocompatibility complex regions that benefit from high variability for immune function (Gonen et al. 2017). Alternatively, hotspots may serve as a guide for meiotic machinery, ensuring proper chromosomal segregation during cell division (Johnston 2024).

Recombination distribution has a significant impact on evolution, as it influences the distribution of genetic diversity and the frequency at which novel genetic variants emerge, and where they emerge in the genome (Harwood et al. 2022). Many selective forces have been suggested to affect the amount of recombination happening in individuals and populations, but that also change the shape of the recombination landscape in the genome. Some of these selective forces include mating system, population size and genetic interference (Roze 2014; Stetsenko and Roze 2022). However, while many indirect pressures to recombination have been studied, the effect of direct selection for an increase or a decrease of recombination rates is still largely unknown. Existing recombination is often assessed in populations, but this is done using variation that might have arisen due to a whole variety of different selective forces (Stetsenko and Roze 2022). The lack of knowledge of the evolutionary biology confounds the observations that can be obtained from such studies.

Recombination has been shown to be a heritable genetic trait. Studies calculating the genetic component of recombination rates have been performed in several organisms, ranging from model species to non-model species (Girard et al. 2023). Heritability estimates of genome-wide recombination rates range from 0.16-0.17 in chickens (Weng et al. 2019), to 0.23 in Soay sheep (Johnston et al. 2016), 0.3 in humans (Kong et al. 2004), and 0.44 in honeybees (Kawakami et al. 2019). Not only general recombination rates are heritable, but so is the distribution of recombination hotspots. PRDM9 determines the location of recombination hotspots in humans and mice, making the presence of motifs necessary for the presence of hotspots in certain areas (Baudat et al. 2010; Parvanov et al. 2010), together with variants in other genes like REC8 and RNF212 (Sandor et al. 2012). Coop *et al.* (2008) also found heritable variation in recombination rates in humans, identifying specific genetic variants associated with recombination phenotypes. The genetic

basis of recombination rates and distribution, hints that recombination rates can be artificially modified with direct selection.

Despite extensive research on recombination rate variation, there is still a significant gap in the global understanding of direct selection on recombination rates. While numerous studies have demonstrated that recombination rates vary greatly across genomes, between individuals, sexes, and populations, the role of direct selection in shaping these patterns is still poorly understood. Much of the existing literature focuses on indirect selection and its effects on recombination rate evolution. Therefore, there is a need of comprehensive understanding of how direct selection act on recombination, a subject that will be partially elucidated in this thesis.

2.2.4 Effects of inversions on recombination

Coldspots are not the only low-recombination parts of the genome. Genomic features or mechanical constraints, for example crossover interference or the presence of structural variants, can also affect recombination rates. Chromosomal inversions have been associated with reduced recombination rates within and around the inverted region (Gong et al. 2005; Li et al. 2023).

Chromosomal inversions occur when a piece of the chromosome is reinserted in the reverse orientation (Cáceres et al., 1999). Chromosomal inversions, when heterozygous, are considered to be the major mechanism of recombination suppression, and maintain allele combinations within the inverted region (Gong et al. 2005; Li et al. 2023). Suppression of recombination plays important roles in divergent adaptation between populations and during sex chromosome evolution (examples in Figure 1a). In divergent adaptation, especially if there is migration between populations, recombination would break allele combinations that have been selected together (Johnson and Lachance 2012; Rifkin et al. 2020). The same happens in sex chromosome evolution, where recombination suppression keeps together beneficial alleles for the heterogametic sex (Wright et al. 2016; Jay et al. 2022). Sex chromosomes typically evolve from a pair of autosomes when one chromosome acquires a sex-determining gene, initiating the differentiation between the two (Livernois et al. 2012; Abbott et al. 2017). Initially, both chromosomes can still recombine, but over time, recombination around the sex-determining region becomes suppressed to preserve sexually antagonistic genes (Murata et al. 2015; Lisachov et al. 2023). This suppression of recombination is a key step in sex chromosome evolution, as it allows the sex chromosome to accumulate mutations and diverge from its partner, leading to further differentiation between the sex chromosomes (Livernois et al. 2012; Sigeman et al. 2024).

The benefits of recombination suppression – either for local adaptation or sexual antagonistic selection – can explain the wide presence of inversions in nature (Kirkpatrick 2010). The generally accepted

mechanism of recombination suppression is that an inversion in heterozygosis disrupts the normal pairing of homologous chromosomes and synapsis formation during meiosis, preventing or strongly reducing crossover formation (Gong et al. 2005; Li et al. 2023). However, crossovers do occur within inversions (Sturtevant and Beadle 1936; Prakash and Lewontin 1971; Ishii and Charlesworth 1977; Hawley and Ganetzky 2016). During such recombination events, an inversion loop is formed accommodating homologous pairing (Figure 1b), which generates chromosomes with duplicated and missing regions, which can even encompass the centromere. Such offspring are often inviable (Stone 1955; Morin et al. 2017), and because most offspring effectively have no recombination in the inverted region, it yields an apparent impression of suppression of recombination (Hoffmann and Rieseberg 2008; Morin et al. 2017; Zanders and Unckless 2019). An even number of crossovers within a heterozygous inversion would lead to normal chromosomes, and therefore movement of alleles within the inverted region would be possible, though in much lower proportion, especially in species with low overall recombination rates.

There are two main types of inversions. Paracentric inversions occur when both breakpoints are on the same chromosome arm, excluding the centromere. Pericentric inversions include the centromere, with breakpoints on different chromosome arms. These two inversions present different outcomes when an odd number of recombination events occurs within the inverted region. For paracentric inversions, this event leads to acentric and dicentric chromatids, which cannot segregate properly (represented in Figure 1b) (Kapun and Flatt 2019). In the case of pericentric inversions, the recombinant chromosomes contain deletions and duplications, which allow for proper segregation but result mostly in viable offspring (Kapun and Flatt 2019).

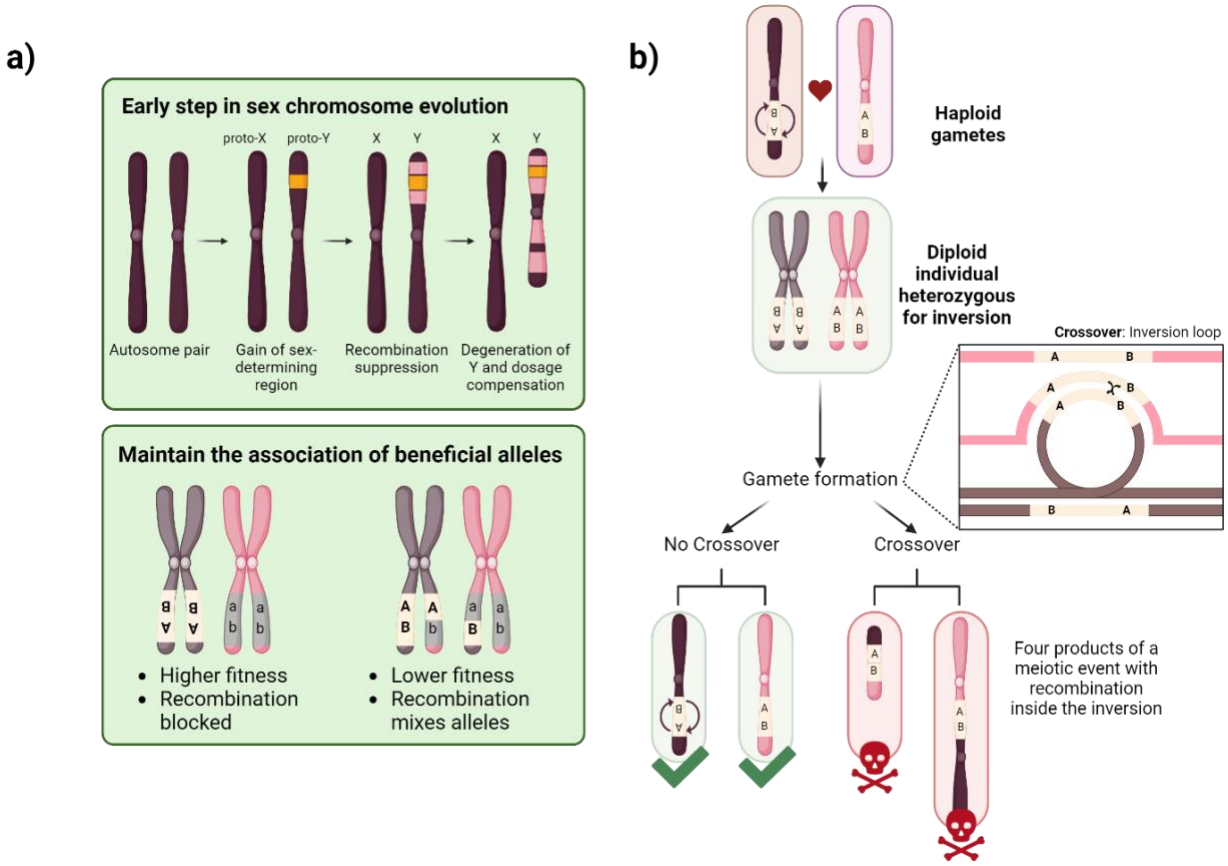

Figure 1. a) Two examples of beneficial inversions. b) Simplified example of a recombination event inside an inversion during meiosis – allowed by the inversion loop. With one crossing over in the inverted region, half of the meiotic products are aberrant.

The size of the inverted region is not stable, but increases stepwise over time (Ponnikas et al. 2018; Jay et al. 2024). Regions that stopped recombining, referred to as evolutionary strata, have been described in various contexts including sex chromosomes, mating-type chromosomes, meiotic-driver loci and supergenes (Bachtrog et al. 2011; Branco et al. 2018; Jay et al. 2018; Stolle et al. 2019; Zanders and Unckless 2019). Many models have been proposed to explain the extension of recombination suppression, depending on neutral processes, dosage compensation, or the sheltering of deleterious mutations (Jeffries et al. 2021a; Jay et al. 2022; Lenormand and Roze 2022; Olito and Abbott 2023; Olito et al. 2024), as well as sexual antagonistic alleles (Charlesworth et al. 2014; Morin et al. 2017; Charlesworth 2021).

Experimental studies on suppression of recombination both within inversions and in the regions flanking them have mostly been performed in *Drosophila.* These studies showed that the effects of inversions can extend beyond the boundaries of the inverted region (e.g. Schultz and Redfield 1951; Kulathinal et al. 2009; Stevison et al. 2011; Crown et al. 2018). These have been shown to affect recombination over much longer distances and even affect crossovers on other chromosomes (Lucchesi and Suzuki 1968; Stevison et al.

2011; Crown et al. 2018). However, while inversions are the most extensively studied mechanism, these have only been observed either through modelling, or through natural existing inversions in populations, which can give a bias towards the presence of different genetic content within the inversion, comparing different haplotypes. These usually are either derived from different populations and thus possess distinct evolutionary histories (e.g. Manoukis et al. 2008; Lowry and Willis 2010; Michel et al. 2010; Korunes et al. 2021), or they coexist within a single population, suggesting that they are under balancing selection (e.g. Coyne et al. 1992; Küpper et al. 2015). Therefore, separating the physical effects of the inversion to those caused by variations in genetic content, is virtually impossible. The lack of concrete research makes it difficult to separate the effects of the presence of an inversion from the effects of the alleles trapped within the inversion itself. Researching the mechanistical properties of the presence of isogenic inversions is, therefore, still needed. With my thesis, I try to elucidate the effects of inversions in heterozygosis on the recombination rates and pattern in isogenic fission yeast cells.

2.3 SCHIZOSACCAROMYCES POMBE

Schizosaccharomyces pombe, commonly known as fission yeast, was first isolated in 1893 by the German biologist Paul Lindner, from East African millet beer (Forsburg 2005; Hoffman et al. 2015 p. 20; Vyas et al. 2021; Chen 2023). The name "pombe" is derived from the Swahili word for beer, reflecting its origin. Although *S. pombe* was initially studied for its fermentation properties, it wasn't until the mid-20th century that its significance as a model organism in research was recognized (Hoffman et al. 2015; Vyas et al. 2021).

The basis of *S. pombe* research was established in 1940 by the scientist Urs Leupold, who studied the mating system of fission yeast. The strains obtained in his reaserach, 968 h^{90}, 972 h^{-}, and 975 h^{+}, are the ancestor strains for almost all studies on *S. pombe*. These three strains derive from one single isolate, and therefore all strains used in laboratories around the world are nearly isogenic, which assures data consistency acquired from all labs working with this organism (Hoffman et al. 2015; Vyas et al. 2021). However, an increasingly large set of natural isolates of this species, as well as resources for its sister species, have become available over the last decade, which can be used to study natural variation in this species (Rhind et al. 2011; Hu et al. 2015; Jeffares et al. 2015a; Tusso et al. 2019). In 2002, fission yeast became the sixth eukaryotic model organism to have its genome sequenced and annotation published (Wood et al. 2002), which provided a robust platform for the ongoing evaluation of genome content. Now, fission yeast is a model organism widely used in molecular and cellular biology. Its unicellular nature makes it simple to study, as one can work with extremely large numbers of individuals at once (Hoffman et al. 2015).

S. pombe is part of the basal Taphrinomycotina clade, within the ascomycetes, the group of fungi thatform sexual spores that are contained within a specialized structure called an *ascus* (pl. *asci*). Its genome size is ~13.8Mb, with three chromosomes of 5.7 (chromosome I), 4.6 (chromosome II, which contains the mating type locus), and 3.5 (chromosome III). It has large modular centromeres, much more similar to multicellular eukaryotes than those of its distant cousin *S. cerevisiae.* It has a high percentage of genes and proteins that are homologous in mammals which are not present in *S. cerevisiae.* This is also the reason fission yeast has been used widely as a model for the study of eukaryotic processes, especially those related to eukaryotic chromatin remodelling and centromere function, due to the conservation of centromere features including size, structure and organisation (Hoffman et al. 2015).

S. pombe has been key in research for eukaryotic organisms. In cell cycle regulation, fission yeast has been instrumental in elucidating the chore mechanisms of cell cycle control, particularly the G2/M transition. The discovery of the cyclin-dependent kinase Cdc2 and its regulatory subunit cyclin B in fission yeast led to the identification of homologous proteins controlling the cell cycle in all eukaryotes (Smith 2009; Fantes and Hoffman 2016). Research performed with fission yeast has also uncovered key components of DNA damage response pathways, including the checkpoint kinase Cds1, homolog of mammalian Chk2 (Cromie and Smith 2008), and of stress response pathways, including the MAPK pathways that respond to environmental stresses (Rosas-Murrieta et al. 2015). Insights into chromosome organisation and segregation, such as the discovery of cohesins and their role in sister chromatid cohesion, were first found in *S. pombe* and *S. cerevisiae*, with homologous proteins later found in higher eukaryotes (Tsubouchi et al. 2021). Finally, fission yeast has been essential for the study of meiotic recombination mechanisms. Key proteins involved in homologous recombination, such as Rad51 and Dmc1, were first characterized in yeasts and later found to have homologs in other organisms (Vyas et al. 2021).

These discoveries highlight the value of *S. pombe* as a model organism for studying fundamental cellular processes that are conserved in higher eukaryotes, including humans. The simplicity of fission yeast, combined with its genetic tractability, has allowed researchers to uncover mechanisms that might be more laborious, difficult and time consuming to elucidate in other eukaryotic organisms. Today, fission yeast continues to be a powerful model for studying recombination and related processes. With advances in genomics and proteomics, researchers can now explore recombination at unprecedented detail.

2.3.1 Life cycle of *S. pombe*

The life cycle of fission yeast consists of asexual (vegetative) and sexual phases, that have been thoroughly described many times (Egel 1989; Nasim et al. 1989). Asexually reproducing *S. pombe* cells go through their cell cycle with distinct G1, S, G2 and M phases, to produce two nearly identical daughter cells

(Hoffman et al. 2015). Both the scientific name "*Schizosaccharomyces pombe*" and the common name "fission yeast" come from its symmetric mode of division during vegetative phase. The cells are rod-shaped, and they grow in length without altering their width. Once they reach about 15µm in length, they undergo a closed mitosis with the nucleus close to the centre of the cell. Shortly after nuclear division, a transverse septum divides the cell through the centre, and the cell is then cleaved to produce two daughters. These two new cells are almost equal in size, similar to cultured mammalian cells, but quite different to the asymmetric division of budding yeast (Hoffman et al. 2015).

When subjected to nutrient starvation, concretely nitrogen starvation, in the absence of a mating partner, haploid cells exit the cell cycle and enter a G0 stationary phase. If a mating partner is present, haploid cells shift from vegetative growth to the sexual cycle (Asakawa et al. 2007; Hoffman et al. 2015; Vyas et al. 2021). Two haploid cells from opposite mating types (called Plus and Minus) respond to nutrient starvation by mating (conjugation). Following conjugation, a zygote is formed, and these enter meiosis and sporulation immediately, producing four spores in a linear tetrad ascus (scheme in Figure 2a). These asci are noticeably bent, showing the shape at which the two haploid cells conjugated (Hoffman et al. 2015; Vyas et al. 2021).

Even though diploids are naturally short lived, diploid cells can be recovered in the laboratory by selection for complementing markers (detailed explanation in materials and methods) (Forsburg 2003). The asci generated from diploid cells that underwent meiosis immediately after zygote formation are called zygotic asci. The asci generated from cells that have been kept artificially in the diploid phase, named azygotic asci, have a short and straight morphology, as they come from a single cell (Hoffman et al. 2015; Vyas et al. 2021). In both types of asci, the wall of the ascus will degrade when in rich medium conditions, and the released spores will germinate and re-enter the vegetative cycle as haploid organisms (Figure 2a).

Fission yeast has two mating types: plus (h^+) and minus (h^-). Most wild-type *S. pombe* strains, including the lab strain, can switch between these mating types and therefore are considered homothallic (h^{90}) (Hoffman et al. 2015; Seike and Niki 2022). The possibility of mating-type switching allows individual cells after a few mitotic cell divisions to perform the sexual cycles by themselves and assures survival when environmental circumstances deteriorate. However, it reduces the possibilities of outcrossing, as most cells will preferably mate with their own clonal sisters (Arcangioli and Gangloff 2023; Nieuwenhuis et al. 2023). Heterothallic strains, however, need a partner of the opposite mating type to enter the sexual reproductive cycle (Seike and Niki 2022). In nature, fission yeast is predominantly homothallic (Nieuwenhuis et al. 2018), and reproduces by haploid selfing with rare amounts of outcrossing (Tusso et al. 2018).

The loci involved in mating-type determination and switching are *mat1, mat2-P* and *mat3-M.* These are located in chromosome II. *mat2-P* and *mat3-M*, located in a silent region, are silent donor sites coding

mating type specific genes, and *mat1* is the transcriptionally active locus (Thon et al. 1994; Klar 2007). During mating-type switching in homothallic strains, the sequence at *mat1* is replaced with the gene of the opposite mating type, situated in the silent cassette (Seike and Niki 2022) (Schematic in Figure 2b). Heterothallic strains, such as the standard laboratory strains 975h^{+} and 972h^{-}, are incapable of mating type switching. Heterothallic strains show diverse modifications of the mating type system, such as the loss of either *mat2-P* or *mat3-M* (making it capable of the expression of one of the factors), or a duplication of the *mat2,3* at *mat1*, avoiding switching of the active locus (Beach and Klar 1984). Artificially heterothallic strains can also be generated in laboratory conditions. Between the *mat2-P* and *mat3-M* there is the so-called k-region, which is a region essentially with no recombination (<0.002 cM), recombining at <0.1% of the genome average of 0.16cM/kb. The reduced recombination seems due to the presence of heterochromatin in this locus (Cromie and Smith 2008).

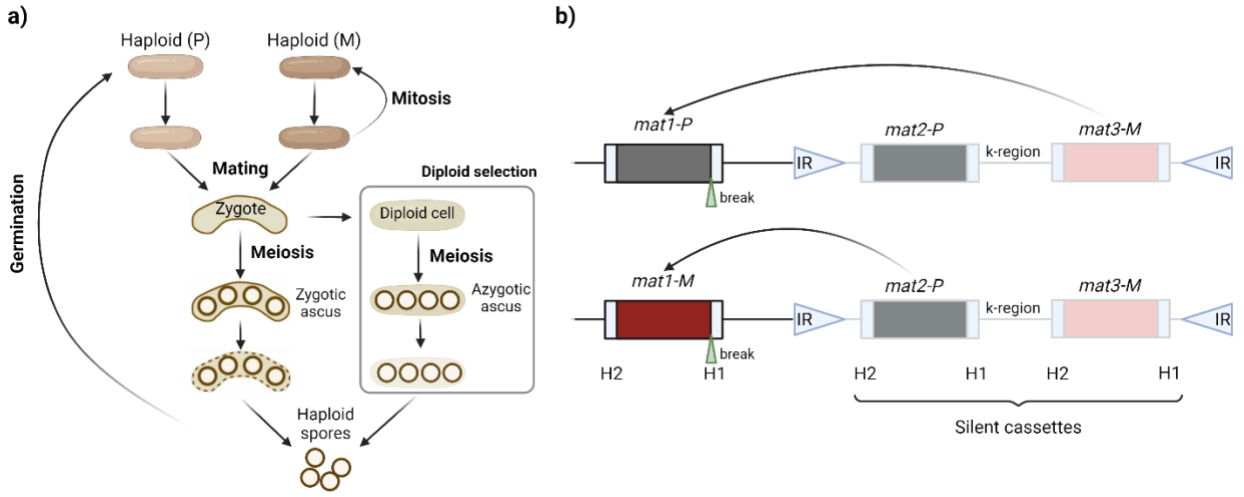

Figure 2. a) Life cycle of heterothallic *S. pombe.* It includes selection for diploid cells. b) Mating type system in the lab strain of *S.pombe.* The three mating type loci are indicated by boxes. The heterochromatic region between the two inverted repeats (IR triangles) contains the two silent cassettes, interspersed with the *k region.* A break is initiated in *H1* in *mat1* to initiate switching, and *mat1* will be substituted by the opposite mating type in the silent cassette. *H1* and *H2* are homology boxes involved in strand invasion during gene conversion. Scheme adapted from Nieuwenhuis, Shraim and Al Ghaithi, 2023.

2.3.2 Role in recombination research

The main focus of research in *S. pombe* since its discovery, has been fundamental research. Research started in the 1940s and early 1950s in two main areas: the mating type system, which led to investigation of the sexual cycle, and the growth and division processes that comprise key regulators of the cell division cycle, for which Sir Paul Nurse got a Nobel prize in 2001 (Hoffman et al. 2015; Fantes and Hoffman 2016). Moreover, due to the silencing of *mat2-P* and *mat3-M* regions, it sparked studies on chromatin structure and its effect on gene expression and recombination (Hoffman et al. 2015; Fantes and Hoffman 2016). As

already pointed out in the previous sections, fission yeast's similarities with other multicellular eukaryotic organisms, together with its unicellular nature, made it a perfect organism for the study of shared cellular mechanisms among eukaryotes. The possible direct analysis of the four haploid spores in the ascus, a feature that is not possible in many multicellular organisms, reveals all products of a single meiotic recombination event at each locus analysed. These features have brought fission yeast to play a crucial role in advancing our understanding of meiotic recombination (Cromie and Smith 2008).

S. pombe has a few more features that make it well suited for recombination research. Where most eukaryotes form a synaptonemal complex (SC), fission yeast lacks this complex. The SC is a protein structure essential for meiosis, that forms a zipper-like assembly between homologous chromosomes and plays a crucial role in mediating chromosome synapsis, facilitating genetic recombination, and ensuring proper chromosome segregation (Zickler and Kleckner 2015). Fission yeast has also a minimal amount of recombination interference (RI). RI is a regulatory mechanism that ensures crossovers are distributed more evenly along the chromosomes. In RI, the occurrence of one crossover event reduces the likelihood of additional crossovers nearby on the same chromosome. These results in crossovers being more spaced than if they were randomly placed. The strength of interference can vary between species, being as long as 50Mb in *Caenorhabditis elegans,* and being practically nonexistent in *S. pombe*.

The lack of synaptonemal complex (SC) in fission yeast, together with the lack of crossover interference except in extremely close distances, and the lack of regulation of the number of crossovers and their distributions along the chromosome, make *S. pombe* an ideal organism for the study of the essential features of recombination without the complexities that are brought by the lack of SC and these regulatory mechanisms (Cromie and Smith 2008). The lack of interference allows for the possibility of modification of recombination rates, as well as the unusually high number of crossovers (Lian et al. 2023). Also at the lower limit of recombination rate, fission yeast is a good model. While recombination assures proper chromosomal segregation, even non-recombining mutants have a relatively high proportion of viable spores. This is due, in part, to the low number of chromosomes, that in the absence of recombination are still expected to segregate correctly 12.5% of the time (Davis and Smith 2001; Cromie and Smith 2008).

2.4 AIMS OF THIS DISSERTATION

The overall aim of this dissertation was to use different techniques to gain a better understanding of not only the current variation in recombination landscape of different fission yeast natural strains, but also to use diverse methods hypothesized to shape the evolution of recombination into what we see today.

My results, divided in three different parts, outline the potential for evolutionary changes of recombination rates in *Schizosaccharomyces pombe.* They begin with the observation of the present variation, through what are the possible selective pressures that have caused this variation, and end with an interesting insight on the possibilities of recombination rate modification and the effects of genomic variants on recombination rates and offspring survival.

Part 1 describes extensive analysis of **the variation in recombination in 57 natural strains** (Jeffares et al. 2015), analysing the proportion of recombination between two artificially-placed markers in each of the three chromosomes of the *S. pombe* lab strain (EBC70). The results show a notable difference between different strains, as well as among the different chromosomes within the same strain.

Part 2 describes an **evolution experiment** performed over 36 sexual cycles, with different selection regimes, which determines whether direct strong selection on recombination rates can generate changes on the recombination landscape. Direct selection for increased recombination (by selecting only recombinant offspring) or decreased recombination (by selecting only parental haplotypes) was done on independent biological lines of the *S. pombe* lab strain. These rounds of selection were performed with a Fluorescence Activated Cell Sorter (FACS). By weekly analysis, I aimed to confirm that recombination can be affected by direct selection on recombination rates.

Part 3 describes the mechanistic **effect of the presence of inversion**, and their size, on recombination and spore germination. The presence of three differently sized inversions, crossed in heterozygosis, show us the pure mechanistic effects when crossed with isogenic strains and analysed by tetrad dissections. When crossed with natural strains we can detect not only the effect of the inversion, but also the incompatibilities between the genes within.

Together these three approaches give an overall new understanding of the present variation in recombination rates among fission yeast strains, and evolutionary mechanisms through which these recombination rates could evolve.

3 MATERIALS AND METHODS

3.1 STRAINS AND GROWTH CONDITIONS

3.1.1 Chemicals and solutions

To generate media used in each section of this dissertation, apart from the ingredients listed in each of the methods sections of the chapters, here are listed the recipes for the components (Table 1, Table 2, Table 3). After mixing all the ingredients in the indicated amount of water, these were filter sterilized (pore size 0.2 micron) and stored in the fridge.

Table 1. Recipe for Salts stock 50x. Used for making minimal medium (EMM, EMMlowN and PMG). Ingredients dissolved in 1L ddH_2O.

Salts stock 50x			
Amount per liter		**Final Concentration**	
52.5 g	magnesium chloride hexahydrate	0.26 M	$MgCl_2 \cdot 6H_2O$
0.735 g	calcium chloride dihydrate	5.0 mM	$CaCl_2 . 2H_2O$
50 g	potassium chloride	0.67 M	KCl
2 g	(di)sodium sulfate	4.1 mM	Na_2SO_4

Table 2. Recipe for Vitamin stock x1000. Used for making minimal medium (EMM, EMMlowN and PMG). Ingredients dissolved in 100ml ddH_2O.

Vitamin Stock x1000			
Amount per 100ml		**Final Concentration**	
0.1 g	pantothenic acid	81.2 mM	pantothenic acid
1 g	nicotinic acid	81.2 mM	nicotinic acid
1 g	(myo-)inositol	4.20 mM	inositol
1 mg	biotin	40.9 µM	biotin

Table 3. Recipe for Mineral stock x10000. Used for making Minimal Medium (EMM, EMMlowN and PMG). Ingredients dissolved in 100ml ddH_2O

Mineral stock x10000			
Amount per 100ml		**Final Concentration**	
5 g	Boric acid	80.9 mM	boric acid
4 g	Manganese sulfate	33.2 mM	$MnSO_4$

4 g	Zinc sulfate heptahydrate	13.9 mM	$ZnSO_4$. 7 H_2O
2 g	Ferric chloride hexahydrate	7.40 mM	$FeCl_3$. 6 H_2O
0.4 g	Molybdic acid	0.32 mM	molybdic acid
1 g	Potassium iodide	6.02 mM	KI
0.4 g	Cupric sulfate pentahydrate	1.60 mM	$CuSO_4$. 5 H_2O
10 g	Citric acid	47.6 mM	citric acid

Supplements and antibiotics

For auxotrophic yeast strains, supplements were added in the following quantities:

Table 4. Available supplements and final concentration

Supplements	
Ingredient	**Amount/L ddH_2O**
Adenine	100mg/L
L-leucine	225 mg/L
Histidine	225 mg/L
Uracil	225 mg/L

The following table contains all the used antibiotics both for fission yeast and bacterial selective selection.

Table 5. Table of antibiotics and final concentrations

Antibiotic list		
Name	**Final concentration**	**Use**
G418 - Geneticin	200 mg/L	Yeast
Nourseothricin	100 mg/L	Yeast
Hygromycin	100 mg/L	Yeast
Ampicillin	100 mg/L	Bacteria
Kanamycin	100 mg/L	Bacteria

3.1.2 Used strains

All strains used in this thesis are described in Table 6. Except for EBC395 and EBC407, all strains indicated with full genotype descriptions are derived from the labstrain from Leupold. Strains starting with “JB” are natural isolates as described in Jeffares et al. 2015, for which only the thallism is given. Strains EBC395 and EBC407 are heterothallic strains with a marker introduced, that are modified from natural isolates JB4 and JB858 respectively.

Table 6. Schizosaccharomyces pombe strains used

Name	Mating type	Genotype / Original name	Original citation
EBC395	M	JB4 with mat1M-H1::hphMX6	
EBC407	M	JB858 with mat1M-H1::hphMX6	
EBC453	P	h+S ura4+-aim2-PSJAG_04227-tdTomato-TPGK1(Skud) ade6+::PSOCG_04642-YFP-TPGK1(Smik) his3+-aim-PSPOG_00147-mCerulean-TPGK1(Sbay) his3-D1? ura4-D18? inv1L::Padh1-kanMX inv1R::ura4+ leu1::hphMX	
EBC455	M	h-S ura4+-aim2-PSJAG_04227-tdTomato-TPGK1(Skud) ade6+::PSOCG_04642-YFP-TPGK1(Smik) his3+-aim-PSPOG_00147-mCerulean-TPGK1(Sbay) his3-D1? ura4-D18? inv1L::Padh1-kanMX inv1R::ura4+ leu1::hphMX	
EBC663	M	h-(H1::kanMX) mat2,3::LEU2 ade6-M216 ura4-D18 leu1-32 I1.45::Peno101_so-mCherry-TPGK_Skud	
EBC675	M	h-(H1::kanMX) mat2,3::LEU2 ade6-M216 ura4-D18 leu1-32 I1.14::Ptif51-tagBFP-Tpgk1_Seub I1.38::Padh1-GFP-TURA3	
EBC687	P	h+(H1::hphMX) mat2,3::LEU2 ade6-M216 ura4-D18 leu1-32 I1.14::Ptif51-tagBFP-Tpgk1_Seub I1.38::Padh1-GFP-TURA3	
EBC746	P	h+(H1::hphMX) mat23::LEU2 ade6-M216 ura4-D18 leu1-32 I1.25::Peno101_so-mCherry-Tpgk1_Smik	
EBC787	P	h+(H1::hphMX) mat23::LEU2 ade6-M216 ura4-D18 leu1-32 II2.34::Peno101_So-GFP-Tpgk1_Seub	
EBC819	M	h-(H1::tagBFP-kanMX) mat23::LEU2 ade6-M216 ura4-D18 leu1-32 II2.76::Plsd90_So-mCherry-Tpgk1_Smik	
EBC832	P	h+s mat23::LEU2 ade6-M216 ura4-D18 leu1-32 inv[II:2.15 - his5::natMX]	
EBC835	P	h+s mat23::LEU2 ade6-M216 ura4-D18 leu1-32 his5::natMX	
EBC836	P	h+s mat23::LEU2 ade6-M216 ura4-D18 leu1-32 Inv[II:ura5-his5::natMX]	
EBC867	P	h+s mat23::LEU2 ade6-M216 ura4-D18 leu1-32 inv[II:his7-his5::natMX]	
EBC871	M	h-(H1::kanMX) mat23::LEU2 ade6-M216 ura4-D18 leu1-32 II2.34::GFP II2.52::ura4 II2.76::mCherry	
EBC961	P	h+ S I-inv1L::Padh1-kanMX inv1R::ura4+ II2.52::Peis_Sjab-mCherry-TPGK_Skud II2.76::Ppil2_Scry-GFP*_TPGK1_Smik leu1::hphMX ade6-M216	
EBC962	M	h+ S I-inv1L::Padh1-kanMX inv1R::ura4+ II2.52::Peis_Sjab-mCherry-TPGK_Skud II2.76::Ppil2_Scry-GFP*_TPGK1_Smik leu1::hphMX ade6-M216	
EBC1051	M	h-S inv1L::Padh1-kanMX inv1R::ura4+ leu1::hphMX ade6-M216 I1.14::Psjeis1-mCherry-TPGK1 I1.25::Pscpil2-GFP*-TPGK1	

EBC1052	P	h+S inv1L::Padh1-kanMX inv1R::ura4+ leu1::hphMX ade6-M216 I1.14::Psjeis1-mCherry-TPGK1 I1.25::Pscpil2-GFP*-TPGK1	
EBC069	homothallic	JB4	Jeffares et al 2015
EBC070	M	JB22	Jeffares et al 2015
EBC073	M	JB758	Jeffares et al 2015
EBC074	M	JB760	Jeffares et al 2015
EBC076	M	JB762	Jeffares et al 2015
EBC077	M	JB837	Jeffares et al 2015
EBC078	homothallic	JB840	Jeffares et al 2015
EBC079	homothallic	JB841	Jeffares et al 2015
EBC080	homothallic	JB842	Jeffares et al 2015
EBC081	homothallic	JB845	Jeffares et al 2015
EBC082	homothallic	JB846	Jeffares et al 2015
EBC083	homothallic	JB848	Jeffares et al 2015
EBC084	homothallic	JB852	Jeffares et al 2015
EBC085	homothallic	JB853	Jeffares et al 2015
EBC086	homothallic	JB854	Jeffares et al 2015
EBC087	homothallic	JB858	Jeffares et al 2015
EBC088	homothallic	JB862	Jeffares et al 2015
EBC089	M	JB864	Jeffares et al 2015
EBC091	P	JB869	Jeffares et al 2015
EBC092	homothallic	JB870	Jeffares et al 2015
EBC093	homothallic	JB871	Jeffares et al 2015
EBC094	homothallic	JB872	Jeffares et al 2015
EBC095	homothallic	JB873	Jeffares et al 2015
EBC096	homothallic	JB874	Jeffares et al 2015
EBC097	homothallic	JB875	Jeffares et al 2015
EBC098	homothallic	JB878	Jeffares et al 2015
EBC099	homothallic	JB879	Jeffares et al 2015
EBC100	homothallic	JB884	Jeffares et al 2015
EBC102	homothallic	JB899	Jeffares et al 2015
EBC103	homothallic	JB900	Jeffares et al 2015
EBC104	homothallic	JB902	Jeffares et al 2015
EBC106	homothallic	JB910	Jeffares et al 2015
EBC107	homothallic	JB913	Jeffares et al 2015
EBC108	M	JB914	Jeffares et al 2015
EBC109	homothallic	JB916	Jeffares et al 2015
EBC110	homothallic	JB917	Jeffares et al 2015
EBC111	homothallic	JB918	Jeffares et al 2015
EBC112	homothallic	JB929	Jeffares et al 2015

EBC113	homothallic	JB930	Jeffares et al 2015
EBC114	homothallic	JB931	Jeffares et al 2015
EBC115	homothallic	JB934	Jeffares et al 2015
EBC118	M	JB938	Jeffares et al 2015
EBC119	homothallic	JB939	Jeffares et al 2015
EBC122	homothallic	JB943	Jeffares et al 2015
EBC124	homothallic	JB953	Jeffares et al 2015
EBC125	homothallic	JB1110	Jeffares et al 2015
EBC126	homothallic	JB1117	Jeffares et al 2015
EBC127	homothallic	JB1154	Jeffares et al 2015
EBC131	homothallic	JB900	Jeffares et al 2015
EBC132	homothallic	JB1174	Jeffares et al 2015
EBC134	homothallic	JB1180	Jeffares et al 2015
EBC135	Sterile	JB1197	Jeffares et al 2015
EBC136	Sterile	JB1207	Jeffares et al 2015
EBC138	homothallic	JB1206	Jeffares et al 2015
EBC139	P	JB838	Jeffares et al 2015

3.1.3 Growth conditions

Temperature

All vegetative yeast growth was performed in incubators at 32ºC. All vegetative growth in liquid media was performed shaking at ~230rpm. Mating temperature (sexual reproduction) for fission yeast was set at 25ºC.

All *E. coli* growth was performed in incubators at 37ºC. All growth in liquid was performed in glass tubes, shaking at ~250rpm.

Media and supplements

Both solid and liquid medium were used for this thesis. These two types of medium have the same compositions. Additionally, solid medium contains 2% Agar-agar (20g/L) (Not indicated individually in the recipes). After mixing all the ingredients with ddH_2O, all media were autoclaved at 121ºC for 15 min. All media are described in Hagan et al. (2016).

- **Growth minimal medium (PMG – Pombe Minimal Glutamate)**

This is a modification of the commonly used fission yeast medium EMM, in which Glutamate is used as a substitute for Ammonium chloride. This has the benefit that antibiotics can be used that do not work on

EMM. In this thesis PMG is used as a defined synthetic growth medium, to avoid possible differences that could occur due to batch differences in rich growth medium (YES; see below).

Table 7. PMG recipe. Supplements added when using auxotrophic strains (see Supplements table)

Ingredient	Amount/L
Potassium Hydrogen Phthallate	3.0 g
$Na_2HPO_4.2H_2O$ (or anhydrous)	2.76 g (2.2 g)
L-Glutamic acid monosodium salt hydrate (or L-Glutamic acid)	5.0 g (3.75 g)
D-Glucose	20 g (=2% final concentration)
Salts Stock x50	20 ml
Vitamin Stock x1000	1.0 ml
Mineral Stock x10.000	0.1 ml
Uracil	225mg/L
Adenine	100mg/L

○ Yeast medium for crosses (EMMlowN)

Crosses were performed on minimal mating solid medium which is PMG as described above (Hagan et al. 2016) with glutamic acid salt reduced to 1g/L, which induces *S. pombe* to sexually mate, and supplements as indicated in Table 4. From now on this type of medium will be called EMMlowN.

○ Growth rich medium (YES – Yeast Extract Supplemented)

YES is a rich medium used for the optimal growth of cells. YES was used to obtain maximum growth of the cells, but not in running experiments, because the composition of yeast extract and CAS aminoacids can differ between batches, possibly introducing non-controlled changes in our experiment.

Table 8. YES recipe. For YES all supplements are always added

YES - Yeast Extract Supplemented	
Ingredient	**Amount/ liter ddH2O**
Yeast extract	5 g
CAS amino acids	2 g
D-Glucose	30 g
Adenine	100 mg
L-leucine	225 mg
Histidine	225 mg
Uracil	225 mg

○ Lysogene Broth (LB) medium for bacterial growth

To perform bacterial transformations we used Top 10 *E. coli*, which were grown in LB medium (Sambrook et al. 1989).

Table 9. Recipe for LB medium (growth of E. coli)

Lysogene Broth	
Ingredient	**Amount/L**
ddH_2O	950 mL
Tryptone	10 g
NaCl	10 g
Yeast extract	5 g

The medium was adjusted to pH7.0 with 5N NaOH, and for solid medium Bacto-Agar was added.

○ Super Optimal Broth with Catabolite repression (SOC medium)

SOC medium is a bacterial growth medium used to grow competent *E. coli* cells after transformation and before plating, to maximize the efficiency of the transformations.

Table 10. Recipe for SOC liquid medium

Ingredient	**Amount per Litre**
ddH2O	100mL
SOB-Medium	3.07g
MgCl2 1M	1ml
Glucose 60%	599µl

3.2 MOLECULAR TECHNIQUES

3.2.1 Extended Golden Gate assemblies

To generate the plasmids necessary for chromosomal integrations and rearrangements, we used the Golden Gate assembly method. This method uses DNA fragments with type IIS restriction enzymes cut sites on the sides, which were generated by PCR and integrated in a plasmid (level1) (Marillonnet and Grützner 2020). Those DNA fragments are designed to have complementary overhangs that can assemble in one specific order into a larger DNA construct (Level 2). We generated a system that is based on Kakui et al. (2015) introducing modifications inspired by Binder et al. 2014. Level 1 and level 2 plasmids contain alternating antibiotic resistance cassettes, and can be transformed into T10 *E. coli* cells. Only *E. coli* that have

integrated the plasmid can then grow in a medium with antibiotic. Level 2 plasmids have been used in this project as a DNA template for PCR, where a Homologous Recombination (HR) fragment was amplified for a yeast transformation (Berenguer Millanes and Nieuwenhuis 2023). Detailed explanations of each step can be found in the following sections.

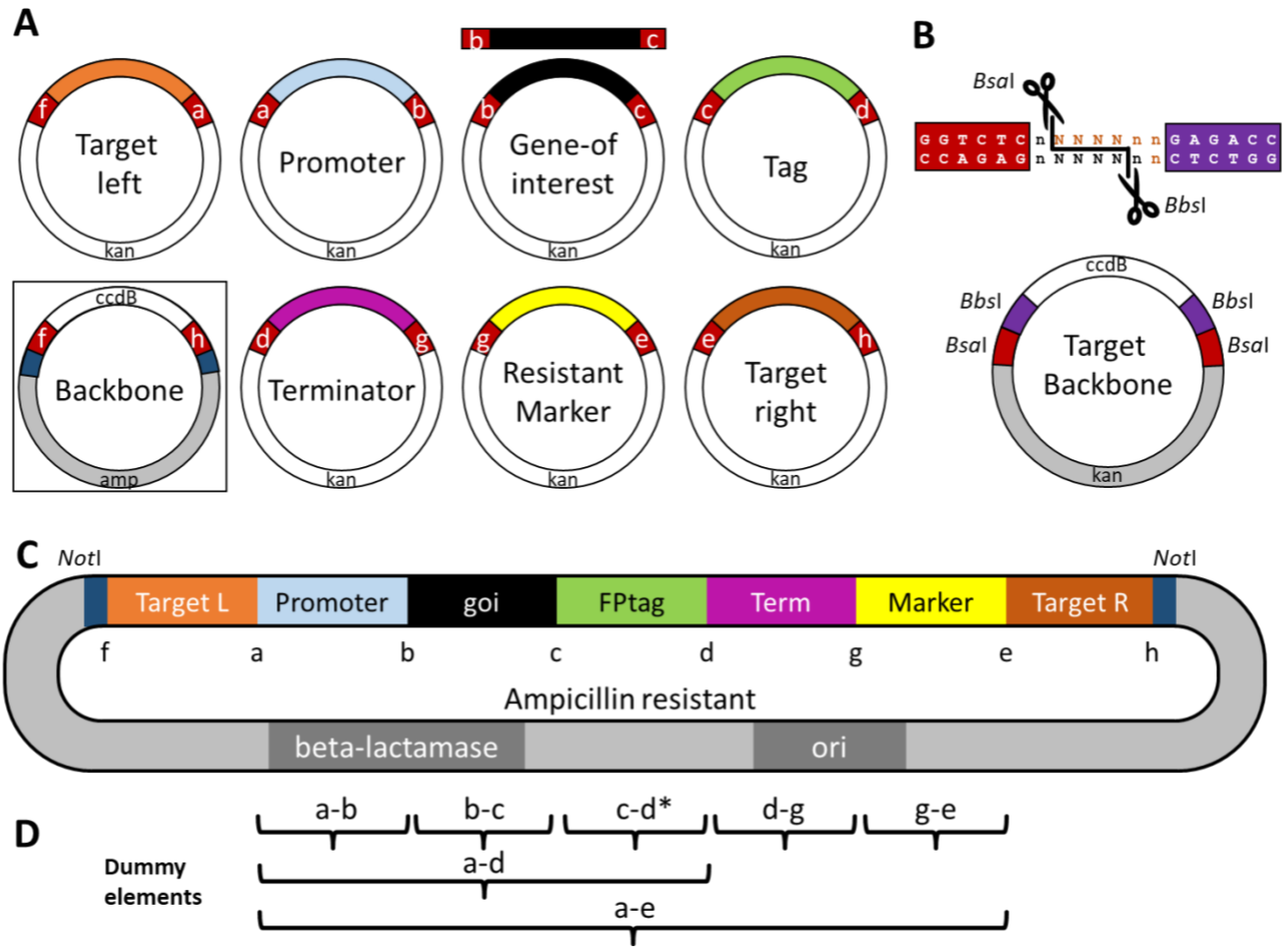

Figure 3. Overview of the golden gate elements and construction of level 1 and level 2 elements. **A** The donor elements with overhangs are indicated by letters and the white parts contain the *BsaI* restriction sites, which will not be present in the final product. Each donor contains a kanamycin resistance gene in the backbone, except for the (f-h) backbone which is ampicillin resistance. This latter plasmid additionally contains a ccdB gene that kills all cells containing undigested backbone plasmids. The (b-c) and (c-d) elements can be reversed for N-terminal tagging as explained in Kakui et al. (2015) **B** Plasmids for Level 1 target elements contain *BbsI* recognition sites that are cut when generating L1 donor plasmids, which can be used to generate L2 plasmids utilizing the *BsaI* sites in the backbone. Additionally, they contain a ccdB that is excised during assembly. **C** Example of a fully constructed Level 2 plasmid. The to-be-inserted fragment can be excised from the backbone using *NotI* digestion and directly used. Alternatively, the fragment can be amplified by PCR using primers M13F and M13R. **D** A set of dummy elements has been produced to span gaps that are not required in an assembly. Figure taken from Berenguer Millanes and Nieuwenhuis, 2023.

Donor elements (Level 1)

The generation of each element's position in the final construct (Level 2) were decided, which dictate the corresponding overhangs of the *BsaI* restriction sites (Figure 3). Followingly, primers were designed with the restriction site and overhangs added to the end of the oligonucleotide sequence. To obtain the fragment, PCR with Phusion DNA Polymerase (Thermo Fisher) were performed using the recipe in Table 11 with the thermocycler program described in Table 12.

Table 11. PhusionPCR recipe with quantity of each component for a total amount of 20µl per reaction

PCR Component	Volume (in µl)
H2O	13.6
Phusion HF Buffer 5X	4
DMSO 100%	0
Primer Fwd (10 µM)	0.4
Primer Rev (10 µM)	0.4
DNA template (~1-10ng/µl)	1
dNTPs (10 mM each)	0.4
Phusion polymerase (5U/µl)	0.2

Table 12. Thermocycle program. Note to modify the time and temperature depending on the primers used and the elongated fragment. Tm calculated with the Tm calculator at Thermofisher.com

Number of cycles	Temperature	Duration	Notes
1 X	98°C	2 min	
30X	98°C	15 sec	
	55-65°C	30 sec	Modify temp to ~(Tm + 5°C)
	72°C	1-5min	Modify time to 30sec / ~1kb
1X	72°C	5 min	
	7°C	Inf	

Once amplified, the presence of the fragment was validated on a 1% Agar gel, and when the correctly sized band is present, the fragment is then inserted in the level 1 backbone pBN111 with kanamycin resistance (Figure 3a), with blunt end cut-ligation (*SmaI).* The reaction (Table 13) was performed in a thermocycler (3.5h at 25°C, followed by inactivation) and the ligate was transformed into chemically competent *E. coli* cell (see 2.3.1). The obtained plasmid was purified with a commercial miniprep kit (Macherey-Nagel) and verified by Sanger sequencing.

Table 13. Recipe for Level 1 element generation. The amount of the PCR fragment and H2O depend on the length and concentration of the PCR fragment

Component	Volume (in µl)
SmaI	0.3
T4 ligase (NEB)	1
CutSmart buffer	1.5
ligase buffer	1.5
pBN111/pBN103 (25ng/µl)	1
PCR fragment	depends
PCR grade H2O	depends

Golden Gate assembly (Level 2)

The assembly of the level 1 elements into a level 2 construct was performed in a single reaction in a thermocycler (Table 14, Table 15). All fragments need exactly one other fragment with a complementary overhang on either side, with the order as shown in Figure 3c, in which TargetL and TargetR indicate the sequences homologous to the chromosomal location where the construct is to be inserted. The dummy elements were created to substitute elements that are not needed in a certain construct, which acts as filler without biological effect. For a correct assembly, all the level 1 elements were isomolar, i.e. diluted to 13.3ng/µl per 1-kilobase DNA. After assembly, the plasmid was transformed into *E. coli* and selected on LB+ampicillin.

Table 14. Golden Gate recipe for level 2 plasmid. The amount of water added will depend on the number of level 1 fragments added to the mix. The total always amounts to 15µl.

Component	Volume (in µl)
plasmids and fragments	1 µl of each
BsaI-HF V2 (5 units)	0.75
T4 ligase (NEB)	0.75
CutSmart 10X	1.5
ligase buffer	1.5
PCR grade H2O	depends
Total	15

Table 15. Thermocycler program for Golden Gate level 2 (BsaI) assembly.

Number of cycles	Temperature	Duration
1X	37°C	5 min
30X	37°C	3 min
	16°C	3 min
1X	37°C	10 min

	80°C	20 min
	8°C	Inf

3.2.2 Generation of CRISPR/Cas9 plasmids (sgRNA)

Plasmids with the guide RNA sequence, for the CRISPR/Cas9 system for yeast transformations, were generated with the spEDIT technique, described in Torres-Garcia *et al.*, 2021. The guide RNA can be inserted in three different backbones, depending on the desired antibiotic resistance gene: natMX, kanMX or hphMX. The plasmids were generated by first identifying a suitable PAM region using CRISPR4P online tool (bahlerlab.info/crispr4p) (Rodríguez-López et al. 2017). Next, the necessary primers needed to be designed and ligated with a touchdown PCR. The ligated primers were then diluted 1:100 and assembled to the backbone with *BsaI* Golden Gate reaction (recipe and thermocycler guide in Table 14 and Table 15). Finally, I proceeded with an *E. coli* transformation (see below) and plated on LB+ampicillin.

The spEDIT system works with fluorescence, in which the GFP marker in the original backbone is replaced when the RNA guide is inserted. *E. coli* colonies that grew on the plate were checked for fluorescence and the non-fluorescent ones were miniprepped, and the sequence for the guide RNA was validated by Sanger sequencing.

3.2.3 Transformations

E. coli transformations

E. coli chemical transformations were performed to generate copies of the desired plasmids, which will afterwards will be extracted and saved at -20ºC. Chemically competent Top10 *E. coli* cells were taken from -80ºC and thawed on ice. Between 5 and 10 µl of spEDIT or Golden Gate (level 1 or 2) ligation was added. After 30 minutes incubation on ice, the cells were heat shocked at 42ºC for 1min, placed back on ice for 2 minutes. After, 250µl of SOC medium was added. The tubes were incubated at 37ºC on a shaker for 1h and plated out on LB plates with appropriate antibiotics. After overnight incubation at 37ºC colonies were assessed for fluorescence or by *E.coli* colony PCR. Good candidate colonies were grown and miniprepped after which the plasmid was stored at -20ºC.

Yeast transformations

All strains used are heterothallic h^+ and h^- strains derived from Leupold's 968 strain (Heim 1990) in which the silent mating-type region (*mat2,3*) was replace by a LEU2 cassette (Klar and Miglio 1986) to avoid reversion to homothallism (Nieuwenhuis et al. 2018). Additionally, the H1 region at *mat1* that contains the

mating type switching initiation point (Styrkársdóttir et al. 1993) was replaced by a kanMX or hphMX marker for plus or minus strains, respectively. These have been genetically modified using CRISPR-Cas9 techniques (Rodríguez-López et al. 2017; Torres-garcia et al. 2021), with HR fragments generated by Golden Gate, following the methods as described in Berenguer Millanes and Nieuwenhuis, 2023, explained on page 25. For detailed genotype information about the used strains, see All strains used in this thesis are described in Table 6. Except for EBC395 and EBC407, all strains indicated with full genotype descriptions are derived from the labstrain from Leupold. Strains starting with "JB" are natural isolates as described in Jeffares et al. 2015, for which only the thallism is given. Strains EBC395 and EBC407 are heterothallic strains with a marker introduced, that are modified from natural isolates JB4 and JB858 respectively.

Table 6).

Using a level 2 plasmid as template, the HR fragment was amplified by Phusion PCR (Table 11 and Table 12). This fragment was then co-transformed with the CRISPR/Cas9 plasmid encoding the appropriate sgRNA. The transformation procedure started by thawing synchronized competent yeast cells by heating them shortly at 42ºC and left on ice. Afterwards, 5µl ssDNA, 20µl of the HR template,10µl of the sgRNA plasmid and 145µl of PEC4000 were added to the cells. 15min of incubation at 42ºC followed, after which the cells were centrifuged and the supernatant removed. Finally, the cells were resuspended with 1ml EMM-N with all the necessary supplements for the strain, which had been reduced to 10% of the standard amount. After ~16h of room temperature incubation, the cells are centrifuged again and plated on solid YES with the appropriate antibiotics for the chosen sgRNA plasmid, incubated until colonies are visible.

To verify that the grown colonies have the correct insertion, yeast colony PCR (with FastGene) were performed. Primers used can be either primers on either side of the insertion, or primers where one is inside the insertion and the other outside. If the first option is used, the colonies will be chosen according to the size of the band in the gel. If the second option is used, the presence of a band itself will show what colonies have the correct insertion.

Table 16. Recipe for FastGene yeast colony PCR

Component	**Volume (in µl)**
H2O	4.2
FastGene	5
Primer F (10µM)	0.4
Primer R (10µM)	0.4

Table 17. Thermocycler schedule for Yeast colony PCR

Number of cycles	Temperature	Duration	Notes
1 X	94°C	2 min	
35X	94°C	30 sec	
	57°C	30 sec	Check by gradient PCR from 52 to 68°C
	72°C	1-5min	Modify time to 1min / ~1kb
1X	72°C	7 min	
	7°C	Inf	

Inversion generation

Inversions were generated with a novel process described in Berenguer Millanes and Nieuwenhuis, 2023. Shortly, the inversions were generated using the same process as the yeast transformations, generating double strand breaks at the inversion break points. To simultaneously generate these breaks, CRISPR/Cas9 with the guide RNA for two PAM sites is introduced. Two sgRNA plasmids with different antibiotic resistances, or one plasmid with two sgRNA sequences are co-transformed into fission yeast strains. To guide the repair towards the inverted configuration, two HR sequences are added during transformation, one for each side of the inversion as indicated in Figure 4a. Three different sized inversions were generated as described in Figure 4b.

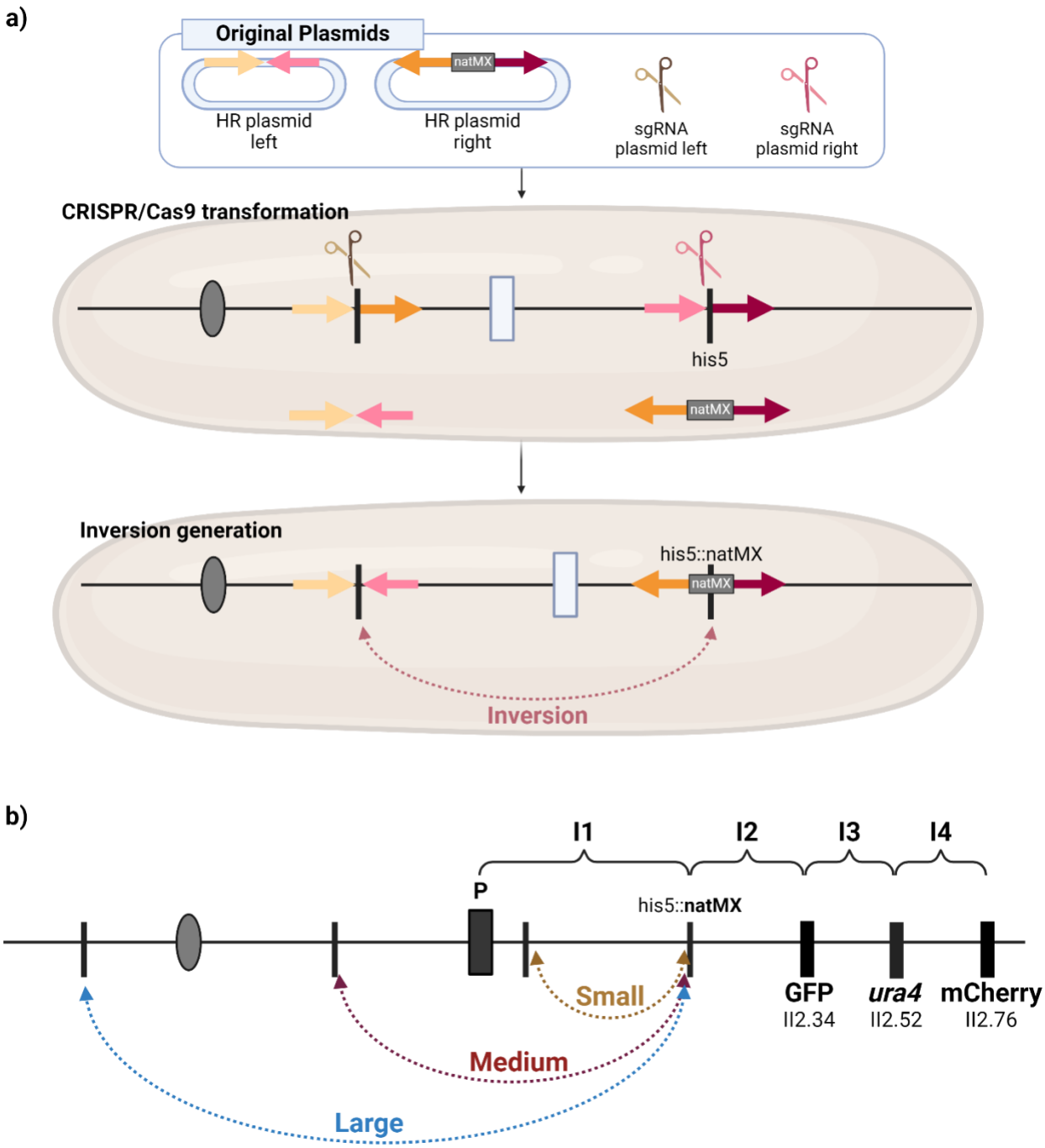

Figure 4. Schematic representations of inversions and their generation. The oval represents the centromere, the large rectangle the mating-type locus, and the smaller rectangles indicate the markers and their location, used to measure recombination. a) Generation of an inversion in fission yeast. The HR fragment is generated by PCR from the HR plasmids, and both sides together with both sgRNA plasmids are put together in the transformation reaction, with the candidate strain. For more information, see main text. b) Representation (not to scale) of the three artificially generated inversions on chromosome II. Small inversion is 110kb long, Medium is 220kb long, and Large Is 1.03Mb long. Also indicated by I1, I2, I3 and I4, the four intervals that I further analyse in this manuscript.

3.3 EXPERIMENTAL PROCEDURES AND ANALYSES

3.3.1 Kill all but spores

To avoid working with several generations of cells at the same time, we used two consecutive treatments that eliminate all the vegetative cells after each mating step but that maintain the spores. Spores are protected during this treatment because the cell wall of spores is thicker than that of vegetative cells (Nieuwenhuis et al. 2018). In this double treatment, first a treatment was performed with Lallzyme MMX (Lallemand), a commercially available enzyme mixture used in wine making (Flor-Parra et al. 2014). Cells were harvested from the mating medium and suspended in 150µl MMX mix (100 mg/ml in ddH_2O, filter-sterilized) and incubated for at least 4h, but preferably overnight, at 32ºC. After the MMX treatment, a second treatment with 30% ethanol was performed by adding ~70µl of 96% ethanol and incubating for 30 min. Cells were then spun down at 1800xg for 3min, the supernatant was discarded and the pellet was re-suspended in water.

After this process we have a suspension of spores in water that can be stored at 4ºC for up to two months. After that time, approximately 90% of the spores will have lost the ability to germinate (Ohtsuka et al. 2022).

3.3.2 Experimental evolution

Experimental setup

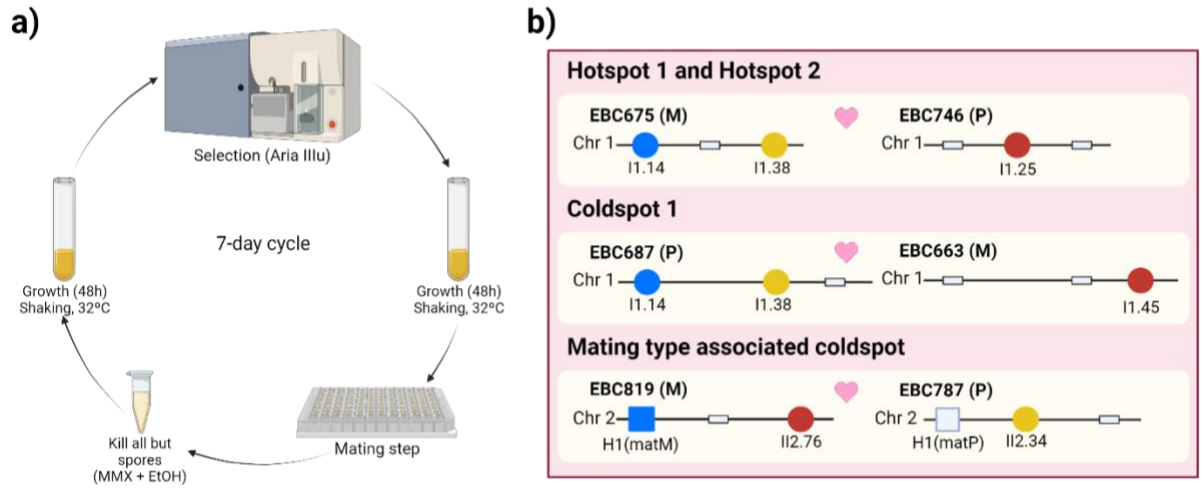

Figure 5. a) Representation of the 7-day sexual cycle for the evolution experiment. b) Graphical representation of the strains and their markers indicated in Table 1. Indicated in the figure what initial crosses were used for each of the selection regimes. Fluorescent markers are represented with coloured dots, and mating types are represented with squares.

For each selection regime we followed the same 7-day cycle of vegetative growth and selection (Figure 5**a**), where the selection step was performed at the Core Facility of Flow Cytometry at the Biomedical Center, Ludwig-Maximilians-Universität München, with Fluorescent Activated Cell Sorting (FACS) AriaIIIu (4-laser). Shortly, all spores were grown for 48h followed by selection on the FACS after which the selected cells were grown for another 48h. The now saturated sample was mated on solid mating medium after which a 'kill all but spores' double treatment as described above was performed. The spores were then used for a next generation. The strains used were generated by transformations as indicated above. Fitness effects of the individual markers were measured by competing each strain with an unmarked strain and no significant differences were measured for any of the markers. The initial crosses done for the experimental evolution were set as indicated in Figure 5b. (EBC675xEBC746 to start Hotspots 1 and 2, EBC687xEBC663 to start Coldspot 1, and EBC819xEBC787 to start the Mating Type associated Coldspot). For each of the crosses, selection was performed since cycle 1, depending on the selection regime. The experiment was run for a total of 36 cycles. Each of the sexual generations was saved in -80ºC, protected with 15% Glycerol.

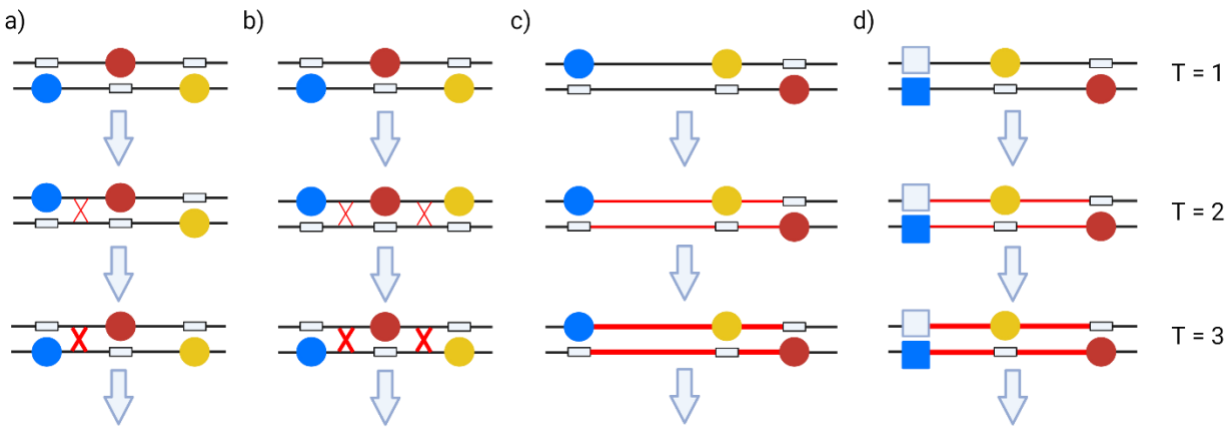

Figure 6. Schematic showing the four selection regimes over three example generations for the selected allele combinations. Blue, yellow and red coloured dots represent the markers tagBFP, GFP and mCherry, respectively. The strains represent the previously indicated initial strains. **a)** Hotspot selection between the first two linked loci in chromosome 1. **b)** Selection for two recombination events between the three loci in chromosome 1. **c)** Selection for the same allele combinations over time, for increased linkage in the same region in chromosome 1. **d)** Selection for association of alleles with opposite mating types, generating antagonistic selection in chromosome 2. Mating types are represented with squares**.**

The selection regime, performed by FACS cell sorting, is schematically portrayed in Figure 6, where the four different regimes are depicted each for three generations. Two regimes select for increased recombination rates (Figure 6a-b), and two select for decreased recombination rates (Figure 6c-d).

The media used for the growth steps was liquid PMG supplemented with uracil and adenine, and for crosses EMMlowN.

Selection step with FACS Aria IIIu

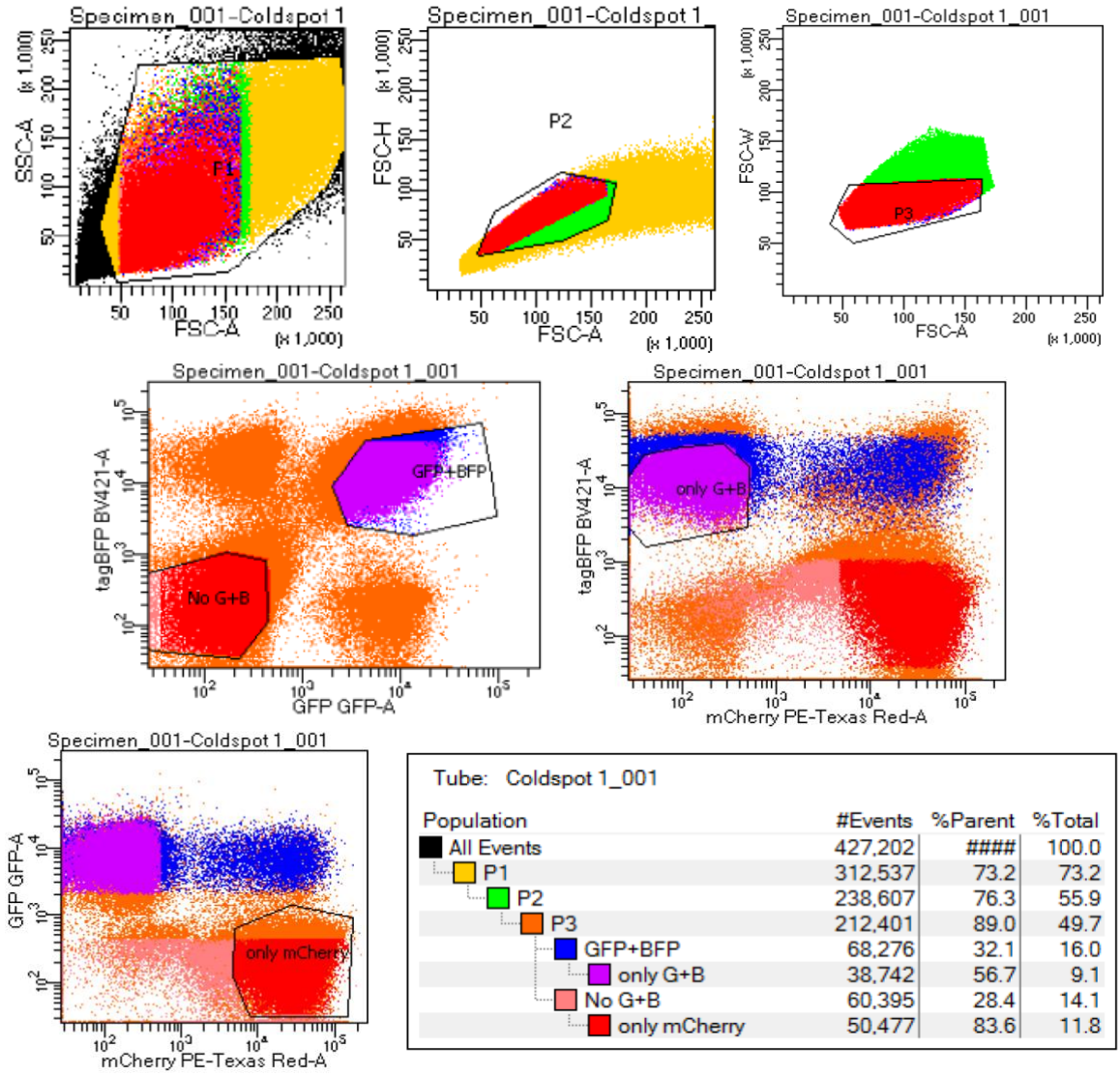

Figure 7. Example of the selection steps for the Aria IIIu. Specimen chosen from "Coldspot in chr1". We can see in each panel, in order from left to right, and starting on the top left, the selection by gates performed. The last panel shows the gating for the samples.

Every generation the samples were taken from the incubator and filtered through a 38µm mesh previously sterilized in 80% ethanol and air-dried. This assured that the samples were adequate to use in the Aria IIIu cell sorter and they did not create cell clumps. For the two coldspot treatments, which kept the same selection step every week (Figure 6c, d), gating was always the same, with the final selection gates chosen as shown in Figure 7. For the two different hotspot treatments (Figure 6a and b) the selection on odd generations differed from the selection on even generations. In all cases 50,000 cells for each genotype were selected each week, which meant a total of 100,000 cells began the growth in each generation.

For Hotspot1, on even weeks selection was done for cells that had tagBFP and GFP, and cells that had mCherry. On odd weeks, selection was performed for cells that had tagBFP and mCherry, and cells that had only GFP (Figure 6a).

For Hotspot2, on even weeks the cells selected were the same as for the Hotspot1, either tagBFP+GFP or only mCherry. On odd weeks on the other hand, selection was performed for cells that had either the three fluorescent markers, or none of them (Figure 6b).

For all four treatments, I used the same three fluorescent proteins (tagBFP, GFP and mCherry) and laser-and-filter combinations in the cell sorter. Laser 405nm with BP filter 450/40 (called BV421) for tagBFP, laser 488nm with long pass 502 and BP filter 530/30 (called GFP) for GFP, and laser 561nm with long pass 600 and BP filter 610/20 (called PE-TexasRed) for mCherry.

For controls 1 and 2, at the beginning of the experiment the first 100,000 cells from P3 (single cells) (Figure 7) were selected. Around week 16 a decrease in certain genotypes was detected in the control tubes, for which we decided to select in the following way: 16,000 cells with BFP marker, 16,000 cells without BFP marker, 16,000 cells with mCherry marker, 16,000 cells without mCherry marker, 16,000 cells with GFP marker and 16,000 cells without GFP marker. In AriaIIIu, selecting for presence or absence of one marker does not affect presence of other markers in the same cell. This type of selection allowed us to avoid selection of haplotypes, while assuring the maintenance of both alleles at each locus. Control 3 was run from the onset using the latter regime.

Data analysis with FlowJo

The flow cytometry results were analyzed using FlowJo v10.10.0 Software (BD life Sciences). The gating pipeline was performed in a similar way as for the selection step in Aria IIIu. For all treatments we did a selection of P1 > P2 > Singlets in order to make sure we are working only with single cells (Figure 8).

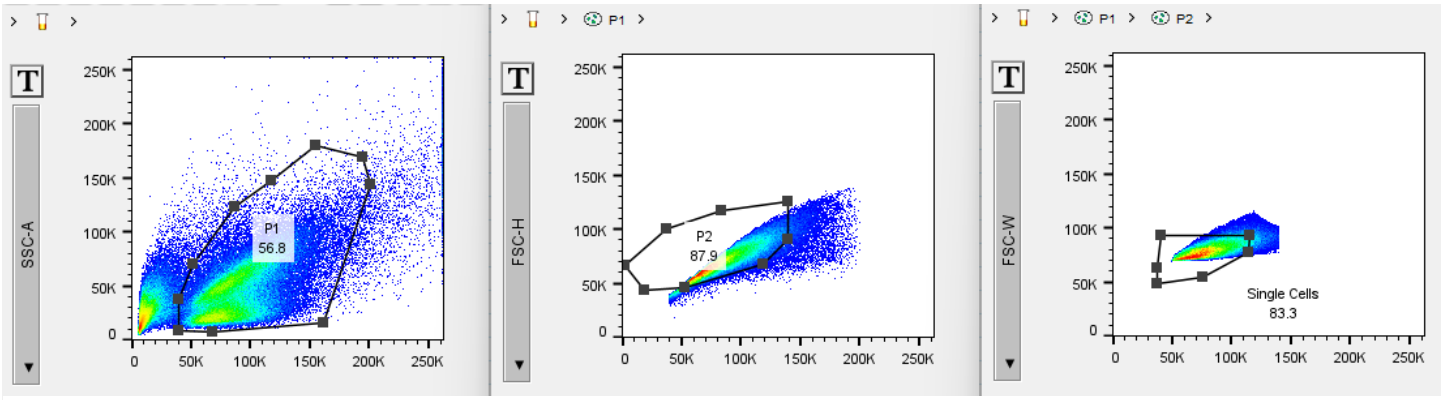

Figure 8. Example of the initial gating used for each sample. From left to right in the panels we can see the P1 > P2 > Single Cells pipeline, and the percentage of hits included in each of the gates.

Gate P1 eliminates most of the debris and other particles in the mix. Gate P2 uses FSC-H to further select only fission yeast cell, and the gate with FSC-W assures that all cells assessed for fluorescence are the single cells, and not doublets that might have two different alleles.

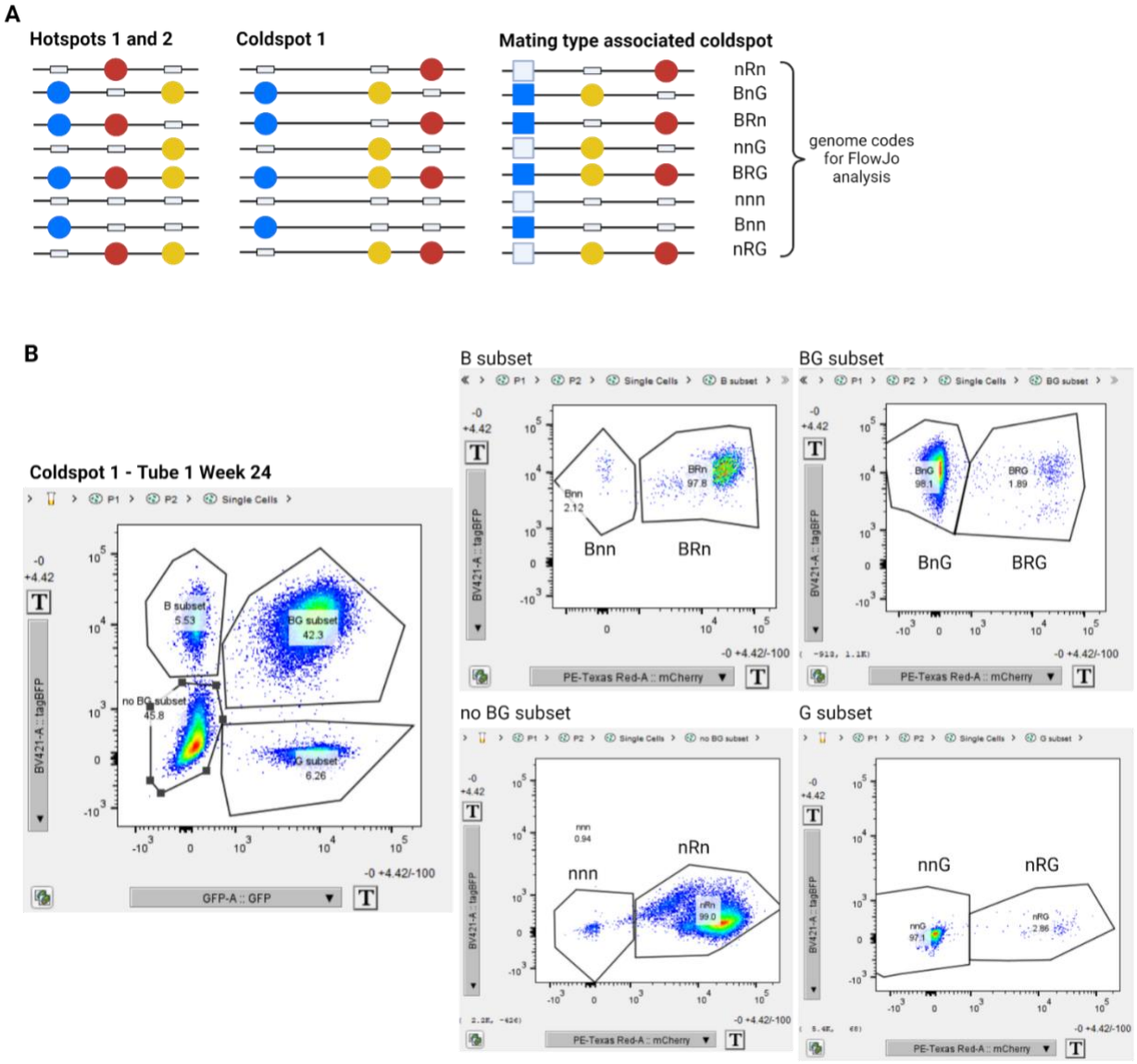

Figure 9 A) Schematic representation of the 8 different haplotypes that can be obtained – according to all the inserted fluorescent markers - for each of the selection regimes, as indicated in the figure. Next to each of the schemes, on the right side, the genome codes used for each of them for the analyses with FlowJo. **B)** Example of analysis for coldspot 1, tube 1 week 24. Here we can see the gating pipeline after selecting for Single Cells, and how to obtain the numbers for each of the genomes. Figure created with BioRender.com

For further analysis, the proportions of every possible haplotype were obtained with the FlowJo software (**Figure 9**). The same haplotype codes were used for all treatments in order to make the pipelines clearer.

3.3.3 Variation in recombination rates

A set of 57 natural strains described in Jeffares et al. 2015 was crossed to tester strains to assess recombination rates. Each of six tester strains indicated in Figure 10a was crossed with each of the natural strains indicated in the strains section (Table 6), to create diploids. Each of these six strains has an inversion in chromosome I which matches them to the natural population to increase crossing compatibility (Jeffares et al. 2017; Tusso et al. 2019), and an *hphMX* marker breaking *leu1*. EBC1051 and EBC1052 contain an mCherry marker in I1.14 and a GFP* marker in I1.25, EBC961 and EBC962 contain an mCherry marker in II2.52 and a GFP* marker in II2.76, EBC453 and EBC455 contain a tdTomato marker in III1.29 and a GFP* marker in III1.32 (Li et al. 2019). All fluorescence proteins are under control of a promoter of either *eis1* or *pil2*, cloned from *Schizosaccharomyces japonicas* and *Schizosaccharomyces cryophilus*, respectively, to avoid gene conversions or non-homologous recombination. These promoters are exclusively activated in the spores, which guarantees an easier filtering of our data, and making it possible to obtain much more precise data by analyzing directly the tetrads (Li et al. 2019).

Most natural strains are homothallic, which means they can switch mating type and mate with cells from the same strain. To assure tetrads analysed were crosses of natural strains with the fluorescently labelled tester strain, I forced outcrossing by generating diploids.

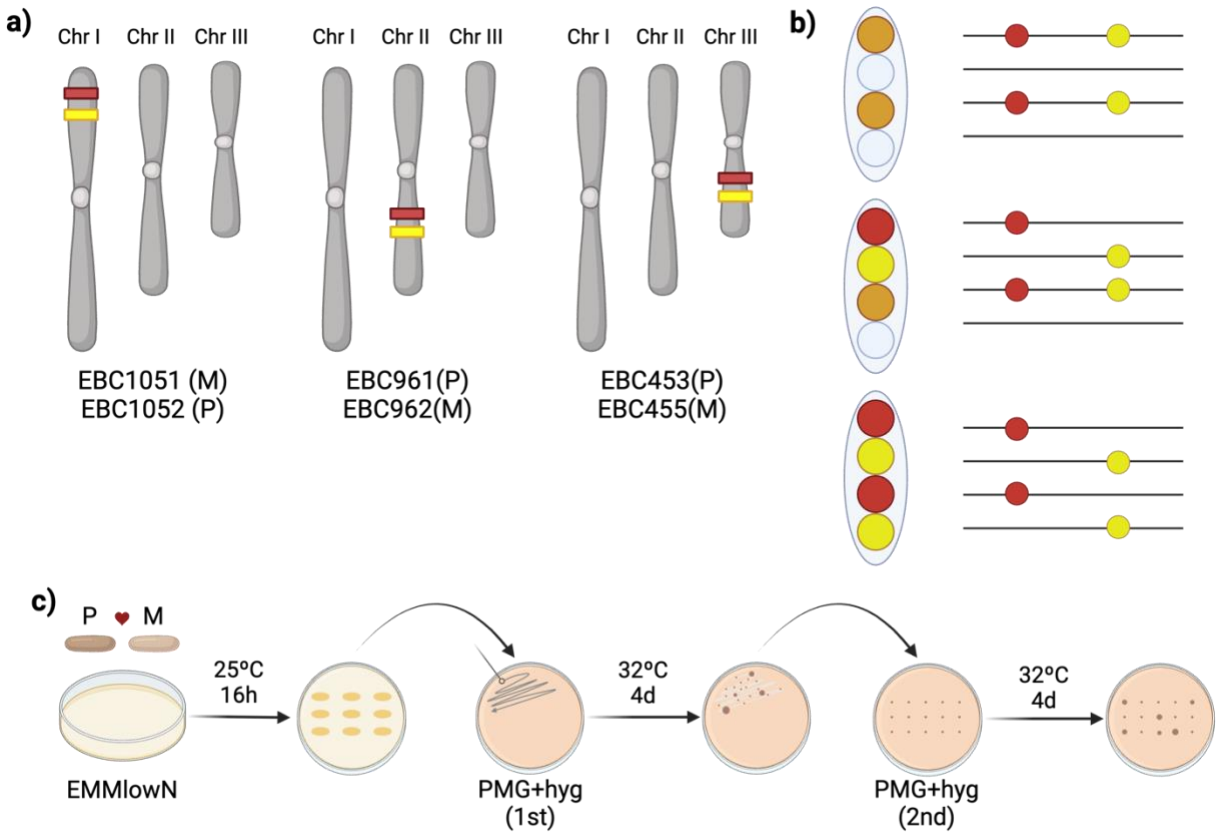

Figure 10. a) Simplified scheme of the position of each marker in each of the strains. b) Scheme of azygotic asci seen in the ImageStream. From top to bottom: no recombination (PD), one recombination event (TT), two recombination events (NPD). c) Process for diploid generation between a lab strain and a natural strain. For a detailed description see main text.

Diploids were created by mixing two strains on EMMlowN solid medium and left for 16h in the 25ºC incubator. After 16h, zygotes have formed, which were streaked on PMG without supplements but with hygromycin. This medium selects for diploids between the lab strain (auxotrophic for leucine and adenine but resistant to hygromycin due to its hphMX marker) and the natural strain (no auxotrophies but sensitive to hygromycin) that are forced to stay together to survive. After 4 days, the diploids form large colonies, which were transferred to a PMG+hygromycin plate to maintain diploids for further analyses (Figure 10c).

Three days before testing for fluorescence, the colonies were transferred to solid EMMlowN 25ºC and incubated for three days to induces sporulation, which results in production of azygotic asci (Hoffman et al. 2015). These colonies were observed under a brightfield microscope to check for sporulation and presence of azygotic asci. Azygotic asci can be recognized because they are completely straight. The colonies that showed the highest number of asci were then selected for data collection using ImageStream.

Data collection with ImageStream

To observe the recombination events between the markers for each of the asci, cells were processed with the Cytek Amnis ImageStream X Mk II Imaging Flow Cytometer, at the Core Facility of Flow Cytometry at the Biomedical Center, Ludwig-Maximilians-Universität München. This machine takes individual images of all particles that pass through the flow. The ImageStream has a wide range of lasers for fluorescence identification, as well as the bright-field (BF) and dark-field (Li et al. 2019). The samples were prepared by transferring cells from EMMlowN into 60µl of sterile H_2O in a 1.5ml Eppendorf tube, making sure the mix was homogeneous and without cell clumps.

○ Data acquisition

Data acquisition was done with the INSPIRE software. In the context of ImageStream, a compensation matrix was generated to correct for spectral overlap between fluorochromes (in our case fluorescent proteins) used in the experiment. Compensation involves measuring the signal for each channel for cells containing a single fluorescent protein and subtract this false positive signal per channel that is due to the emission of other fluorochromes. This allows for accurate quantification of fluorescence of different fluorescent proteins in the same sample. In this experiment, only the channels Ch02 (green, opt. detection: 480-560nm), and Ch04 (red, opt. detection: 595-642 nm) were used for the compensation matrix.

To acquire the data, ImageStream was set at “Slow” flow, and gating and selection of populations was performed to obtain images of asci that showed fluorescence both in channels 02 and 04.

○ Data filtering with IDEAS v6.0

Further filtering of the data was necessary. This was achieved by added gating of the images, selecting for (1) had the correct “rod” shape, (2) were in focus and centered, and (3) had the right intensity in channels 02 and 04. The final filtered images were downloaded for channels 01, 02, 04 and 09.

Sorting real azygotic asci

After obtaining the images from IDEAS, these needed to be further processed in order to be manually scored for quality and recombination events. To handle the large dataset, we applied a machine learning algorithm to preselect images before manual curation. I applied a Convolutional Neural Network (CNN) that was designed by Dr. David Hörl (Human Biology & BioImaging, LMU).

Data pre-processing

The 4-channel ImageStream data were transformed for batched training by cutting the central square region of the images and resizing it to a common shape of 64x64. As we encountered oversaturated columns in the data from one of the fluorescent channels, we set columns with less than 4 unique gray levels to zero.

Data architecture and training

We implemented our CNN model for automatic quality control in PyTorch and PyTorch-Lightning. Our network consists of 4 blocks with 3 convolutional layers followed by ReLU activation each. In each block, all convolutions have the same number of output channels, the first additionally performs downsampling via strided convolution (stride 2). Furthermore, we added residual connections by adding the output of the first convolution to the final output of each block.

After the convolutional blocks, we used adaptive max-pooling to 1x1 and fed the resulting feature vectors through two fully connected layers to reach a final output size of 2. Dropout was performed before each fully connected layer during training.

We used cross entropy loss with class weights inversely proportional to the fraction of good or bad images in the training dataset. The network was trained using Adam and an 85%-15% training-validation split. To prevent a bias of the model towards tetrads with co-localizing fluorescent signals in both channels – which indicates no recombination and makes up a high proportion of the tetrads – we only included the first of the fluorescent channels.

For inference on new data, we kept the checkpoint at the epoch that had the lowest loss on the validation split.

Detection and Matching of Spores

To detect fluorescent spores, we applied a Laplacian-of-Gaussian filter to the images and recorded the two strongest local minima in each channel. The detected spores of the two fluorescent channels were matched into two pairs using linear assignment and distances between the closest and second closest pair were recorded.

Training was done on a compute server equipped with 2 Intel Xeon E5-2680 v4 CPUs, 256GB of RAM and a NVIDIA Tesla V100 GPU. Analysis of the data was done with a smaller computer which was possible due to the small size of the model.

Final images

After processing the individual images generated by the sorting program, this generated a grouped image containing the transmitted light channel, green fluorescence, red fluorescence, and the overlay (Figure 11). These were scored by their quality, according to the transmitted light and green fluorescence channels, and saved in a new folder from highest to lowest quality hit.

After sorting, the 1000 highest ranking pictures were manually scored for the presence of asci with two spores shining in Ch02 and two spores shining in Ch04, and the recombination events counted. For the crosses in which the total of pictures was less than 1000, all pictures were scored.

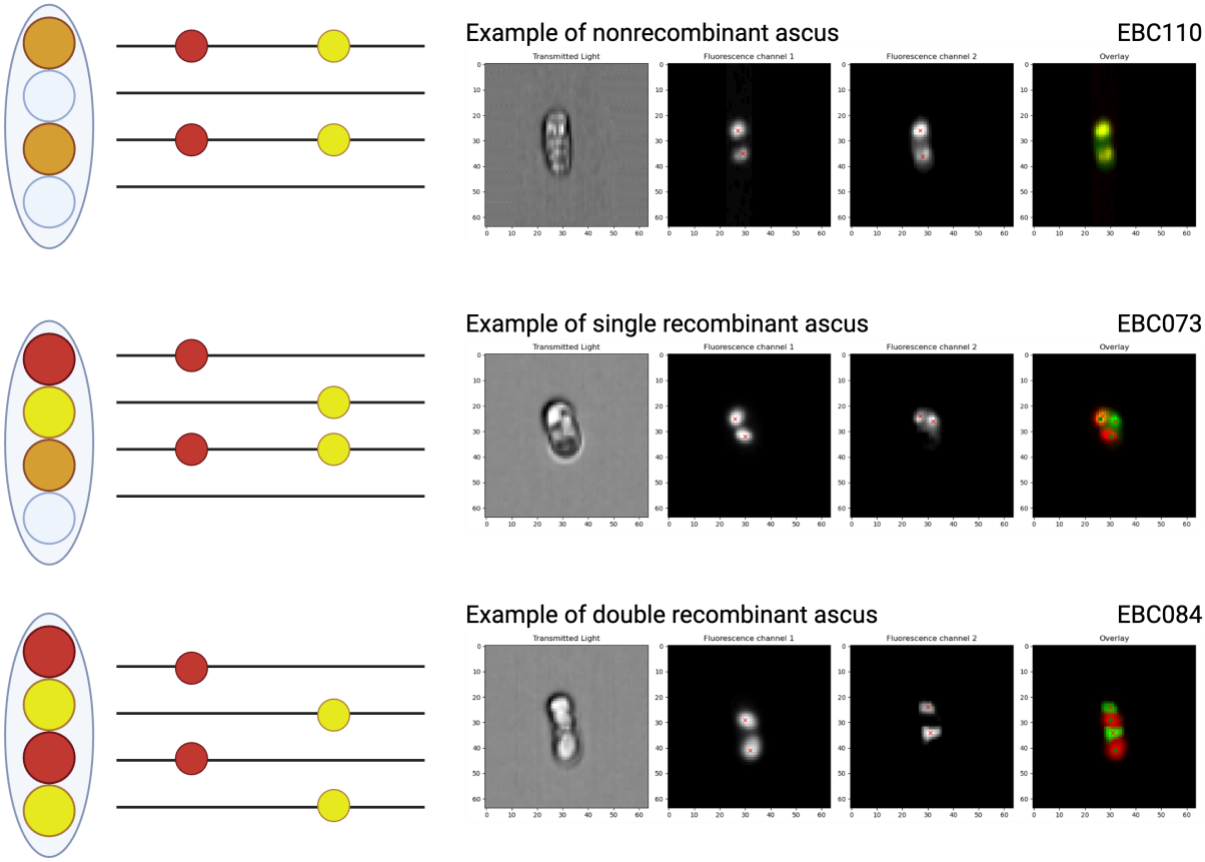

Figure 11. Examples of resulting images after the program. From top to bottom: PD, TT, NPD of three different crosses. These images were scored manually.

Frequencies and map distance calculations

Recombinant and non-recombinant asci were manually counted according to their segregation types. Thee types of tetrads can be scored. Non-recombinants (Parental Ditype), tetrads with one recombination event (Tetratype), and tetrads with two recombination events (Non-Parental Ditype) (represented in Figure 10b) (Perkins 1949).

Using counts for the three tetrad categories, recombination rates between the two markers were calculated using the formula from Perkins, 1949:

$$cM = \frac{6NPD + \mathrm{TT}}{2(PD + NPD + TT)} * 100$$

Where PD: “Parental Ditype”, NPD: “Non-Parental Ditype” and TT: “Tetratype”

Statistical tests, correlations and dataframe manipulation

All statistical tests described in this section were performed with R (version 4.3.2). Dataframe manipulation prior to all statistical tests was done with the “tidyr” and “dplyr” packages in R. Correlations and linear models explained in the Results section were done with base R functions. ANOVA between chromosomal grouping was performed using the “aov” base R function.

3.3.4 Inversions

I analysed the effect of inversions of different sizes when in heterozygosity on gamete viability and their role in recombination rates within the inversions and in the chromosomal regions flanking the inversion breakpoints. For this, I applied tetrad dissections and bulk segregant analyses. To gain further insights into the data and assess robustness, a model was generate to which the data was fitted.

Tetrad dissections

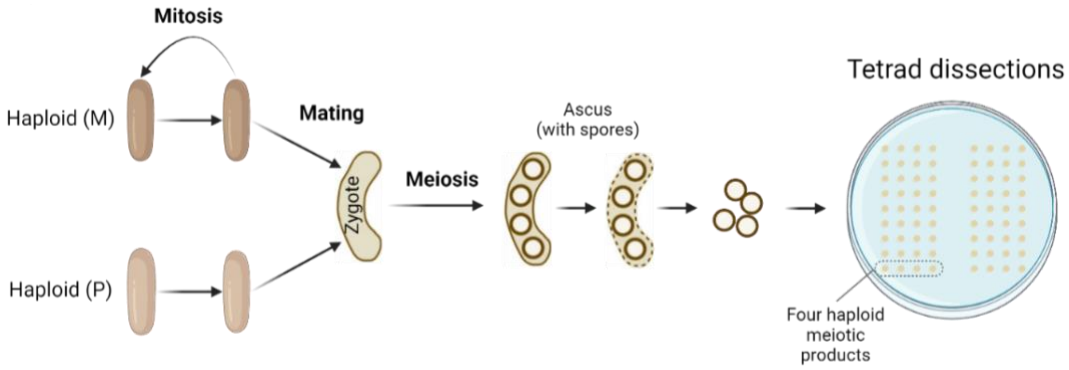

Figure 12. Simplified schematic representation of the fission yeast life cycle, and the steps performed for tetrad dissections

To assess the effect of the inversions on recombination rates, tetrad dissections were performed using the Singer MSM400. A plus strain with an inversion (Figure 4) or the control strain without inversion with the natMX cassette in *his5*, were crossed with a Minus strain containing three markers on the right side of the inversion as indicated in (Figure 4). GFP on II2.34, a *ura4* cassette in II2.52, and mCherry in II2.76. The dissection plates were prepared by pouring 35ml of YES solid medium on 9 cm petri dishes. A small amount

of a cross consisting of a mix of cells and asci was mixed with 50µl of sterile ddH_2O and well suspended. A drop of the mix was added on one side of the petri dish and completely dried before tetrads were isolated. Each tetrad was moved to a location on the grid, after which the plate was incubated at 32°C which induces breakdown of the ascus wall. After 5h, the spores for each tetrad were separated and distributed on the grid. Each plate fits 18 tetrads (schematic in Figure 12). After 4 days, the plates were replica plated onto YES with the antibiotic nourseothricin, G418 or hygromycin to score *natMX*, *kanMX* or *hphMX*, respectively, and PMG-dropout for the *ura4* marker.

Calculation of genetic distances

Genetic distances were calculated with the data obtained from tetrad dissections, using the tetrads for which genotypes of all four spores were known. Calculations were performed implementing the formulas in Perkins (1949) (as described in 0).

Recombination model

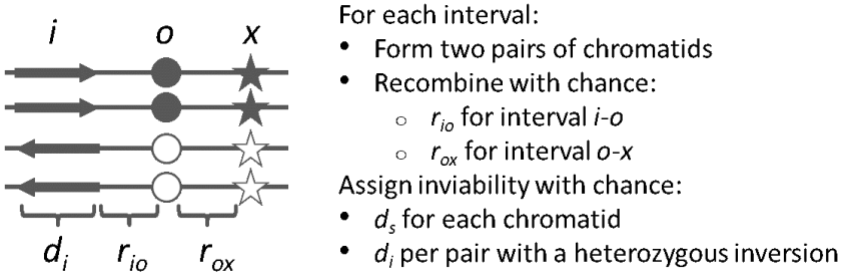

Figure 13. Summary of the simulation model used to fit observations

Genetic distances calculated above depend on the tetrads for which the genotypes for all four spores can be observed. However, especially for crosses with heterozygous inversions many tetrads showed death of two or more spores. To avoid biasing our results by analyzing only surviving tetrads, we modelled the changes in recombination rates caused by the presence of an inversion in heterozygosis. To the data of all observations, including incomplete tetrads, were fitted a model using a maximum-likelihood approach. This model assumes no recombination interference or recombination competition and thus serves as a null model for testing the presence of these effects. This part of the project was performed by Prof. Dirk Metzler (Evolutionary Biology, LMU).

In the model, we call the locus of the inversion i and the marker loci x and o, where o refers to the marker locus closest to i. The initial state is a tetrad with two chromatids that have the inversion and alleles 1 at both loci x and o and two chromatids that do not have the inversion and alleles 0 at the two marker loci. We assume that all three possible recombination events – recombination between x and o, recombination

between o and i, recombination within i – happen independently in the following way: for each interval, the chromatids find each other in two random pairs and each pair recombines independently of the other pair with a certain probability. The probabilities are r_{ox} for recombination between o and x, r_{io} for recombination between i and o and d_i for recombination within the inversion. In the latter case, recombination will lead to death of both chromatids if exactly one of the two has the inversion. Finally, there is a background death probability of d_s for each spore. Note that also the random pairing is independent for the three types of recombination events and any death event happens at the end, such that chromatids that die were not excluded from any possible recombination pairings.

For any given quadruple of parameter values for r_{ox}, r_{io}, d_i and d_s we provide the R script `recombprob.R` (see Supplementary Materials) to calculate the probabilities for all possible tetrads. Further, we provide the R script `recombsim.R` to simulate these outcomes and which is implemented independently from `recombprob.R`, such that the results of the scripts can be checked against each other. We used the `recombprob.R` in combination with the *optim* command in R (with option `method="L-BFGS-B"' for using the method from (Byrd et al. 1995)) to fit the model to various data sets. To test for deviations between the model predictions and the observed frequencies of the different types of tetrads, we applied a parametric bootstrapping approach (Efron and Tibshirani 1993). For this, we simulated 1000 data sets according to the model with the fitted parameters, re-fitted the model to the simulated data and calculated the chi-square statistic of the fit and used as a p value the fraction of the bootstrap repetition for which the chi-square statistic had a greater (or equal) value than for the original data.

Bulk segregant re-sequencing

To obtain a higher resolution of recombination around the inversions, crosses between strains with the inversion and natural isolates were performed. Crosses were incubated for four days, after which presence of asci was confirmed microscopically. The cells were harvested and all unmated cells were killed as described above, to ensure only meiotic spores in the final mix. The surviving spores were germinated overnight in YES at 32°C. This culture was divided into two batches: one third of the mix was transferred into fresh liquid YES medium which act as control, and the other two thirds into liquid YES with nourseothricin (100µg/ml), to select only genotypes with inversion. These fractions ensure a similar number of cells in the two pools, because under Mendelian segregation half of the cells are sensitive to nourseothricin and will die.

After growth to saturation, DNA was extracted from the totality of the cell population using the Quick-DNA Fungal/Bacterial Miniprep Kit (Zymo Research). Libraries were prepared using the Illumina PCR-Free Prep (Illumina) with UDI barcodes from IDT. The samples were sequenced at NovoGene with 150bp

paired-end reads with 450insert size with a mean coverage of 120X. Shortly, the obtained reads were cleaned with trimmomatic v0.38 (Bolger et al. 2014), mapped to the reference genome (Wood et al. 2002) using *bwa-mem* (Li 2013) and variants were called using *bcftools mpileup* (Danecek et al. 2021). The vcf files were processed in R 4.3.2 (R Core Team 2023) using *vcfR* (Knaus and Grünwald 2017). Variants were filtered by quality score and matched to the known variants per strain from Jeffares et al. (2015) after which frequencies of the reference allele were calculated.

Statistical tests

All statistical tests described in this section were performed with R (version 4.3.2). For calculation of statistical differences in germination rates, we performed a Chi-squared test with Yates' continuity correction, with one degree of freedom between each of the pairs. The same test was done to calculate significant differences in recombination events in each interval. A Pearson's Chi-squared test with four degrees of freedom was performed to detect the significant differences between the tetrad patterns among each of the groups. The percentage of spores resistant to nourseothricin from the tetrads with two germinated spores was also calculated with a Chi-squared test with Yates' continuity correction, with one degree of freedom. Statistical differences between the ratios of PD/NPD/T (changes in genetic distances) were calculated with chi-squared tests for goodness of fit with two degrees of freedom.

Data availability

Raw tetrad dissection data, as well as vcf files, primer sequences and plasmid maps in GenBank format are available on figshare under doi:10.6084/m9.figshare.26068201. All scripts used for the analysis and for parameter estimates are available. Files containing the raw reads (Illumina fastq and nanopore fasta) are available at NCBI SRA in BioProject PRJNA1126042 under BioSamples SAMN41919296-SAMN41919305 and SAMN43045027-SAMN43045034.

3.4 FIGURES

All figures were generated with the "ggplot" package in R (versions 4.3.2 and 4.4.0), and statistical analysis for this thesis was generally performed with the package "tidyverse" and with base R functions.

Explanatory figures and graphs were generated and polished with BioRender.com

4 RESULTS

4.1 VARIATION OF RECOMBINATION RATES

The genome of *S. pombe* natural strains shows a recent hybridization event between two ancestral populations, here called Sp and Sk (Tusso et al. 2019). This hybridization is believed to have occurred during the 14th to 16th centuries, coinciding with intercontinental trade, leading to pure strains being found in Europe, Africa, and Asia, while hybrid strains were identified in the Americas (Tusso et al. 2019). The resulting hybridization has significantly increased phenotypic variation among these strains, with recombination rates evolving under both genetic influences and environmental pressures.

Here, I tested the hypothesis that there is recombination variation caused by differences in ancestry. This was done by inserting two fluorescent markers (red and green) in each of the three chromosomes in the reference strain of *S. pombe* (Figure 10a) with promoters that were only activated in the spores, creating a set of six different strains. These were crossed with each of the available natural fission yeast strains, and their tetrads were analysed.

According to literature (Cromie and Smith 2008; Lian et al. 2023) crossovers in *S. pombe* occur throughout most of the genome with nearly uniform intensity of 0.16cM/kb, except for the so-called "K region", between the two silent mating-type loci *mat2* and *mat3,* and within the centromeres, where recombination is well below the genomic average. Using these calculations, the loci analysed in each of the three chromosomes were expected to show a genetic distance of ~18cM in chromosome I (markers in I1.14 and I1.25), ~35cM in chromosome II (markers in II2.52 and II2.76) and ~5cM in chromosome III (markers in III1.29 and III1.32). These values were calculated from crosses within the reference strain (here EBC70/JB22).

4.1.1 Initial data visualization

I assessed variation in recombination rates of 57 natural isolates at three intervals, each at three chromosomes. For each cross, tetrads were scored, and with these values, I calculated the recombination rate expressed in cM implementing the formula from Perkins (1949) (page 43). Data of the genetic distance for each chromosome, in all crosses, shows a varying pattern. The strains in Figure 14 are arranged from lowest to highest recombination in the analysed area. The strains are not arranged in the same order for all chromosomes, which suggests that recombination in one chromosome does not correlate in any way to the other two chromosomes.

Apart from the very noticeable variation in recombination rates, ranging from barely any recombination to the maximum expected recombination between two loci (50cM), there is also an apparent difference in the distribution of recombination rates among the strains. Where in chromosome I and III there is large variation at higher recombination rates, in chromosome II the variation increases gradually. Chromosome I also shows the absolute maxima of recombination rates (Figure 14).

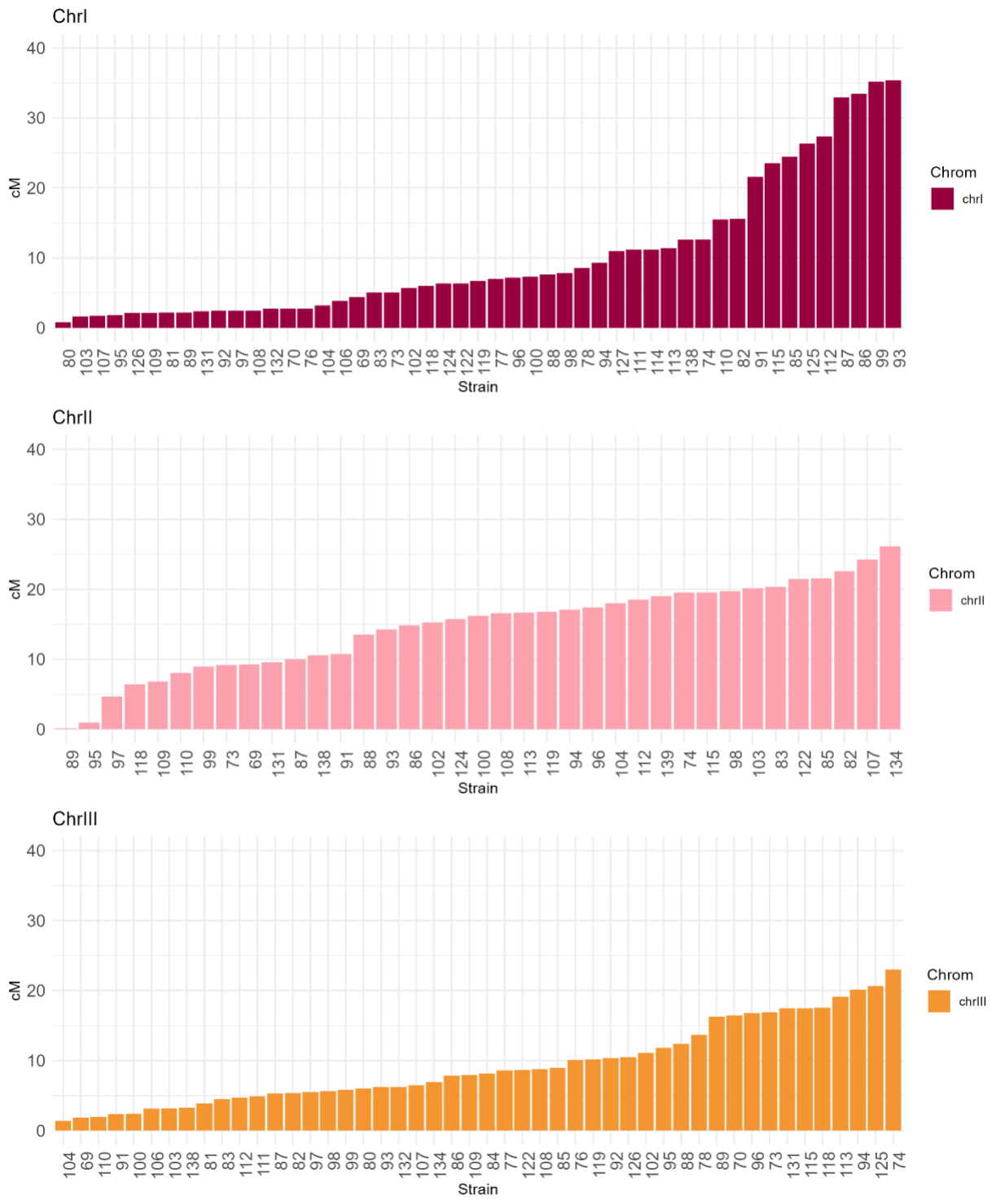

Figure 14. All strains in order from lower to higher recombination rates between the red and green marker, in each of the three chromosomes. From top to bottom, chromosome I, II and III respectively.

Surprisingly, crosses with the reference strain (EBC70) showed recombination rates very different from the expected 0.16cM/kb average. In chromosome I, observed recombination for the measured interval was

2.71cM (expected = ~18cM), and in chromosome III it was 16.42cM (expected = ~5cM). Due to technical difficulties, I was not able to obtain data for chromosome II for the reference strain. Crosses between wild type strains in Li et al. (2019), gave a distance in chromosome III of 1.97 cM, calculated only using the number of visible recombination events:

$$Crossover\ frequency\ (CF) = \frac{Recombination\ events}{Total\ tetrads/2} * 100$$

When calculating the genetic distance in the same manner in our case, the distance in chromosome III for the cross between the two reference strains is 8.9 cM, which is lower, but not as low as the distance found in Li et al. (2019). In their study, though, they used strains where markers were inserted, and that were heterothallic, therefore measuring recombination in zygotic asci. Azygotic asci are known to have higher recombination rates, and the addition of several markers in both strains might have an unknown effect on recombination rates (*Dr. A. Lorenz, personal communication*).

For the rest of the analysis, I used the genetic distances calculated using the formula from Perkins (1949). This is a more precise formula, as it accounts for the complexities of genetic recombination, compensating for multiple crossover events in the same chromatid (Perkins 1949; Gowans 1965). If two crossover events happen in two different pairs of chromatids, they result in NPD, but if they happen in the same two chromatids, they can result in PD, which would look like no recombination occurred. The inclusion of NPD in the formula corrects the underestimation of genetic distance when calculated by number of recombinants, which means there is a reduction of bias, especially in larger distances where multiple crossovers are more likely (Perkins 1949; Gowans 1965; Ma and Mortimer 1983).

The median recombination rate of 6.73 cM, 16.2 cM and 8.05 cM, for chromosomes I, II and III, respectively is also different from the expected distances of 18cM, 38 cM and 5 cM. To make direct comparisons possible between the measurements among the chromosomes which differ in the physical distances between the markers (110.2kb, 240kb, and 26.5kb for chromosome I, II and III respectively), I normalized the map distances by dividing by the physical distance in kb

Table 18. Average genetic distances per kb in each of the three chromosomes

	Chr I	**Chr II**	**Chr III**
average Genetic dist (cM)	10.7	14.6	9.33
physical dist (kb)	110.2	240	26.5
Average cM/kb	0.093	0.061	0.352
Median cM/kb	0.061	0.068	0.304

(Table 18). Chromosome III shows the highest average and median genetic distance, which was expected due to the proximity to the *ade6* hotspot. Chromosome II now shows the lowest recombination and distribution, closely followed by chromosome I (Figure 15, table).

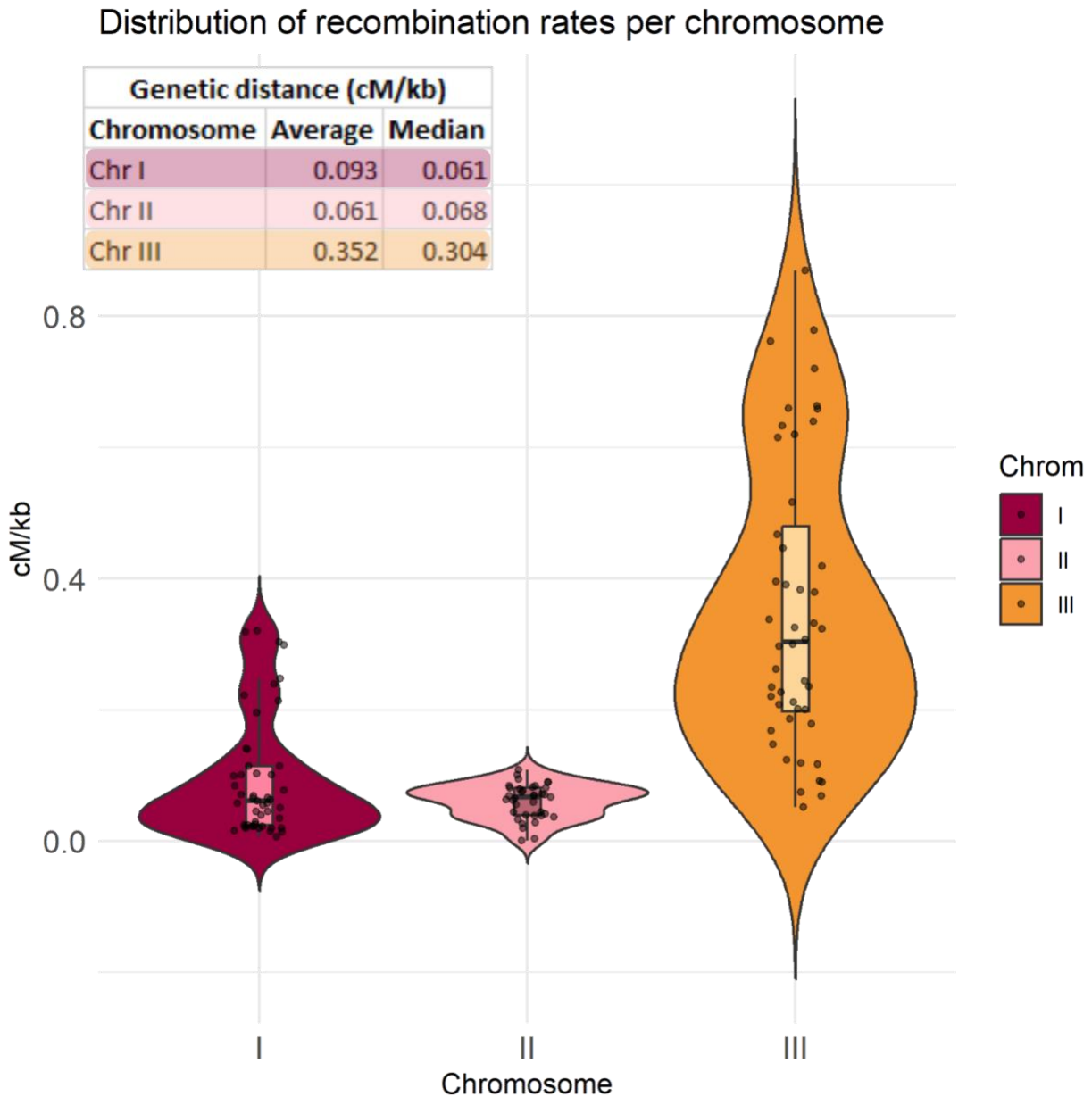

Figure 15. Distribution of strains, according to recombination rate in the analysed locus, per chromosome. On the top left side, a table with the average and median genetic distance (in cM/kb) for each chromosome.

4.1.2 Recombination is variable in the genome

Recombination rate for an interval can be dependent on features of the interval itself (*cis* effect) or be regulated by loci at different locations in the genome (*trans* effect). If recombination changes genome-wide depending on the strain, an increased recombination in the analysed area of any of the three chromosomes would translate to an increased recombination in the other two. In other words, the recombination rates among chromosomes would be correlated.

Table 19. Pearson's correlations between recombination rates (cM/kb), for each chromosome pair. P-value of each comparison in the highlighted cells.

	chrI	**chrII**	**chrIII**
chrI	1	0.1	-0.164
chrII	*0.58*	1	-0.068
chrIII	*0.76*	*0.62*	1

None of the recombination rates are significantly correlated with those at another chromosome. A correlation of -0.164 indicates a weak or very moderate negative relationship between chromosome I and chromosome III (Table 19). There are no positive correlations, which suggests recombination rate does not appear to be regulated at a genome wide level (Figure 16). If anything, the correlation indicates a negative relationship for all three chromosomes, however these are all non-significant (Table 19). From this analysis, I conclude that recombination is not regulated at the strain level.

]

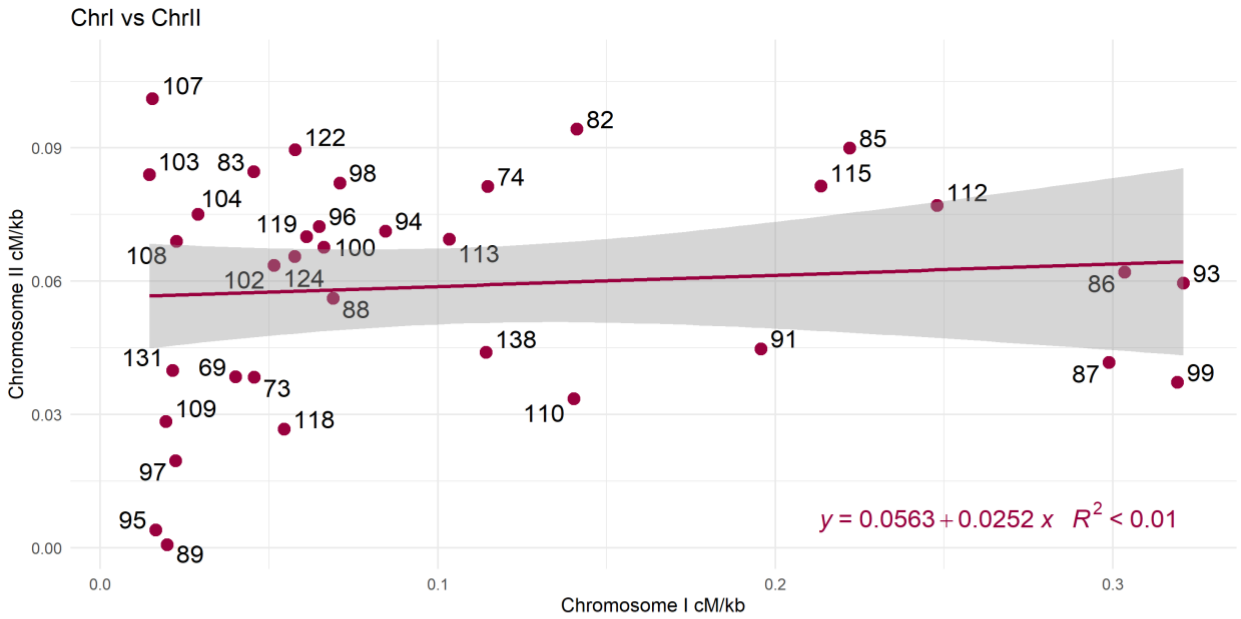
ChrI vs ChrII
Chromosome II cM/kb
Chromosome I cM/kb
0.00
0.03
0.06
0.09
0.0
0.1
0.2
0.3
107
122
82
85
103
83
98
74
115
112
104
119
96
94
108
100
113
102
124
88
86
93
138
91
131
69
73
87
99
109
118
110
97
95
89
y = 0.0563 + 0.0252 x R² < 0.01

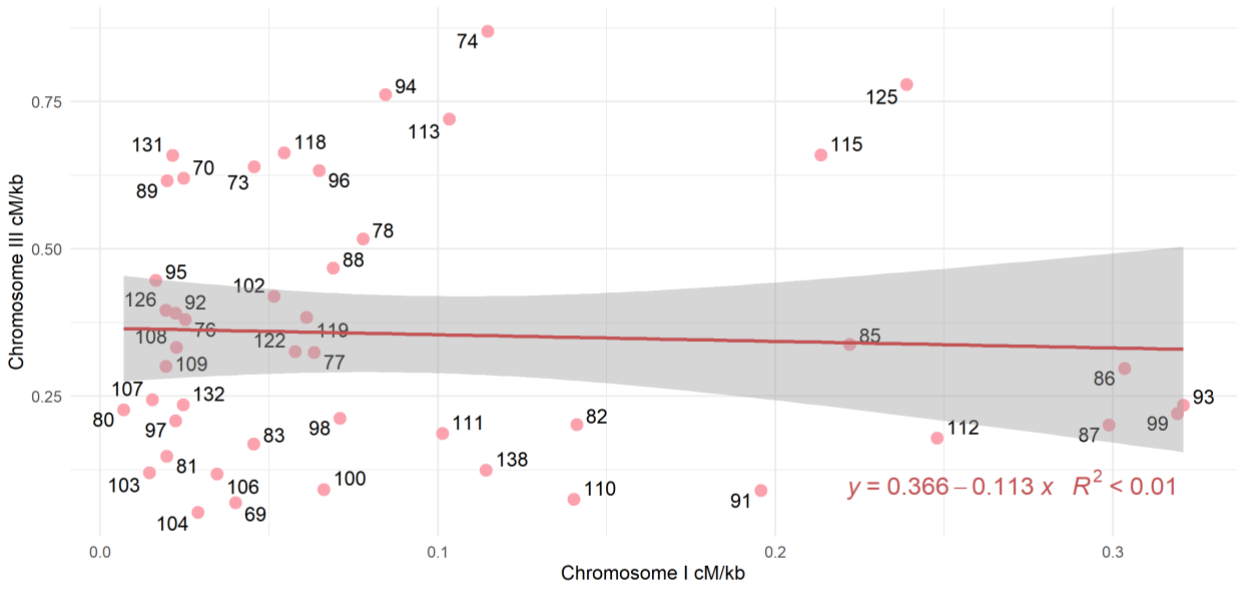
ChrI vs ChrIII
Chromosome III cM/kb
Chromosome I cM/kb
0.00
0.25
0.50
0.75
0.0
0.1
0.2
0.3
74
94
125
113
131
118
115
70
73
96
89
78
88
95
102
126
92
108
76
122
119
85
77
109
86
107
132
93
80
97
83
98
111
82
112
87
99
81
138
103
106
100
110
91
69
104
y = 0.366 − 0.113 x R² < 0.01

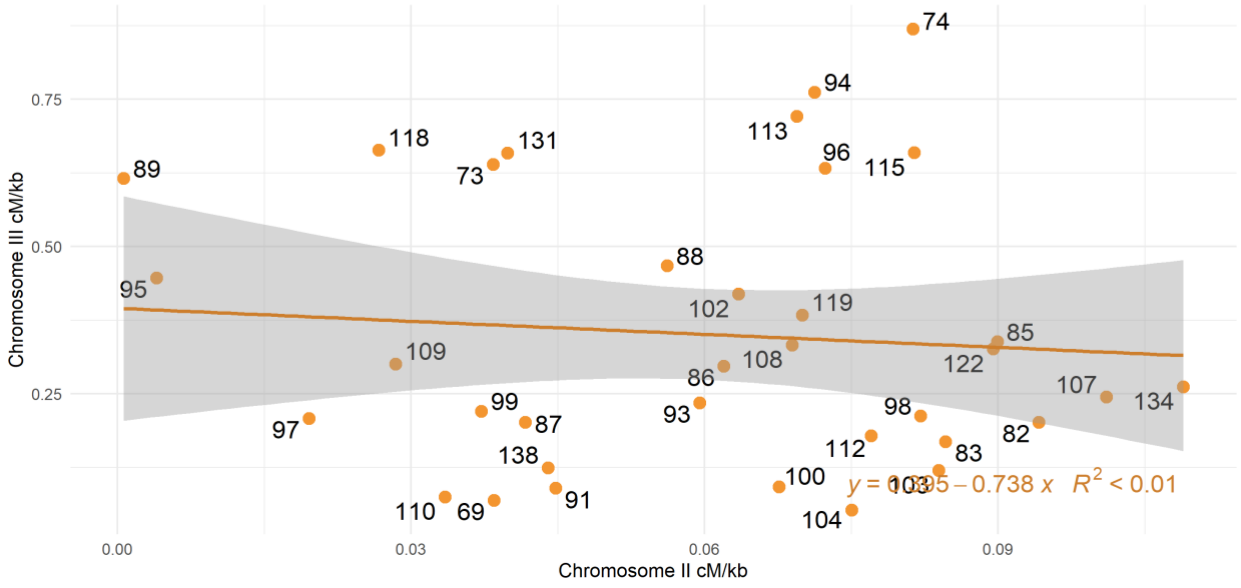
ChrII vs ChrIII
Chromosome III cM/kb
Chromosome II cM/kb
0.00
0.25
0.50
0.75
0.00
0.03
0.06
0.09
74
94
118
131
113
73
96
115
89
88
95
102
119
85
109
108
122
86
107
134
93
99
87
98
97
82
138
112
83
91
100
110
69
104
y = 0.395 − 0.738 x R² < 0.01

Figure 16. Correlations between pairs of chromosomes. a) linear model between chromosome I and II. b) linear model between chromosome I and III. c) linear model between chromosome II and III.

4.1.3 Differences in recombination rates are not directly affected by hybridization blocks

To test whether recombination rate variation observed among the strains depends on divergence between the strains, I asses if recombination depends on the ancestral origin of the intervals. As described above, two ancestral fission yeast populations hybridized and most current natural strains descend from that cross (Tusso et al. 2019). Using the inferred ancestry (Sp or Sk) of the genomic overlapping windows generated in that study, I could infer whether recombination depended on the percentage of Sp or Sk found at various genetic levels. The reference strain is almost 100% Sp, so the expectations were that a higher percentage of Sp in the natural strain used for the cross would correlated with a higher recombination rate. This expectation is based on the observation that increased divergence between homologous DNA sequences has been shown to cause a decline in recombination (Greig et al. 2003; Jeffries et al. 2021b). In some cases, even a single diverging nucleotide inhibited recombination (Claverys and Lacks 1986; Datta et al. 1997). This shows genomes become incompatible not only because of structural rearrangements, but also at a sequence level. Crossover blockages can be caused by incompatibilities in the mismatch repair system, which has a disproportionately large effect on inhibiting crossing-over and conversion between sequences with low divergence (Greig et al. 2003; Opperman et al. 2004).

The unusually high recombination rates of *S. pombe* reference strain, compared to other studied organisms, could be caused by the lack of sequence divergence, and might be lower when the cells cross with a more diverged strain. Local changes in recombination rates, as measured in this section, are unlikely to be caused by overall background differences in ancestry, as there was no correlation in recombination among the chromosomes (Figure 16). They are more likely affected by local changes in ancestry around and within the measured interval. In this section, I analyse both the *cis* and background effects of strain ancestry in recombination rate variation.

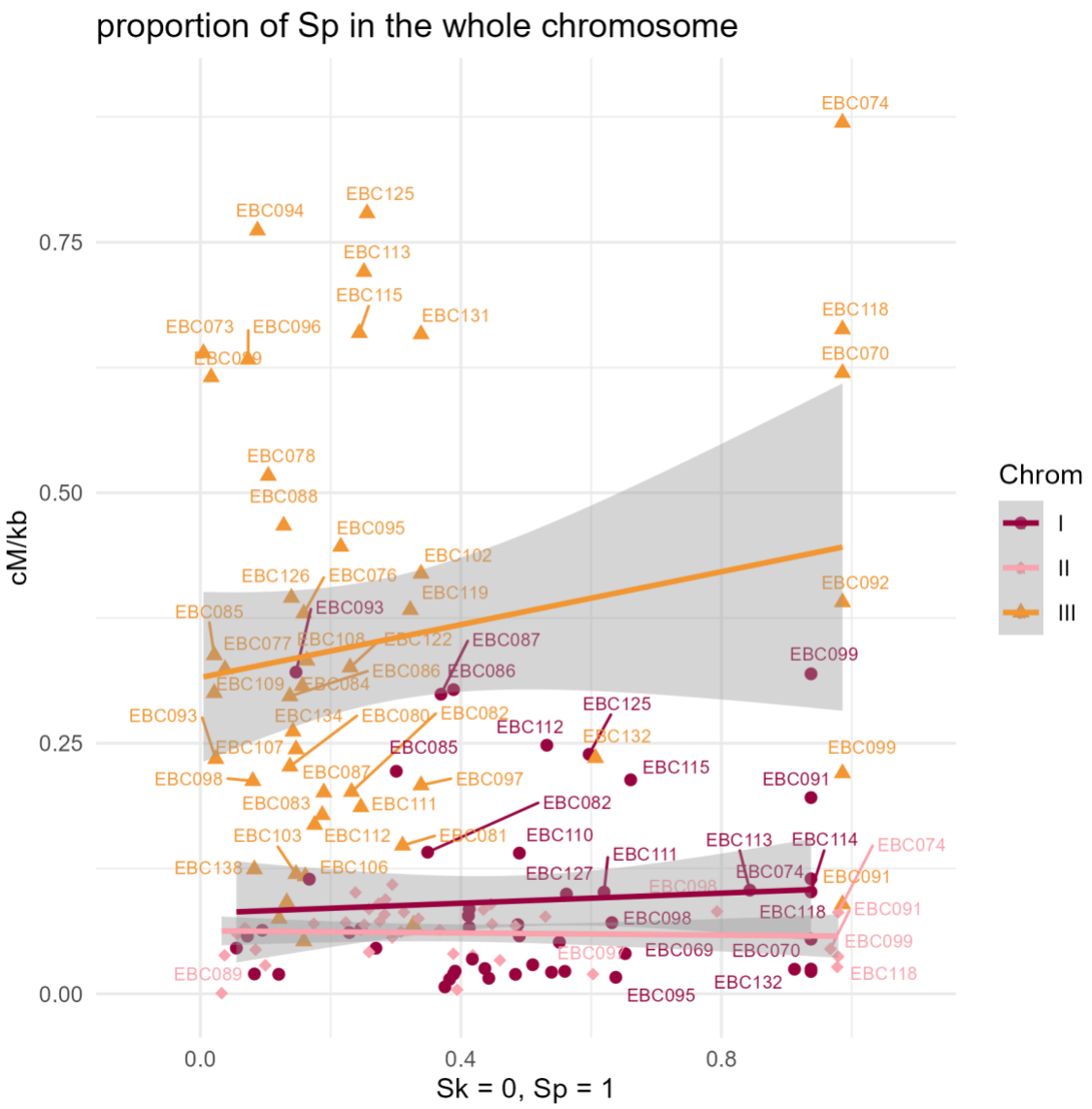

Figure 17. Scatter plot with the average of Sp in each chromosome, per strain, correlated to the calculated cM/kb. Linear model included per chromosomal group. Kendall's tau calculated per chromosomal group. Chromosome I: tau = 0.08 p-value = 0.43, Chromosome II: tau = -0.001 p-value = 0.98, Chromosome III: tau = 0.02 p-value = 0.8.

An initial analysis of the percentage of "Sp" in the whole analysed chromosome, as expected, showed no relationship with recombination rates (non-parametric Kendall's Tau test p>0.43; (Figure 17).

To find whether the ancestry affects the recombination rates locally, I performed the same analysis but only using the genetic windows contained within the two fluorescent markers (Figure 18). Due to the two markers being close in physical distance and the recent occurrence of hybridization which has not yet allowed for the mixing of ancestral sequences over shorter distances, in almost all strains the percentage of ancestral DNA in that window is either 100% Sk or 100% Sp. Again, no relation between the fraction Sp and recombination rates was observed (Kendall's Tau test; p>0.12).

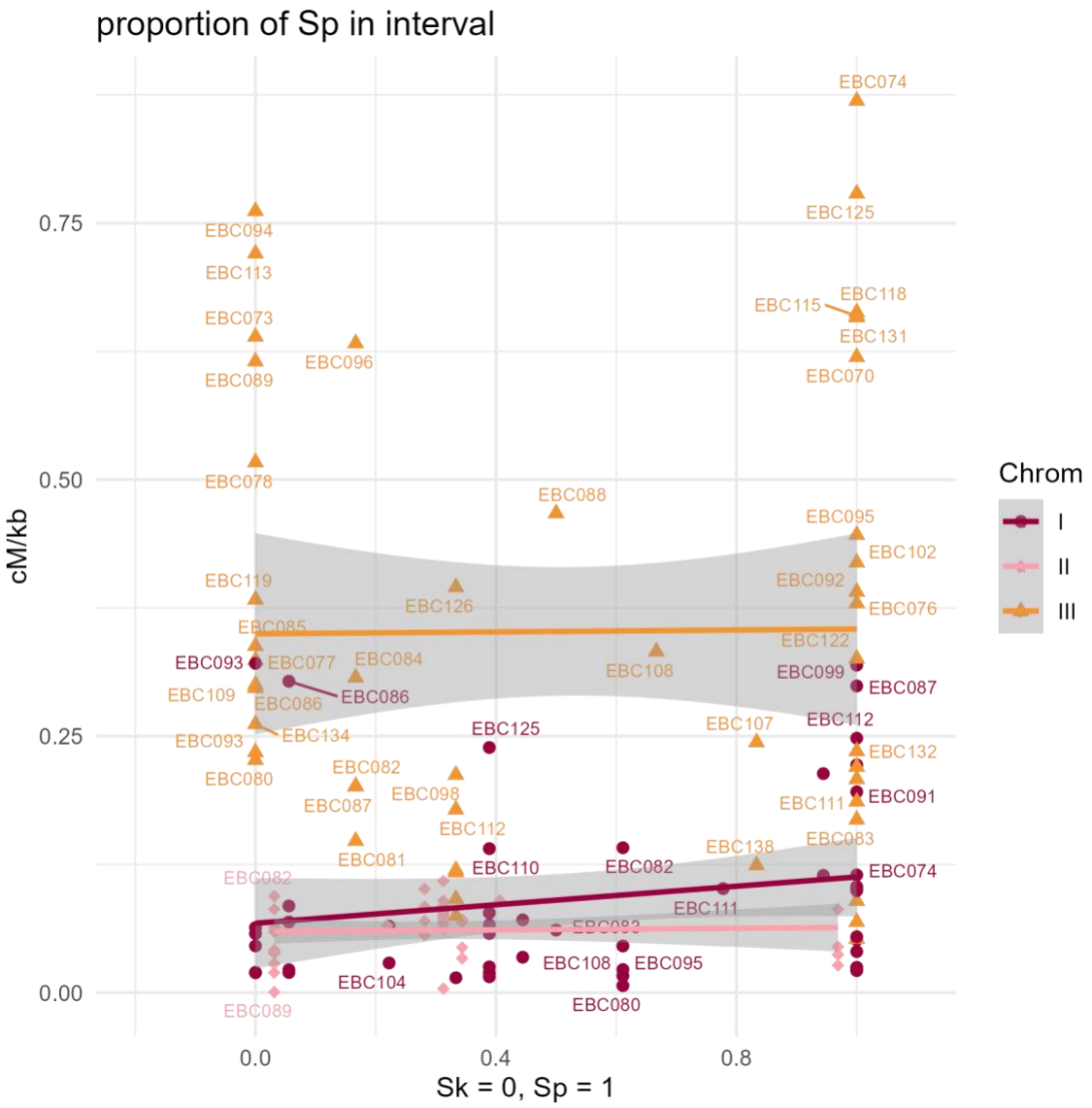

Figure 18. Percentage of Sp (red) within the interval between the two markers in each strain and chromosome, compared to the recombination rate in that area, expressed in cM/kb. Linear model included per chromosomal group. Chromosomes indicated by colour. Kendall's tau calculated per chromosomal group. Chromosome I: tau = 0.16 p-value = 0.12. Chromosome II: tau = 0.12 p-value = 0.33. Chromosome III: tau = -0.06 p-value = 0.56.

Recombination machinery predominantly attaches to specific regions of the genome, such as intergenic regions, open chromatin areas, and replication fork barriers. The recombination process begins with DSB formation at these hotspots and proceeds through a series of well-coordinated steps leading to crossovers. The distance between where the recombination machinery binds and where crossovers occur, typically spans from a few hundred to a few thousand base pairs, depending on the genomic context and the specific proteins involved. Therefore, I also repeated the analysis using the average percentage of Sp extending the analysed interval beyond the two markers by a small window of ~22 kb on each side (Figure 19). Also in

the wider interval, no significant correlation between the recombination rates and the ancestral block where recombination happens was observed (Kendall's Tau test; p>0.13).

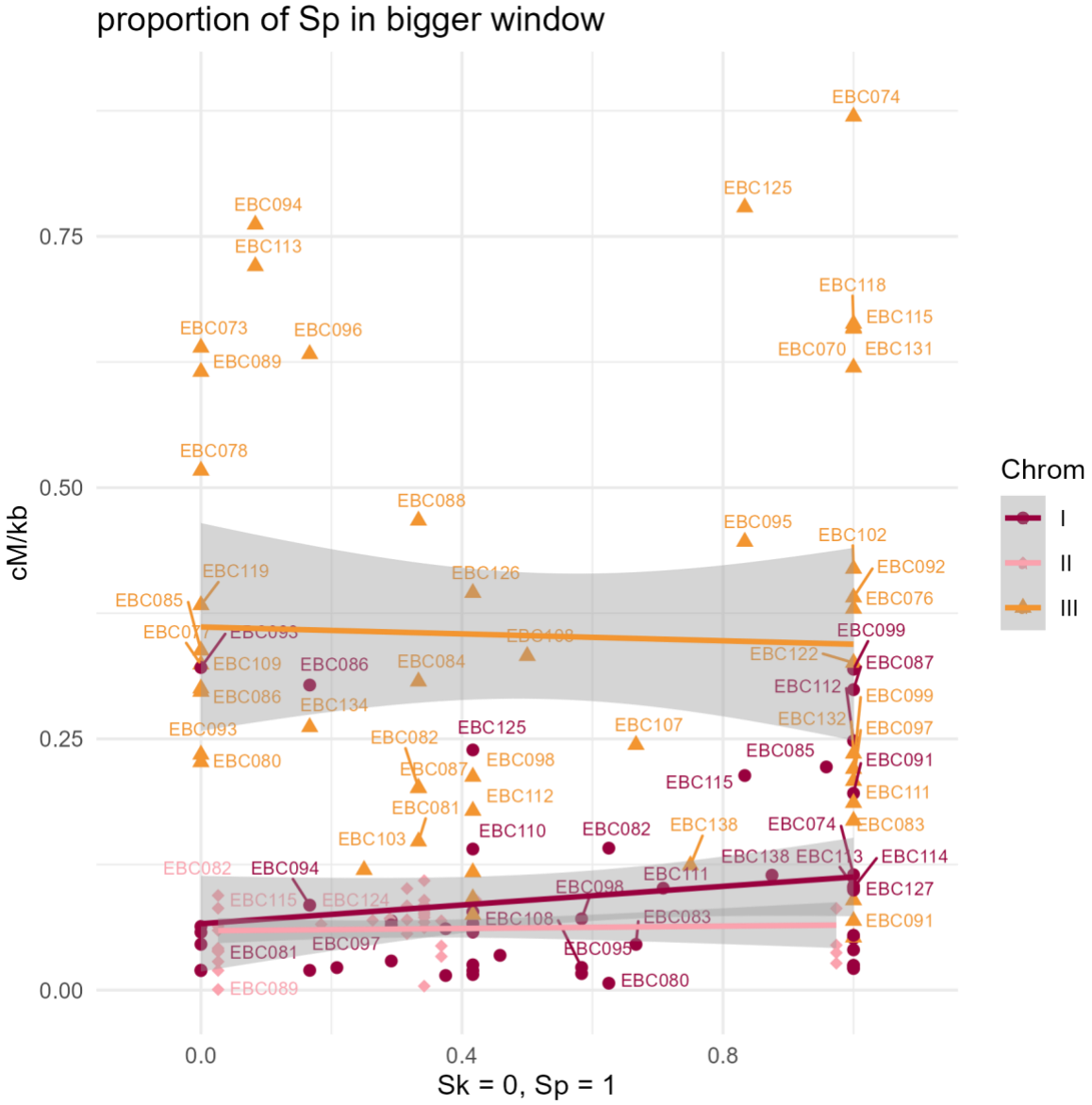

Figure 19. Scatter plot comparing proportion of Sp in the analysed locus, with a window of ~22kb extra on each side, and recombination rate expressed in cM/kb. Linear model included per chromosomal group. Kendall's tau calculated per chromosomal group. Chromosome I: tau = 0.156 p-value = 0.13. Chromosome II: tau = 0.14 p-value = 0.24. Chromosome III: tau = -0.08 p-value = 0.43.

These analyses suggest that recombination is affected by something completely different from the hypothesized ancestral divergence.

4.1.4 Data quality does not correlate with similarity between crossed strains

Some strains have higher crossing compatibility than others. These range from strains that are ancestrally similar to the *S. pombe* that is widely used in research, to strains that are very diverged. To rule out that the lack of correlation was caused by imaging quality, I tested if variation in quality is associated with the recombination rate.

Of all images taken with the ImageStream, even after the double filtering with the IDEAS software and AI supported asci sorting, a certain amount of images were unusable. Due to the labour intensity of the manual curation of the data, a maximum of 1000 pictures were checked for each cross. Those were the highest quality ones. However, each cross presented a varying amount of usable pictures within the first 1000 ones. After the filtering with IDEAS software, some crosses presented less than 1000 pictures for scoring. The difference in the initial amount of data can introduce biases in the quality as calculated here, as by definition there is a higher probability of finding 1000 good images if the total are 20,000, than if the total are 1500.

The cause of the difference in quality of the crosses could be due to biological reasons. Worse sporulation rates in some strains could lead to lower quality in the final images due to the lower proportion of asci, which would mean that the quality of the data correlates with the strain. These differences were hypothesized to be caused by the percentage of ancestral similarity between the two strains in the cross.

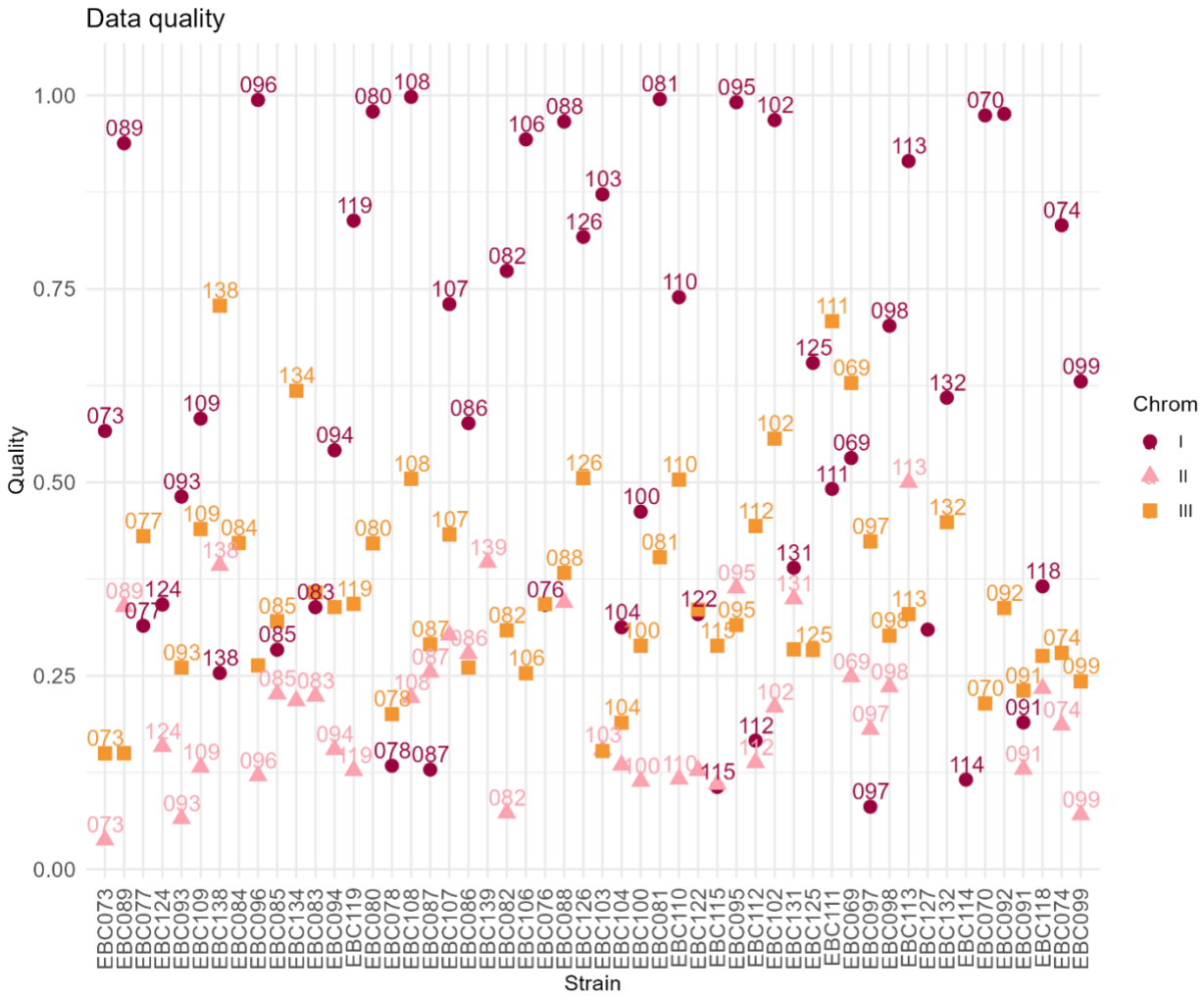

Figure 20. Quality of the sample versus strain number. Quality is calculated by the proportion of good pictures in the total analysed pictures per strain (usually first 1000). The strains in this graph are in order of Sp percentage in the total strain. From left (most Sk) to right (most Sp).

I analysed if quality might affect the calculated recombination rates. I found no correlation between the strain and the quality of the obtained data –expressed as the fraction of useful images in the top 1000 ranked images. Instead, it seems like chromosomes group together and the sample quality is correlated with the chromosome. Chromosome I seems to group in higher quality levels than II and III. The strains in Figure 20 are ordered from the lowest percentage of Sp in the genome (left) to the highest percentage (right). If the level of similarity between the crossed strains was correlated with the quality of the obtained data, there would be an increase in quality with the increase in Sp percentage in the genome.

An ANOVA comparing the effect of the strain and the chromosome, as well as their interaction on the quality of the data, shows that there is no effect of strain (p-value = 0.9), or effect of the interaction between the strain and the chromosome (p-value = 0.08). There is, however, a significant effect of the chromosome

on data quality (p – value = 1.18^{-13}). After performing a Tukey post-hoc correction among the chromosomes, all three chromosomes are significantly different from each other (Figure 21).

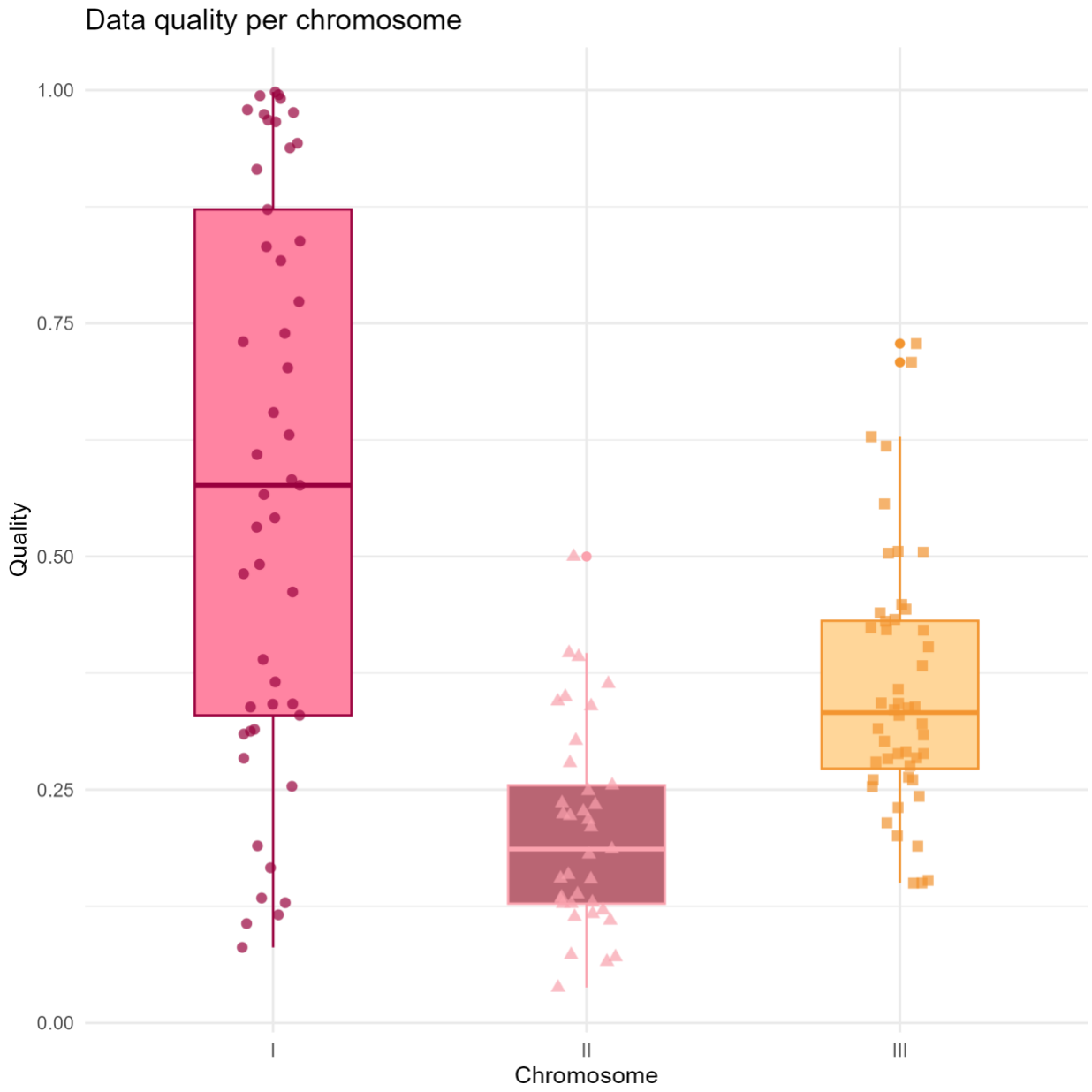

Figure 21. Plotted quality of the samples against each of the three chromosomes. Significant difference in the media between the three groups.

This analysis rejects the hypothesis of biology having an effect on the quality of the images. Rather than some inherent biological quality of the strains, related to ancestry or allelic differences, it seems like there is an effect of the chromosome that contains the fluorescent markers. There could be an effect of the fluorescent markers because of (i) the area of the genome where they are. They could affect sporulation or

reproduction in some way by breaking the promoter of an important gene for gamete formation. Even though the insertion loci were chosen so no gene would be truncated, intergenic spaces can also affect fitness in unexpected ways. (ii) Partial inactivation of the inserted genes that leaves some tetrads without fluorescence. (iii) Differences in promoters. While the same set of promoters was used in all inserts, they were not in the same promoter-fluorescent protein combination, which could affect the quality of the images.

Another possibility is that the effect was caused by the moment of measurement. The measurements and pictures per chromosome were taken in different batches and different numbers of images were taken per strain. In general, the total amount of pictures in chromosome I crosses was much larger than in chromosomes II and III. This would imply that the total of usable pictures with good tetrads would also be lower. This result reflects the effort in total data capture, which was highest for chromosome I and lowest for Chromosome II. However, also within each chromosome, no correlation is observed between quality and recombination rate. Even the grouping itself could have an effect in the crosses. In any case, after grouping by chromosome, there was no correlation between the quality of the images in each cross and the recombination rates, so I conclude that the effect is negligible. For future research, it is important to maintain a high total number of images when measuring the crosses, which allows for a higher total number of usable tetrads.

Seeing the high variability between recombination rates in the same locus (Figure 14), and the high variation in quality within strain (Figure 20, Figure 21), it is apparent that recombination rates are affected by some internal cellular changes. In this experiments, the yeast was maintained at all times in a controlled environment, and therefore I assume that changes in recombination due to environmental cues can be considered negligible. I have found no correlation between the analysed parameters, neither in longer distances (chromosomal level) nor in short distances (locus level/cis effects), and not by the quality of the images. These results open the possibilities for further research in recombination rate variation, in the search of the effect of diverse genetic qualities in recombination rates.

4.2 DIRECT SELECTION ON RECOMBINATION RATES ALTERS THE RECOMBINATION LANDSCAPE IN FISSION YEAST

While heritability of recombination rates has been shown to exist many times, as explained in the general introduction of this manuscript, the possibility of its evolution under direct selection has not been researched

extensively (but see Charlesworth 1976). To discover how evolvable recombination rate is, we need to understand the potential response to direct selection. For this reason, I designed an evolution experiment in which repeated selection is performed for different allele combinations. In the experiment described in this section, repeated selection either for recombinant offspring, or non-recombinant offspring in the different lines is expected to change recombination rates within these experimental lines, and generate either a novel hotspot or a novel coldspot in the region.

4.2.1 Recombination responds to direct selection

To assess whether recombination rates changed over time, I analysed if the number of recombinants over time follow the expected changes over the course of the evolution experiment (Figure 22). During selection, each generation two haplotypes are maintained, but due to recombination all eight different haplotypes are generated again which are observed after germination before growth. If increased or decreased linkage arises, the two selected haplotypes would gradually increase their frequency in the total population over the course of the evolution experiment. The two selected haplotypes chosen as example in the figure are BRn and nnG.

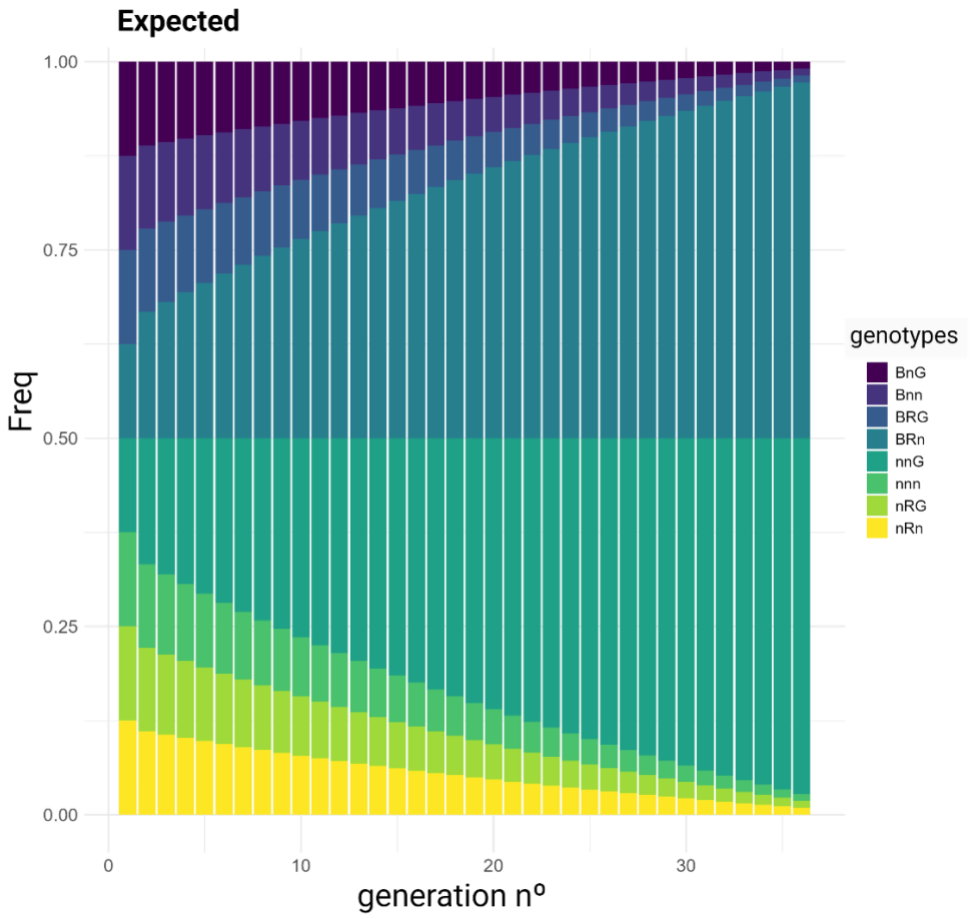

Figure 22. Simplified expectations at the end of the evolution experiment, using ChrI Coldspot as an example. Representation of selection for haplotypes BRn and nnG over the generations.

I started this experiment with four different selective regimes, two hotspots and two coldspots. Short Hotspot, where there was selection for recombinants exclusively in the first interval, Long Hotspot, where there was selection of double recombinants in each generation, Chromosome 1 (Chr1) Coldspot where there was selection for non-recombinants in chromosome I, and Mating Type Associated (MTA) coldspot, where there was selection for non-recombinants around the mating type locus. Hotspots 1 and 2, and coldspot 1 have the markers in chromosome I, while the MTA coldspot has the markers in chromosome II. Together with the selected lines, controls were performed to assess how recombination might evolve without selection for recombinants. Initially, each generation the first 100,000 cells were selected. However, over the course of the experiment fitness effects of marker combinations resulted in near loss of fluorescent markers. The regime was changed, selecting for the same number of cells for each individual marker (details in materials and methods). Note that Hotspots 1 and 2 share the same control (Hotspots control), as they were started from the same two ancestral strains.

Adaptation of Coldspots' haplotypes along the generations

In ChrI Coldspot, where I selected always for the same two haplotypes (BnG and nRn) with markers on chromsome I, there is an immediate increase in these two haplotypes in the first generation, followed by a stabilisation throughout the whole experiment (Figure 23). These two reach an apparent maximum. This is in contrast with its control, which towards the end has balanced haplotype frequencies.

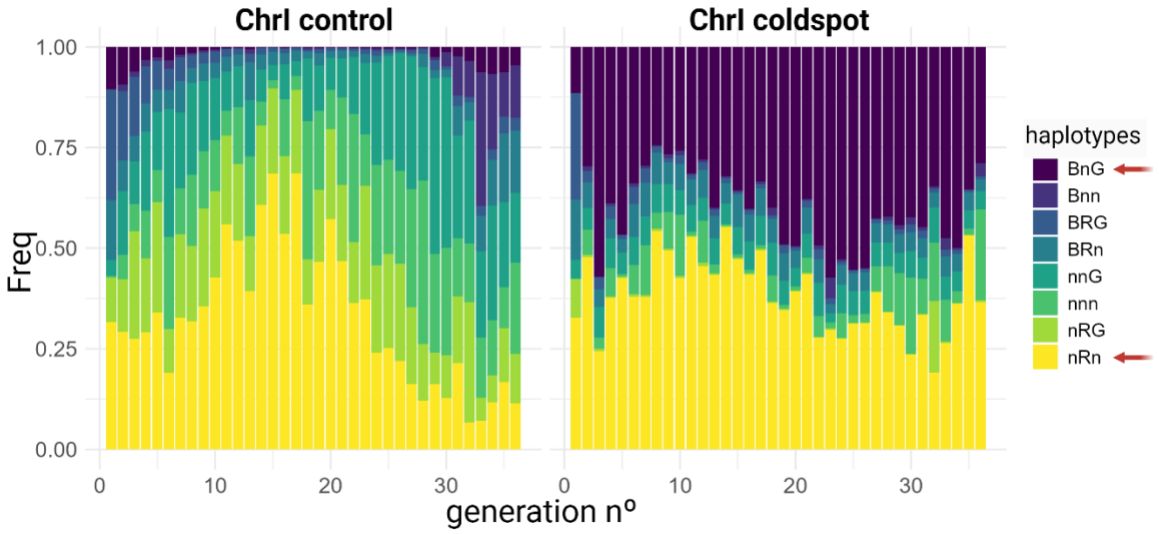

Figure 23. Mean proportions for 6 replicate populations of each of the eight haplotypes along the generations for ChrI coldspot and ChrI control. Selected haplotypes indicated with red arrows

MTA Coldspot, in which selection for the markers (BRn and nnG) on chromosome II, with one of the markers linked to the mating type, shows a very stable presence of the two selected haplotypes from start to finish of the experiment (Figure 24). In this treatment, there is also more stability in the control for all haplotypes. The slower increase in the proportion of selected haplotypes, compared to the ChrI coldspot, was also expected in this selection regime, as in this case the fluorescent haplotypes are related to the mating type. Here, the selected haplotypes are always going to be crossed against each other. In the other regimes, 50% of the parental haplotypes will come from two parental cells that already had the same fluorescent haplotype, and therefore these recombination events are not selected against, nor can they be observed.

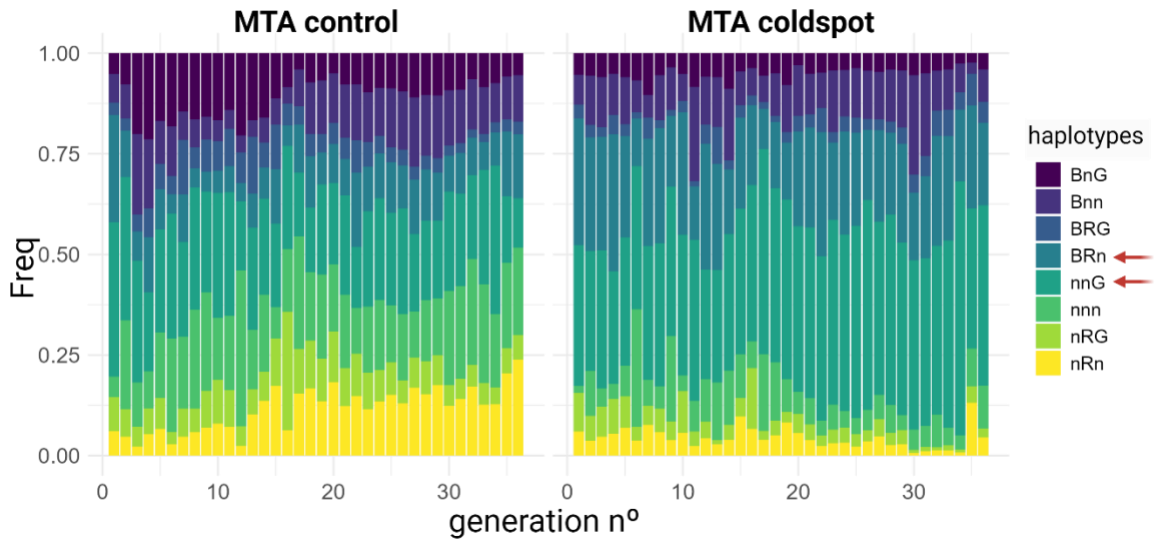

Figure 24. Mean proportions for 6 replicate populations of each of the eight haplotypes along the generations for MTA coldspot and MTA control. Selected haplotypes indicated with red arrows.

Adaptation of Hotspots' haplotypes along the generations

An important distinction between the two hotspots and the two coldspots is that in the hotspots, the two selected haplotypes were switched every week, in order to select only for recombinant offspring. In the case of the short hotspot there was selection for recombination exclusively in the first interval, and in the case of the long hotspot there was selection for double recombinants – cells that had recombined both in the first and second interval. For clarity, the odd and even generations are separated for the hotspots and their control (Figure 25 and Figure 26).

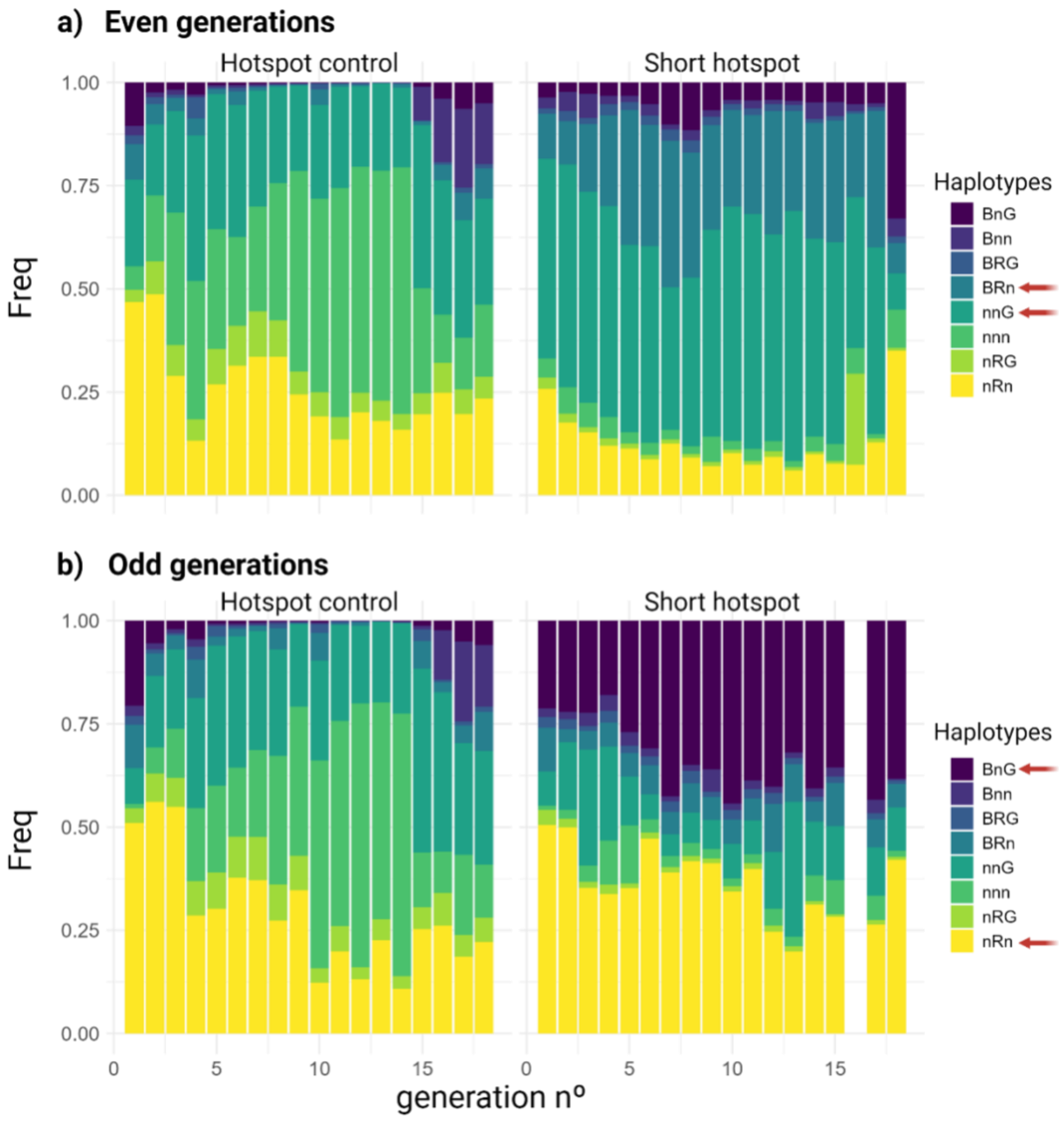

Figure 25. Mean proportions for 6 replicate populations of each of the eight different haplotypes along the generations, for hotspot Control (left) and Short hotspot (right). The generations are separated between odd (a) and even (b) because we switched the selected haplotypes, as to select for recombinants. Selected haplotypes signalled with red arrows. Note that one week of data is missing for short hotspot.

In Figure 25, controls (left panels) both odd and even generations show a very similar pattern because no selection occurred at either week. The two figures for short hotspot (Figure 25, right panels) show a strikingly different pattern, as the selection was different for even and odd weeks. Note that the two haplotypes selected for in odd generations (BRn and nnG) will be more abundant in even generations, and the two haplotypes selected for in even generations (nRn and BnG) will be more abundant in odd generations, as the linkage between the used markers guarantees a higher proportion of non-recombinant haplotypes. If recombination increased, after selection, more recombinant haplotypes would be expected to arise over the course of the experiment, gradually reducing LD.

However, LD does not show a clear decrease through the weeks. There is a stabilisation of the haplotypes, but not a visible increase in total recombinants. The same patterns are visible for long hotspot (Figure 26, right panels).

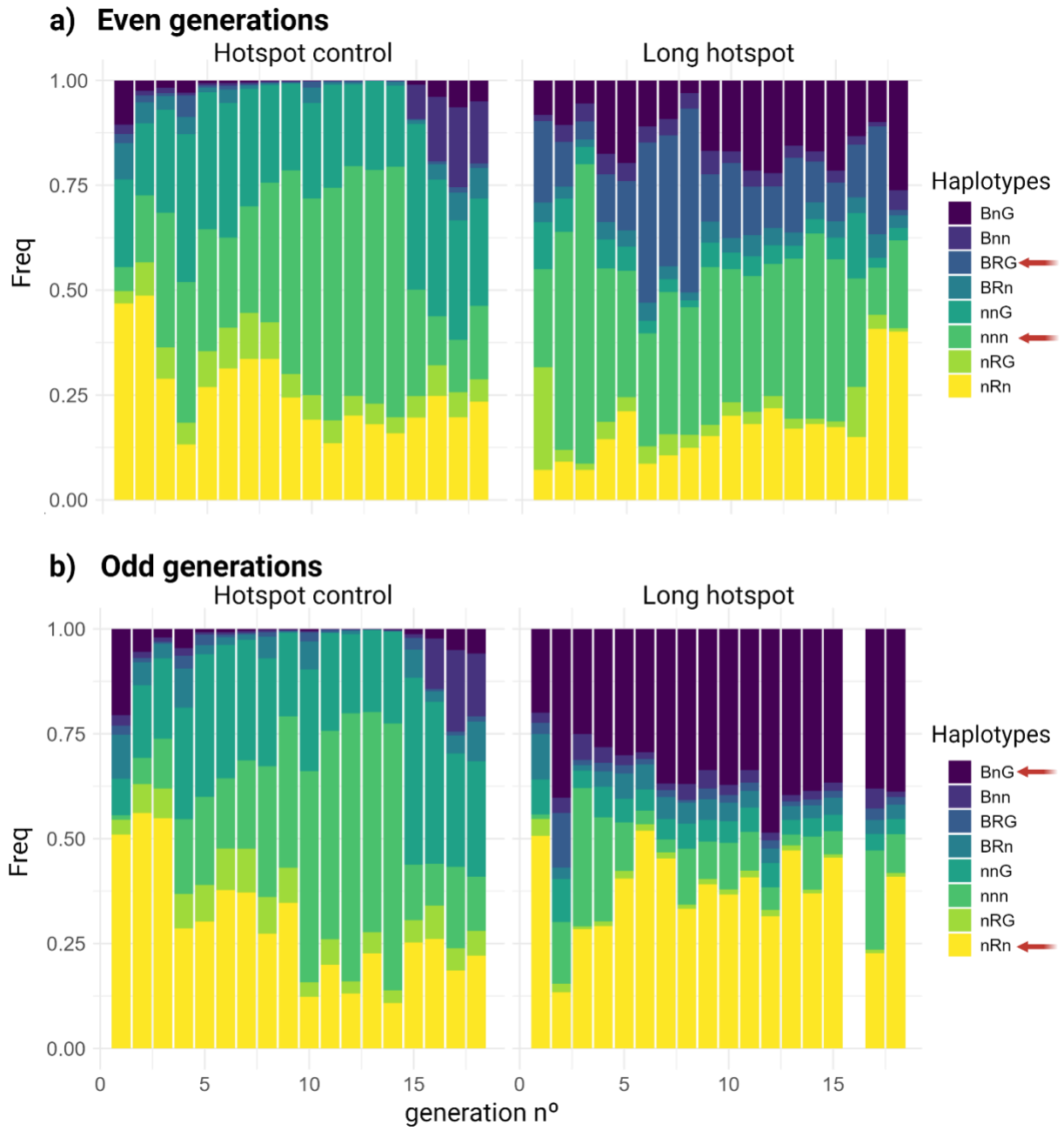

Figure 26. Mean proportions for 6 replicate populations of each of the eight different haplotypes along the generations, for hotspots control and long hotspot. The generations are separated between odd (a) and even (b) because I switched the selected haplotypes in each alternate generation, to select for recombinants. Note that one week of data is missing for long hotspot.

The controls for both hotspots and ChrI coldspot show an almost complete disappearance of certain haplotypes in the population that contain the tagBPF marker. This appears to be a noticeable effect of the fluorescent markers on the vegetative fitness of the cell. To maintain all markers, but without selecting for any genotypes we changed selection to maintain equal allele frequencies per locus as explained in the materials and methods. The fitness effect of the fluorescence proteins might also explain the changes in frequencies among some haplotypes in the selected treatments (both hotspots and chrI coldspot), as the non-selected haplotypes of "coupled haplotypes" are expected to always have the same proportions to one another. Additionally, if all markers were neutral, the two selected haplotypes should have the same proportion in the population, which is not always the case (see selected haplotypes especially in Figure 24b – MTA coldspot, Figure 25– short hotspot, and Figure 26 – long hotspot). I will discuss this in further sections.

4.2.2 Recombination landscape changes, but not always in the expected direction

To analyse if recombination rates changes relative to the ancestor, over the course of the evolution experiment, I performed a well controlled measurement over one or two full cycles for all lines.

In addition to the evolved strains and their controls, I added for each treatment six replicates of a cross between the unevolved ancestral strains: EBC675 x EBC746 for the two hotspots, EBC687 x EBC663 for the ChrI coldspot and EBC819 x EBC787 for the MTA coldspot. These were added for direct comparison of recombination rates between the original strains and the evolved strains. The results varied greatly for each of the treatments.

The expected frequencies in the offspring, when crossing two haploid parentals that are heterozygous at three loci under random mating, can be calculated as follows:

$\underline{Original}$:

$$\boldsymbol{freq(nRn) = freq(BnG) = \frac{1}{2}}$$

$\underline{Expected\ offspring}$:

$$\boldsymbol{freq(nRn) = freq(BnG) = \frac{1}{2} * (1 - r1) * (1 - r2)}$$

$$\boldsymbol{freq(BRn) = freq(nnG) = \frac{1}{2} * r1 * (1 - r2)}$$

$$\boldsymbol{freq(nRG) = freq(Bnn) = \frac{1}{2} * (1 - r1) * r2}$$

$$\boldsymbol{freq(nnn) = freq(BRG)} = \frac{1}{2} * r1 * r2$$

where $r1$ and $r2$ are the recombination proportions in the first and second intervals, respectively (Figure 27). The proportion of total recombination in the whole interval is represented as r.

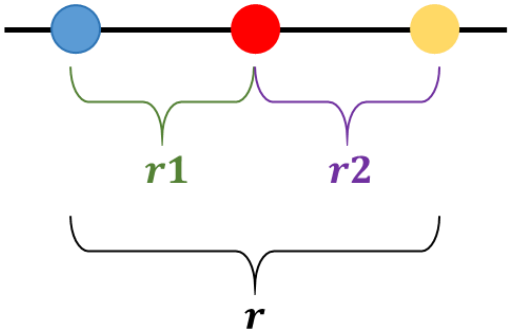

Figure 27. Schematic of the markers and representation of r1, r2 and r.

To calculate $r1$ and $r2$, the proportions of recombinants after the first initial cross between nRn and BnG (F0) are measured. $r1$ will be the sum of the proportions of all the genotypes that include a recombination event in the first interval. $r2$ is the sum of the proportions of all the genotypes that include a visible recombination event in the second interval, and r is the sum of the proportion of all recombinant genotypes:

$$\boldsymbol{r1} = freq(BRn + nnG + nnn + BRG)$$

$$\boldsymbol{r2} = freq(nRG + Bnn + nnn + BRG)$$

$$\boldsymbol{r} = freq(total - nRn - BnG)$$

Using these equations, and applying the obtained proportions from the results of the crosses between the ancestral strains (F0), I obtained the following results:

$$\boldsymbol{Hotspots}: \boldsymbol{r} = 0.29;\ \boldsymbol{r1} = 0.22;\ \boldsymbol{r2} = 0.12$$

$$\boldsymbol{ChrI\ Coldspot}: \boldsymbol{r} = 0.5;\ \boldsymbol{r1} = 0.29;\ \boldsymbol{r2} = 0.32$$

$$\boldsymbol{MTA\ coldspot}: \boldsymbol{r} = 0.4;\ \boldsymbol{r1} = 0.27;\ \boldsymbol{r2} = 0.29$$

Effects on recombination rates are not only restricted to the haplotypes that have been selected during the experiment. For this reason, I also calculated the changes in proportions of each pair of complementary haplotypes, presented in each of the following sections.

The calculations above are only valid when mating results in heterozygosity at all loci in the diploid. This is true in F0 and for individuals where the mating type is always linked to a fluorescent haplotype, as it is

the case for the MTA coldspot. However, for both hotspots and for ChrI coldspot, after F0, recombination rates are calculated differently, as mating types and fluorescent haplotypes are no longer linked. This is represented in Figure 28.

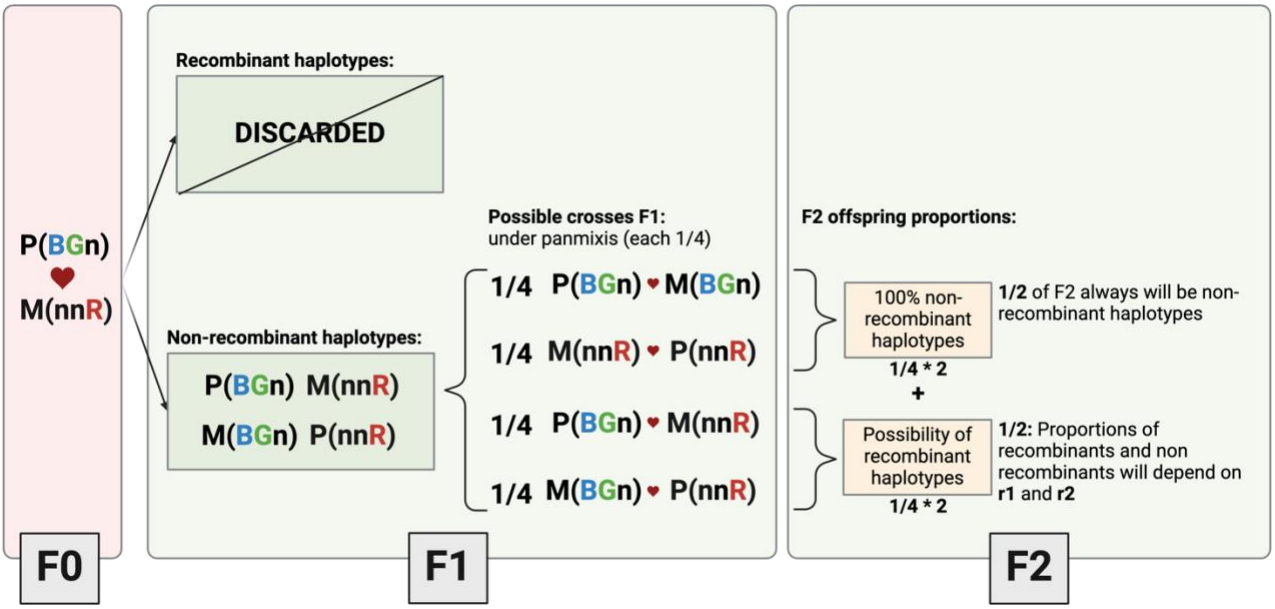

Figure 28. Schematic of the expected recombinants and non-recombinants after the first (F0) and subsequent generations, for an example cross, where there is selection for non-recombinants and there is no linkage between the mating type and the fluorescent haplotype. All recombinant haplotypes are discarded in each generation for the experiment's purposes, so they are not represented in the scheme after F1. After F1, mating types and fluorescent haplotypes are completely mixed, so 50% of every generation starting from F2 will be non-recombinant haplotypes.

To calculate recombination rates for the second generation, the expected proportions will change, and the equations previously presented will change in the following manner, using the $r1$ and $r2$ as calculated in F0:

Original:

$$\boldsymbol{freq(M[nRn]) = freq(M[BnG]) = freq(P[nRn]) = freq(P[BnG]) = \frac{1}{4}}$$

Expected offspring:

$$\boldsymbol{freq(nRn) = freq(BnG)} = \frac{1}{4} + \frac{1}{2} * (1 - r1) * (1 - r2)$$

$$\boldsymbol{freq(BRn) = freq(nnG)} = \frac{1}{4} * r1 * (1 - r2)$$

$$\boldsymbol{freq(nRG) = freq(Bnn)} = \frac{1}{4} * (1 - r1) * r2$$

$$\boldsymbol{freq(nnn) = freq(BRG)} = \frac{1}{4} * r1 * r2$$

Mating-Type Associated Coldspot (MTA Coldspot)

This treatment started with the cross between EBC819 and EBC787 and was expected to show an increase in the proportion of the parental genotypes after crossing. Meaning, LD was expected to increase over time while we selected for non-recombinants.

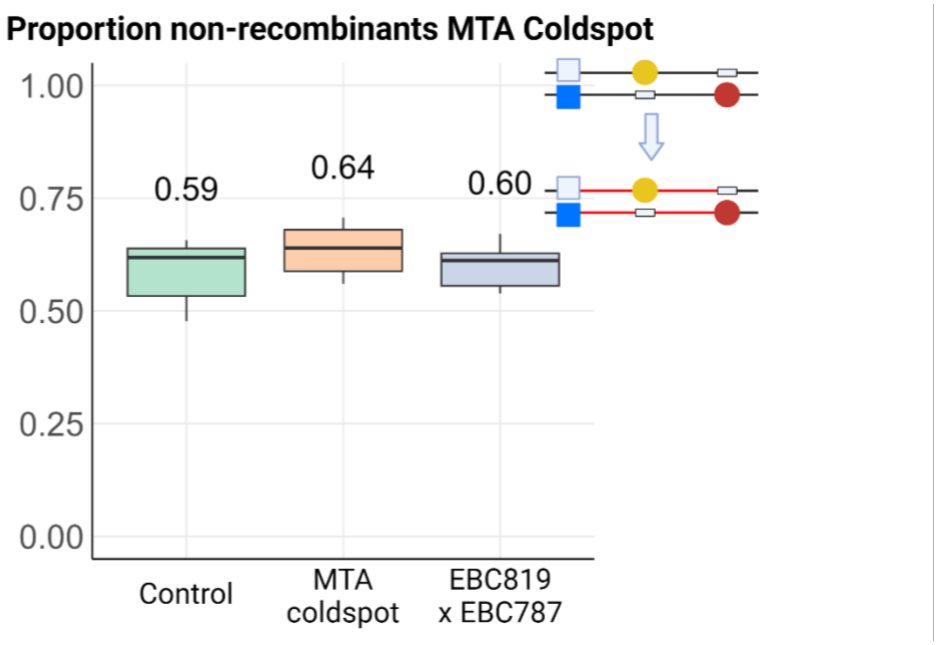

Figure 29. Proportion of parental (non-recombinant) haplotypes for the Mating Type Associated lines. Boxplots represent the sum of the haplotypes indicated on the right side of the picture (nGn + BnR). Anova between groups with Tukey correction gave non significant results.

The proportions of the non-recombined cells ($1 - \boldsymbol{r}$) did not significantly differ between the control and ancestral strains, and the evolved strains. The values are similar to the expected value of $\boldsymbol{r} = 0.4$ (Figure 29; $\boldsymbol{r} = 0.4$ and 0.39 for the ancestral and control respectively). The evolved lines have a lower recombination rate on average, however, there is no significant difference ($\boldsymbol{r} = 0.36$, $p > 0.85$ in both comparisons). There is a tendency towards LD increase, which could be the first onset of recombination suppression, and there might be a possibility of increase.

Regarding the other haplotypes, MTA coldspot shows no significant differences with respect to the ancestral proportions (Table 20).

Table 20. Comparison between the averages of the evolved strains, ancestrals and controls for Mating Type Associated Coldspot.

	MTA ancestral	**Evolved MTA Coldspot**	**MTA control**
$freq\ parentals\ (BRn + nnG)$	0.6	0.64	0.59
$freq\ rec\ I1\ (BnG + nRn)$	0.11	0.11	0.12
$freq\ rec\ I2\ (nRG + Bnn)$	0.13	0.07	0.11
$freq\ double\ rec\ (nnn + BRG)$	0.16	0.18	0.18

The MTA coldspot is the only treatment in which the two fluorescent genotypes that were selected for, mate exclusively with each other, as they are linked to the mating type. This results in heterozygosity in each zygote each generation, and selection for suppression of recombination was thus expected the have the largest effect in this treatment. Nevertheless, no significant change was observed. Because in the other three treatments mating types are unlinked to the markers, heterozygosity is expected only in half of the formed zygotes. I will discuss these other treatments in the following sections.

Chromosome I Coldspot (ChrI Coldspot)

With an r = 0.5, the first and last markers in ChrI coldspot interval were completely unlinked. Starting from F2, as previously schematized (Figure 28), half of the population will always have the non-recombinant fluorescent haplotypes. In this case, as r = 0.5, an extra ¼ will also be non-recombinant haplotypes, which leaves already ¾ of the population as non-recombinant from F2 onwards.

This brings down the selection coefficient. From these ¾ of the population that have non-recombinant fluorescent haplotypes, only 1/3 are true non-recombinants that come from a cross where recombination was possible. The other 2/3 come from a cross where recombination would not be detectable (nnR x nnR or BGn x BGn, Figure 28). While this does not eliminate selection, it does lower it. We did not observe any change in the MTA coldspot where selection was higher, and thus are unlikely to see a change in this treatment. The measurement show that recombination did not differ from the expected proportion of non-recombinants 0.75 (Figure 30)

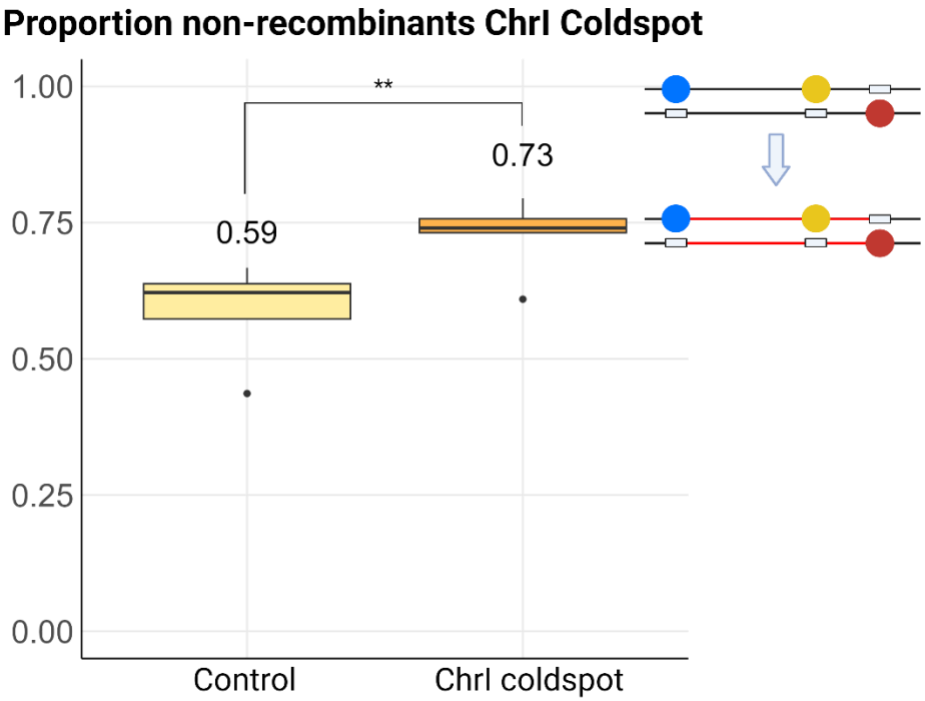

Figure 30. Proportion of non-recombinant haplotypes for the ChrI Coldspot lines. Boxplots represent the sum of the haplotypes indicated on the right side of the picture (BGn +nnR). Anova between groups with Tukey correction gave significant results. Cross between ancestral strains (EBC687 x EBC663) not included in this picture, as the measurements are not comparable to each other (Read main text and Figure 28 for further detail). Significant differences indicated with asterisks (*: p<0.05, **:p<0.01, ***:p<0.001).

Data for the proportion of non-recombinant haplotypes in the evolved likes of ChrI coldspots (Figure 30) is as expected after generation F2, without any selection (0.73 is very similar to 0.75 expected with random mating (Figure 28,

Table 21)). A proportion of 0.25 recombination is, assuming random mating, the maximum possible in this setup. The ChrI control lines though, have increased the recombination above this possible maximum (r = 0.41, Figure 30).

Proportions of all haplotypes started from the cross between EBC687 and EBC663 (ChrI Coldspot and ChrI Control) do show unexpected changes. Note that in the first column of

Table 21, “Calculated Ancestral proportions” I do not use the proportions obtained from the experiment, but the calculated ones using the equations introduced in the end of section 4.2.2. Therefore, significance can only be calculated between the evolved lines and the control.

Table 21. Comparison between the averages of the evolved strains, and controls, and the expected values in the ancestral crosses. Note that the "Calculated Ancestral proportions" column has the calculated numbers expected after F2, and therefore significances cannot be calculated. For more information read main text. Significances ANOVA with tukey's post-hoc test indicated with the letters in each box. In boxes without letters no significance was found.

	Calculated Ancestral proportions	**Evolved ChrI Coldspot**	**ChrI Control (c)**
$freq\ parentals\ (nRn + BnG)$	0.7414	0.73 (a)	0.59 (b)
$freq\ rec\ I1\ (BRn + nnG)$	0.0986	0.11	0.13
$freq\ rec\ I2\ (nnn + BRG)$	0.1136	0.15 (a)	0.23 (b)
$freq\ double\ rec\ (Bnn + nRG)$	0.0464	0.01	0.05

The significant increase in recombination in the control compared to the evolved lines, already shown in Figure 30, is due to the significant increase in recombinants in interval 2 (

Table 21). This increased the total recombination of the measured interval above the possible maximum (50cM).

Changes in the short and long Hotspots

To measure the change in recombination rates of the evolved strains relative to the ancestor, I performed selection for two generations for the evolved hotspot strains, their control and the ancestral cross (EBC675 x EBC746), and measured the number of recombinants after the second cycle. As shown in the previous section (Figure 28), in strains where the mating type and the fluorescent haplotype are in different chromosomes, from generation F2 half of the population will always have non-recombinant haplotypes.

Therefore, performing two crossing cycles (generations 37 and 38) with the ancestral strains avoided the difference in the proportion of each haplotype in the population by measuring all strains after F2. For these measurements, the control was also selected, and as the two hotspots had a different selection regime, the control had to be separated in two different controls, now called short hotspot control and long hotspot control (Figure 31). Although in both hotspot treatments the expected results were slightly different, in both cases recombination was expected to increase, compared to the ancestral lines and the controls.

In the short hotspot, I started with a cross between BRn and nnG genotypes and show the proportion of resulting haplotypes with a recombination in the first interval exclusively (nRn + BnG). In the long hotspot, I started with a cross between BRG and nnn, and I show the proportion of resulting haplotypes that were double recombinants. The shown haplotypes are the ones selected for during the whole experiment (Figure 31).

Short hotspot does not show a significant difference for recombinants in the first interval, compared to the parental strains (Figure 31a).

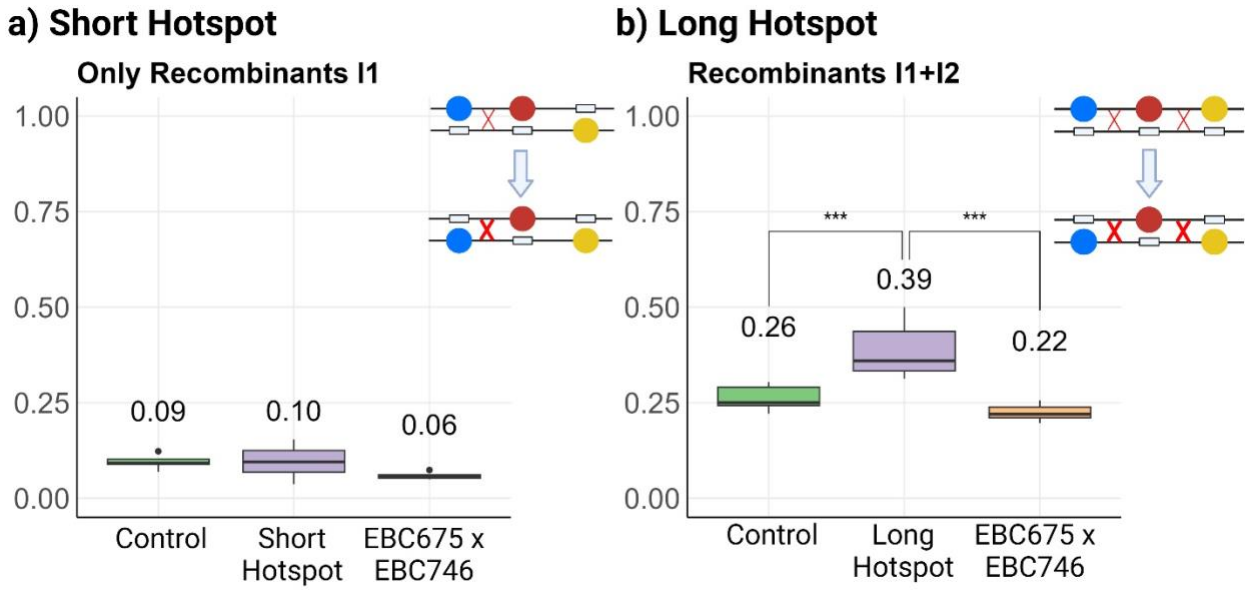

Figure 31. Frequency of the recombinants (indicated next to each figure) for short and long hotspot in generation 38). The two haplotypes shown in each graph at the top are the haplotypes that were crossed and the haplotypes below the arrow show the two haplotypes as would have been selected during the evolution experiment. **a)** Results for recombinants in interval 1 for short hotspot. **b)** Double recombinants for long hotspot. ANOVA between groups corrected with Tukey multiple comparison of means, with a 95% family-wise confidence level. Significant differences indicated with asterisks (*: $p<0.05$, **:$p<0.01$, ***:$p<0.001$).

Double recombinants in the long hotspot show a significant increase with respect to both the control and the ancestral lines (Figure 31b). The fraction of double recombinant genotypes (nRn + BnG) did not differ between the control and the ancestral cross, which is what I expected without selective pressure.

Short hotspot shows a slight increase in the recombination rates in interval one, but as shown before, this is not significant (Figure 31a). There is a significant difference in the recombination rate for interval 2, between the ancestral cross and the other two lines (Evolved short hotspot and controls), where surprisingly the recombination rate has decreased (Table 22). All comparisons done with ANOVA between groups, corrected with Tukey multiple comparison of means.

Table 22. Comparison between the averages of the evolved strains, controls, and ancestral crosses for short hotspot in generation 38. Significant differences ANOVA with tukey's post-hoc test indicated with the letters in each box. Boxes without letters indicate no significant differences were found.

	Ancestral short hotspot	**Evolved short hotspot**	**Control short hotspot**
$freq\ parentals\ (BRn + nnG)$	0.731	0.771	0.678
$freq\ rec\ I1\ (nRn + BnG)$	0.0585	0.1	0.1
$freq\ rec\ I2\ (BRG + nnn)$	0.173 (a)	0.0541 (b)	0.108 (b)
$freq\ double\ rec\ (Bnn + nRG)$	0.0369	0.0789	0.12

The decrease of recombination in the second interval could be due to the unexpected selection for non-recombinants in interval 2. As I only selected for increased recombination for interval 1, I always selected haplotypes where there was no recombination in interval 2. This though, clashes with the fact that recombination has also lowered for the control lines in interval 2. An alternative explanation might be a difference in fitness between some haplotypes. The complementary genotype pair BRG + nnn, which are expected to be in equal frequency, has generally a ratio that deviates a lot from 1, as the proportion of nnn in the population is always much higher than the proportion of BRG. Differences in asexual fitness could cause these differences between complementary haplotypes. An even small difference in fitness caused by the presence of markers in the cell can affect the growth speed, and when working with high numbers of individuals, these differences become later very apparent. This might influence the results and will be further discussed later.

The largest effect of selection of the four treatments was observed in the long hotspot. Shown in Table 23, the proportion of non-recombinant genotypes is significantly lower in the evolved lines, which shows a general increase in recombination. This increased recombination is all in the double recombinants, that in the evolved lines are significantly higher than both in the parental lines and the controls.

Table 23. Comparison between the averages of the evolved strains, controls, and ancestral crosses for long hotspot in generation 38. Significant differences after ANOVA with tukey's post-hoc test indicated with the letter in each box. Boxes without letters indicate no significant differences.

	Ancestral long hotspot	**Evolved long hotspot**	**Control long hotspot**
$freq\ parentals\ (BRG + nnn)$	0.605 (a)	0.488 (b)	0.556 (ab)
$freq\ rec\ I1\ (Bnn + nRG)$	0.0607	0.0493	0.0672
$freq\ rec\ I2\ (BRn + nnG)$	0.11	0.076	0.115

$freq\ double\ rec\ (nRn + BnG)$	0.224 (a)	0.386 (b)	0.262 (a)

The proportion of single recombinants for intervals 1 and 2 shows a lowered tendency in the evolved lines. Interestingly not only the double recombinant haplotypes have increased, but also a (non-significant) decrease in the single recombinant types can be observed. This is as expected, because these genotypes were eliminated during the evolution experiment.

The control strains used for the measurements of the two hotspots were the same, and were treated the same way for most of the experiment. All changes observed for generation 38 should thus result from the selection applied in generation 37. Even though the parental haplotypes (among the two new control treatments) differed for this last cross, the recombination rates for each of the intervals are not expected to differ. Therefore, the ancestral lines and the controls for the hotspots were expected to give the same recombination values between each other in generation 38. However, the measurements of the hotspots control lines and the ancestral lines show differences within generation 38 after selecting for different genotypes (Table 24). These unexpected differences among lines hint towards an effect of the fluorescent haplotype either on recombination rates, or on the asexual growth fitness that might skew the frequencies of some haplotypes before measurement, after spores have germination and growth.

Table 24. Average proportions of haplotypes in generation 38 for controls and ancestral crosses. Highlighted the cells that show statistical significance ($p<0.05$) between the following pairs: Ancestral short vs. Ancestral long, and Control short vs. control long. ANOVA between groups corrected with Tukey multiple comparison of means, with a 95% family-wise confidence level. Summed haplotype pairs indicated in each cell.

	Ancestral short Hotspot	**Ancestral long Hotspot**	**Control short Hotspot**	**Control long Hotspot**
$freq\ parentals$	0.731 $(BRn + nnG)$	0.605 $(BRG + nnn)$	0.678 $(BRn + nnG)$	0.556 $(BRG + nnn)$
$freq\ rec\ I1$	0.0585 $(nRn + BnG)$	0.061 $(Bnn + nRG)$	0.1 $(nRn + BnG)$	0.067 $(Bnn + nRG)$
$freq\ rec\ I2$	0.173 $(BRG + nnn)$	0.11 $(BRn + nnG)$	0.108 $(BRG + nnn)$	0.115 $(BRn + nnG)$
$freq\ double\ rec$	0.0369 $(Bnn + nRG)$	0.224 $(nRn + BnG)$	0.12 $(Bnn + nRG)$	0.262 $(nRn + BnG)$

4.2.3 Effects of the fluorescent haplotype on asexual fitness

So far, I have assumed that complementary pairs of genotypes are equally present in the population, as would be expected under Mendelian segregation. A deeper look into those proportions showed that some of these pairs are not equal as expected, and could affect the changes in recombination rates that happen in the ancestral crosses and controls for hotspots (Table 24). Some haplotypes seem to have dominance over the rest. Additionally, there are unexpected changes in recombination rates between generations, visible in the differences between haplotypes in the Ancestral and Control lines for long and short hotspots (Table

24), between generations 37 and 38 that should not appear in only one generation. These differences might affect the amount of inferred recombination.

Using a pair of genotypes that does not grow at the same rate in the asexual phase will likely skew the calculation of recombination rates. To assess how strongly the recombination rate estimates might be affected by these potential fitness differences, I assessed the skew in ratios between the complementary haplotypes. When calculating the ratio of the average proportion (among the six tubes) of two complementary haplotypes, the ratio should be as close as possible to 1, as these complementary haplotypes are generated at the same rate by meiosis. If there is no difference in vegetative growth between the two different haplotypes, the proportion of these two in the population should be practically equal. A small skew suggests little influence of fitness on our calculated recombination rates. This was calculated for each of the treatments for each of the last two generations, to see whether the used genotypes are suitable for this analysis (Table 25).

Table 25. Deviations in frequencies per haplotype pair, calculated as the absolute log10 of the ratios of each haplotype pair. Highlighted in green, for each line, the haplotype with the smallest ratio difference. In some lines, Hotspot is abbreviated to HS, and coldspot to CS.

log(BnG/nRn)	log(nnn/BRG)	log(BRn/nnG)	log(Bnn/nRG)	Line
0.08	0.71	0.24	0.85	Control short HS
0.06	0.80	0.28	1.24	Control long HS
0.08	0.59	0.23	1.04	Short hotspot
0.03	0.63	0.05	0.50	Long hotspot
0.03	0.57	0.35	0.90	Ancestral Short HS
0.09	0.78	0.05	0.63	Ancestral Long HS
0.01	1.21	0.18	0.82	Chr I control
0.26	0.70	0.14	0.13	MTA control
0.05	1.22	0.03	0.50	Chr I coldspot
1.90	0.50	0.44	0.52	MTA coldspot
0.39	0.94	0.36	1.23	Ancestral ChrI CS
0.11	0.52	0.14	1.23	Ancestral MTA CS

In Table 25, calculations are done by initially taking the ratio (haplotype1/haplotype2) of the average proportions for each haplotype among that treatment (average of 6 lines per treatment). When the expected is that genotype1 = genotype2, the ratio should equal 1 (haplotype1/haplotype2 = 1). To normalize the ratios, I calculated the $|\log_{10}|$ of each ratio, and the closest to 0 shows the best fit.

The ratios are the smallest in the pairs used for the final calculations in this project, for almost all lines. For the Mating type associated coldspot, the best genotype couple is BRn/nnG, which coincides with the two genotypes that had been selected along the experiment. Chr I Coldspot also shows the best pair is the selected genotype couple BnG/nRn, although the obtained results already are non-significant and our results for this experiment are non conclusive.

For the hotspots, the most reliable generation will be generation 38, because we are comparing the same kind of treatments, and in this case for all treatments except one (Ancestral Long HS, and not for a large difference) the best pair of genotypes are the ones we are measuring in Figure 31.

These analyses suggest that the observed changes in recombination rates are likely not to be affected by differences in vegetative growth. Even though the genotypes do not only affect each other in the pairs, but also affect the proportion of all genotypes in the population, the effect of each of the genotypes will stay the same along generations. If in the same population the growth rate of each genotype stays the same, the evolved strains can be compared with the original parental strains, and the detected changes will be caused by changes in recombination rates.

4.3 INVERSIONS LOWER GERMINATION AND ALTER RECOMBINATION RATES

Inversions are one of the most important structural variant, when talking about changes in recombination rates. As discussed in the introduction, inversions can affect recombination within the inverted region, as well as beyond their flanks and in some cases, the effects alter genome-wide recombination rates. All previous studies, though, either have inferred the effects of inversions through modelling, or have studied natural existing inversions, including differences in haplotypes in the region. Consequently, this has left a knowledge gap in the true mechanistic effects of the presence of an inversion in the genome.

Here, I tested the effect of the size of three inversions on viability and on recombination rates in regions flanking the inversions. This makes it possible to measure the effect of inversions in isolation by analysing genotypes that are isogenic except for the inversion. Comparisons can be made between the inverted strains because all inversions end in the same location, *his5*. These were tested both through crosses in heterozygosis, with a non-inverted strain containing three markers on the right side of the inversion (Figure 1), and with an strain containing the same inversion. This setup, allowed me to asses the effect of the inversion on crossovers in the region flanking the inversion through tetrad dissection analysis. Additionally,

strains were crossed to natural isolates and segregants were sequenced in bulk to assess recombination rates and LD decay at a finer resolution.

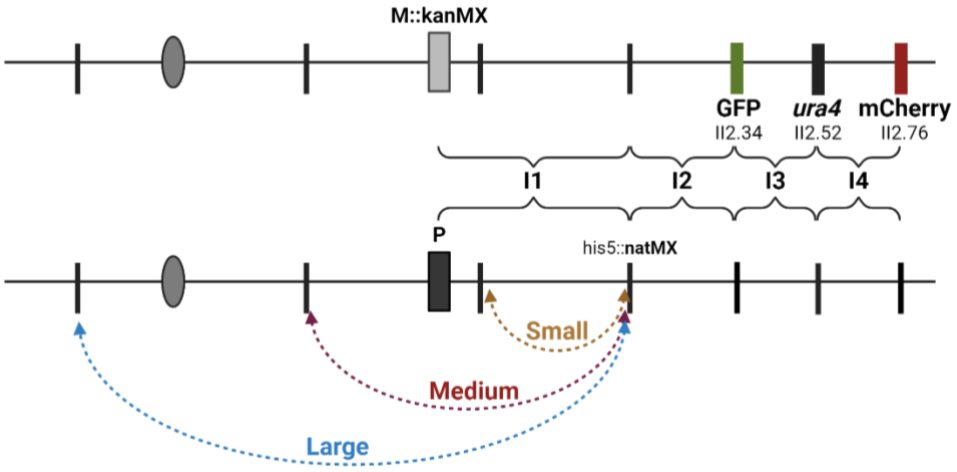

Figure 32. Schematic representation of the strains generated for the experiments. In M strain, I inserted three markers on chromosome II (GFP, ura4 and mCherry), and a *kanMX* resistance marker in the mat1 region. In P strain, three artificially generated inversions on chromosome II that span 110kb, 220kb and 1.03Mb for the small, medium and large inversions respectively. The inversions share the same right side breakpoint at the *his5* locus in which the *natMX* resistance marker was introduced. The Large inversion is pericentric. For both strains, the oval represents the centromere and the rectangle the mating type. The smaller rectangles indicate marker locations used to measure recombination rates for the intervals I1 to I4.

4.3.1 Spore viability is directly affected by the presence of inversions in heterozygosis

Recombination inside an inverted region in heterozygosis is expected to lead to aneuploidy and, therefore, lowered germination rates. Tetrad dissections show a lowered spore viability of the inverted strains in heterozygosis versus the control strain (Figure 34a) measured by counting the total amount of colonies formed after spore germination.

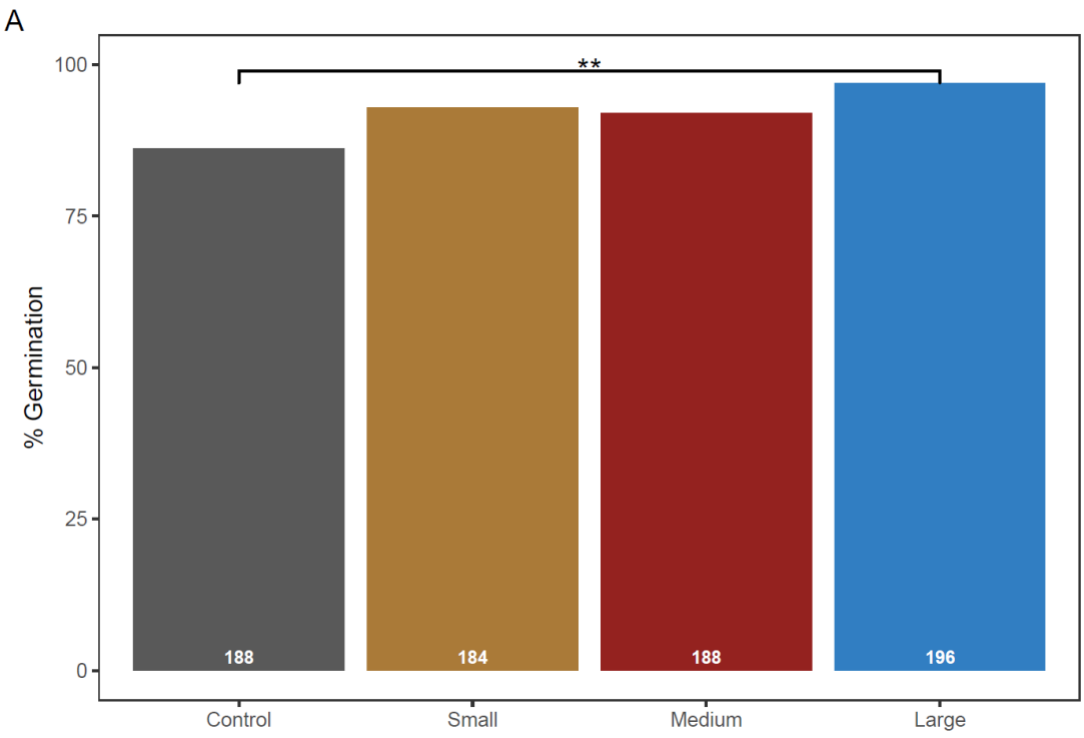

Figure 33. Percentage of total germinating spores when crossing two strains with the same inversion in homozygosis. There is significant difference in spore germination between the control strains and the strains with the largest inversion.

This reduction is not observed in crosses between two strains with the same inversion, which confirms that in order to have a biological effect, inversions need to be in heterozygosis (Figure 33). Furthermore, it is not only the presence of the inversion but the size of it that affect germination rates. The viability of the crosses is affected by 6.4%, 13.5% and 45.4% for the small, medium and large inversion, respectively, which is a significant difference among all strains.

Table 26. p-values for the comparisons between the germination rates of spores for each of the inversions and the control, and the inversions to each other. The fraction of the viable spores from the total (given in parenthesis) spores tested is given.

Strain	Fraction alive	Small	Medium	Large
Control	84.0 % (n = 1188)	0.001913	7.29E-12	≤2.20E-16
Small	78.6 % (n = 1356)	-	0.000373	≤2.20E-16
Medium	72.7 % (n = 1408)	-	-	≤2.20E-16
Large	45.9 % (n = 1728)	-	-	-

To confirm the inversion in heterozygosis is the cause for lower germination rates, in Figure 34b I show the results, for each of the crosses, of the number of spores germinated per tetrad. If a death of a spore was

independent of the other spores in the tetrad, a binomial distribution would be expected for spore survival per tetrad. If for any reason there were a higher background mortality, this would change the peak of the distribution but not the shape. When the mortality is due to recombination inside the inverted region in heterozygosis, however, every time it happens two meiotic products should die together, which would shift the shape of the distribution towards an increase in 0, 1 and 2 germinating spores per tetrad, leading to a

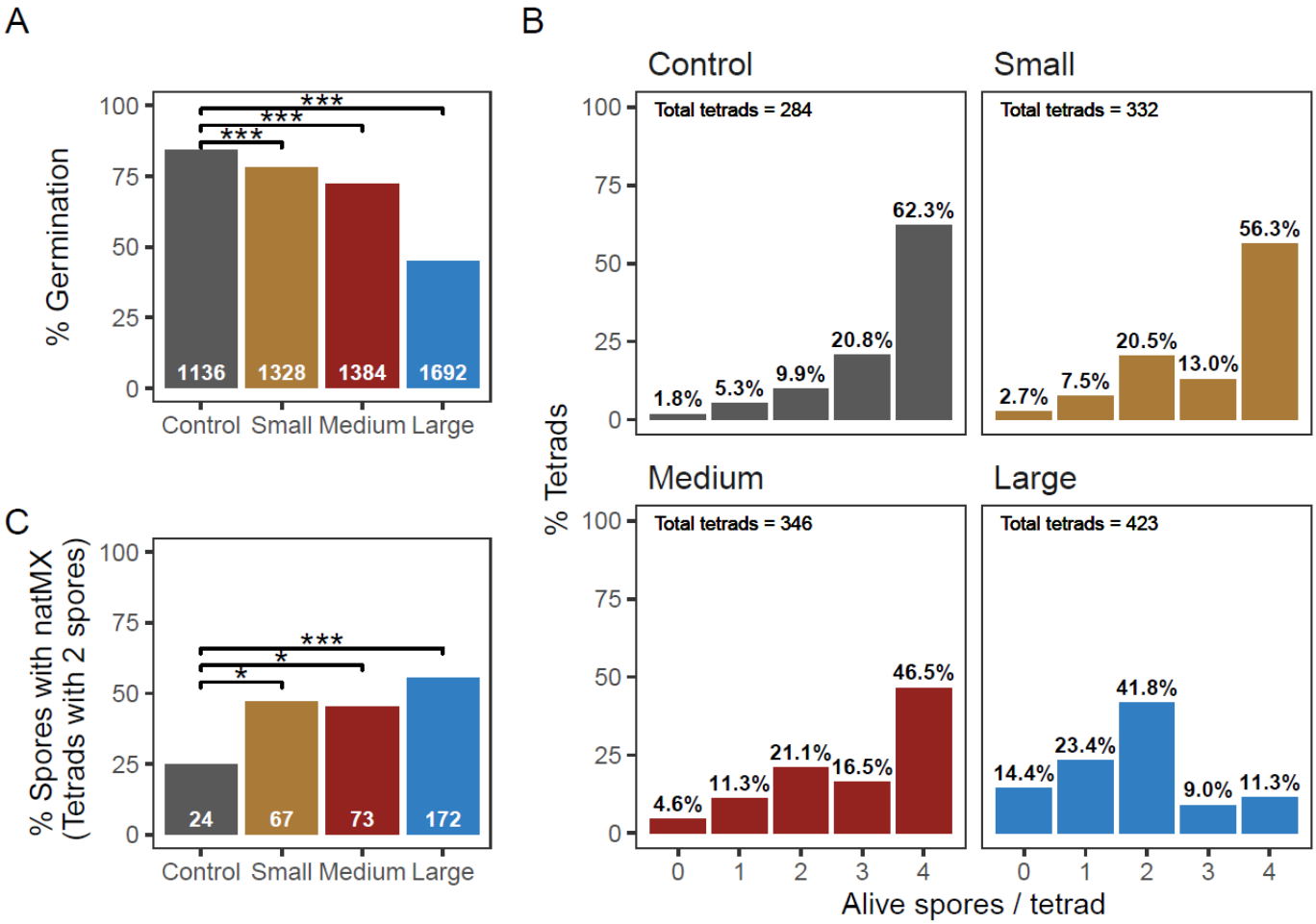

reduction of the number of tetrads with 3 or 4 alive spores. This is what happens in Figure 34b when comparing the control to the inverted strains, and the shift towards a peak in 2 alive spores per tetrad increases proportionally with the size of the inverted region, showing the highest change in the largest inversion (Table 27).

Figure 34. Spore survival of crosses between the four P strains (control or one of the inversion strains) and strain EBC871, which is M and contains four markers. a) Bar plot showing the germination percentage for the total of spores in each of the inversions compared to the control. b) Bar plots showing, for each of the inversions and the control, the percentage of tetrads with a certain number of spores germinated (from 0 to 4). c) For each of the inversions and the control, percentage of germinated spores that are resistant to nourseothricin among tetrads with two viable spores (total tetrads indicated in each bar. Asterisks in a) & c) indicate significance levels of Pearson's χ^2 with df = 1 (*: p<0.05, **: p<0.01, ***: p<0.001).

If fitness is not affected by the presence of markers in the strain, the same percentage of non-germinating spores with and without the inversion would be expected. The nourseothricin resistance marker *natMX* has an unexpected effect on the fitness of the control cells, which creates a skew in the frequency of the marker in the tetrads with two surviving spores in the control (Figure 34c, control shows only 25% spores with *natMX*). However, this deviation from 1:1 is not observed on the two-spore tetrads in the strains with the inversions, in which the *natMX* marker is located at the inversion breakpoint (Figure 34c, all inverted strains show close to 50%). Assuming the same effect of the *natMX* marker in all strains, this shows that in the inverted strains, when a pair of spores is dying one contains the inversion and one does not. The presence of the inversion in heterozygosis is causing the spores to die in pairs due to an odd number of recombination events within the inverted region, and the inviability caused by this is stronger than the inviability caused by the presence of the *natMX* marker.

Table 27. Results of a chi square test for homogeneity across the groups (nº of spores alive per tetrad) shown in Figure 34b. All inversions show significant differences with the control

Comparison Inversion Small-Control							
Chi-squared	19.472						
df	4		***Residuals***				
p-value	0.0006347	Control	-0.57253	-0.80141	-2.44405	1.746109	0.708776
		Small	0.529523	0.741219	2.260473	-1.61496	-0.65554
Comparison Inversion Medium-Control							
Chi-squared	31.473						
df	4		***Residuals***				
p-value	2.45E-06	Control	-1.45173	-1.89363	-2.59798	0.927622	1.995483
		Medium	1.315243	1.715596	2.353734	-0.84041	-1.80788
Comparison Inversion Large-Control							
Chi-squared	279.7						
df	4		***Residuals***				
p-value	2.20E-16	Control	-4.17792	-4.55048	-5.98903	3.209681	9.11104
		Large	3.42333	3.728602	4.907336	-2.62997	-7.46547

4.3.2 Inversion presence and size affect genetic map distances

Table 28. Calculations of map distances per interval in cM in the different intervals. The interval in which a significant difference in the proportion of PD/T/NPD relative to the Control was observed are grey shaded (difference between map distances is greater than twice the standard error). The rows in bold correspond to intervals 1 to 4 described in Figure 32. Analysis was performed using only tetrads with information for all four spores.

Interval	**Map distance (cM)**			
	Control	**Small**	**Medium**	**Large**
MAT - his5	**14.9**	**3.56**	**1.88**	**41.2**
MAT - II2.34	15.3	8.40	3.75	35.0
MAT - II2.52	33.5	21.1	25.7	65.7
MAT - II2.76	45.7	29.9	32.1	56.1
his5 - II2.34	**7.08**	**6.72**	**2.10**	**4.29**

his5 - II2.52	27.4	19.7	24.1	41.7
his5 - II2.76	43.6	28.3	32.1	37.0
II2.34 - II2.52	**22.3**	**19.7**	**21.8**	**35.4**
II2.34 - II2.76	39.6	25.5	29.2	36.1
II2.52 - II2.76	**19.1**	**17.9**	**19.2**	**36.6**

I assessed genetic map distances by performing tetrad dissections with crosses between the inverted and control strains (EBC832, EBC867, EBC836 and EBC835) and the M strain with three markers (EBC871) (Table 6 and Table 28). First, I present the analysis that used exclusively tetrads where information of the four spores was available for each marker pair. Below I give analyses using all surviving spores. Using the tetrad data, map distances were calculated per interval, and then compared to the non-inverted control (Table 28 and Figure 35a). Highlighted on the table the intervals where there has been a significant change in the proportion of PD/T/NPD from the control, calculated with a Chi-squared test.

In the strains EBC867 and EBC836 (with medium and large inversions respectively) the first interval between the right breakpoint and the mating type was in the inversions, as the inversions encompass the mating type (Figure 1). The recombination of a marker outside of an inversion without killing the offspring, requires at least two crossovers within the inversion, one on each side of the marker. I assessed the changes in recombination rates between the *kanMX* marker, located at the *mat1* locus, and the *natMX* marker located at the right breakpoint, which showed a much shorter map distance in the medium inversion than in the control crosses (2 cM and 19 cM, respectively). Meaning that while recombination happens, it is visible at a much lower rate, because the recombining spores with a single crossover die, skewing the measure to shorter map distances in the surviving spores. In the large inversion, the mating type appeared completely unlinked from the *natMX* marker (77 cM). It is important to note that after inverting that segment, the distance between the *mat1* locus and the *natMX* marker increase from 15kb to almost 1Mb, but a recombination event is still needed in each of the two sides of the *mat1* locus for the spores to germinate. For strain EBC832 (small inversion), the map distance was strongly reduced to 5cM. This was expected, because this inversion does not include the *mat1* locus inside, but rather there is a small distance between the left breakpoint and the *mat1*. This leaves only this small interval of 4kb, between 2.11 Mb and 2.15 Mb, for a recombination event to occur. It might be slightly higher than the distance in the medium inversion due to the fact that only one recombination event was needed to recombine the *natMX* and *kanMX* markers.

Next, I checked the intervals outside of the inversion. The interval flanking the inversion was expected to show a reduction in map distance (Crown et al. 2018; Koury 2023). All three strains show a reduction (10cM for the control, versus 9cM, 2cM and 4cM for the small, medium and large inversion respectively).

However, after correction for multiple testing, none of these differences shows significance (Table 28 and Figure 35a). The large inversion showed the loci for interval 3 and 4 to be unlinked (>50cM). however, as shown in the previous section, inversions decrease viability of meiotic products, and the decrease in viability is directly proportional to the size of the inversion (Figure 34a). Using only surviving tetrads might introduce bias due to differences in spore survival between strains, and tetrads with different recombination events are likely surviving at different rates. The data used to calculate map distances was based only on tetrads for which information on all four spores was available and therefore, differential survival cannot be excluded as the cause for changes in map distance.

Analysis of the total fraction of recombined spores from all viable spores came next. This measure ignores double cross-over events in the intervals, and thus gives a relatively conservative estimate for recombination per interval. These results show a slightly different result for some of the intervals (Figure 35b). Specifically, recombination in the flank of the large inversion is no longer reduced, but actually increased, even though not significantly. Discarding or adding part of the information seems to affect the recombination rates for certain intervals.

It is important to differ the two methods of analysis. In general and regarding recombination rate analysis, it is widely accepted that the Perkins' (1949) formula counting the complete tetrads is more accurate. However, studies with tetrad dissections do not usually have markers with a mortality as high as the one caused by the presence of inversions in heterozygosis. In our case, and when talking about evolutionary strategies, all alive progeny matters, and therefore it is important to take into account all alive spores and their recombination rates. This is the reason why I used both the Perkins' (1949) formula, and the total spore bulk for a more complete analysis.

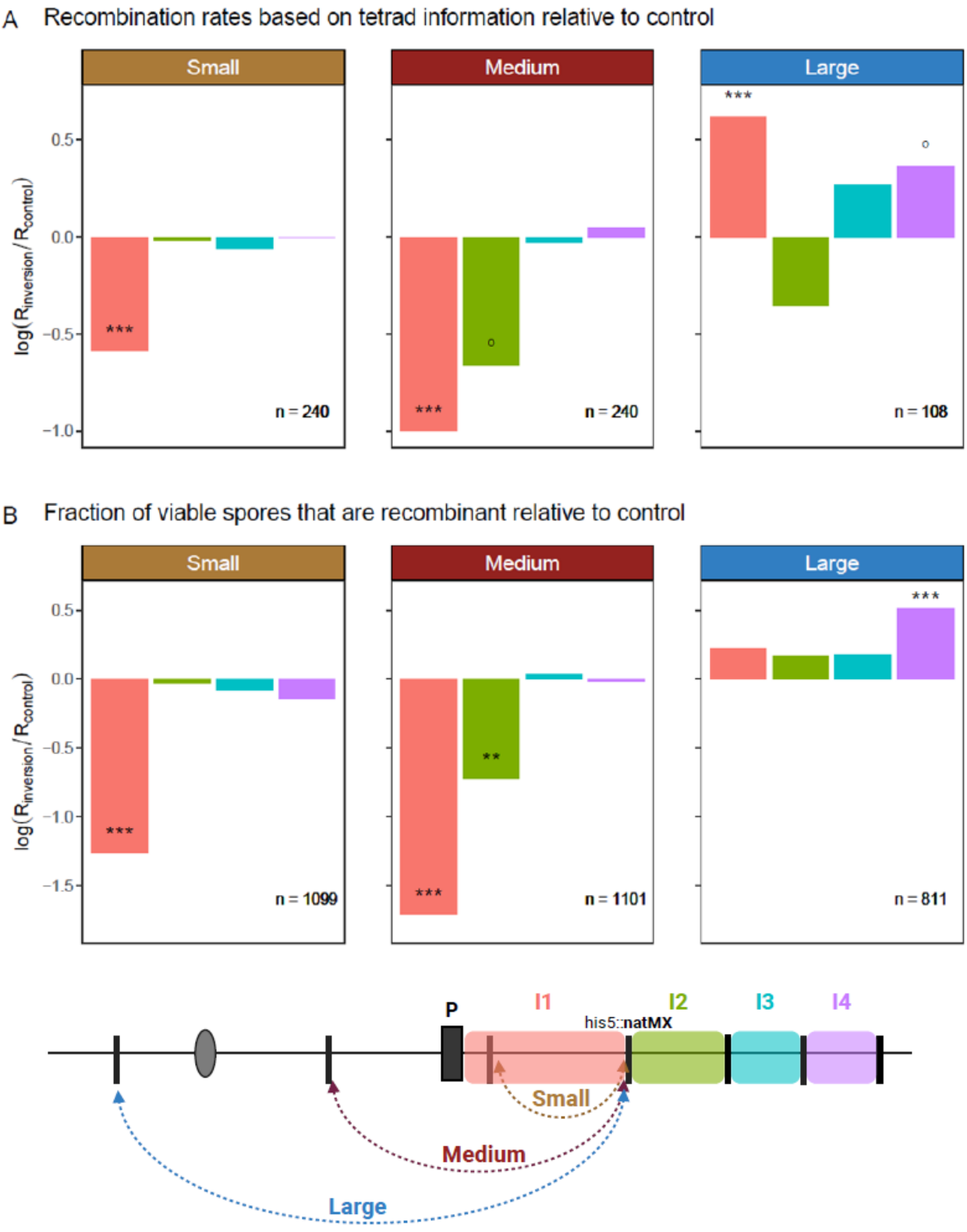

Figure 35. Change in recombination of inversion strains relative to the control (log transform ratio). A) the map length compared to the control strain for each of the strains with inversions, calculated by taking the log of the ratio, calculated using Perkins 1949 for complete tetrads only. B) similar, but comparing the fraction of non-parental genotypes for all

alive spores. The line at zero represents no difference from the control. Pearson's $\chi 2$ after Bonferroni correction (*: $p < 0.05$, **: $p < 0.01$, ***: $p < 0.001$, °: $p < 0.05$ before correction, df = 2 for a and df = 1 for b). Number of analysed tetrads (a) or spores (b) given per cross.

As mentioned above, with increasing inversion size spores' viability strongly reduces. To asses whether the differences in observed recombination rates are caused by a change in recombination rates and is not due to spore survival of certain genotypes influencing the recombination rate calculations, I used a stochastic computer model that simulates recombination and survival. The model allowed independent recombination within each interval, assumed a constant background death, and that recombination within the inversion causes death of the two meiotic products produced. This allowed for the estimation, for a given parameter set (A certain inversion and pair of loci used) the expected number of each tetrad type, including tetrads with dead spores. I fitted in this model my raw counts of each of the possible tetrad combinations, obtained from the tetrad dissections, to estimate the recombination rates for each interval.

Table 29. Parameter estimates for the data fittedto the model, for each locus combination (o and x) with the his5 marker (i) for each of the tested strains, estimating recombination per interval (r), as well as background death rate (d_s) and death due to recombination within the inversion when heterozygous (d_i).

Strain	r_{io}	r_{ox}	d_s	d_i	**Loci**		
					i	***o***	***x***
Control	0.083	0.266	0.112	0.070	Control	II2.34	II2.52
Control	0.083	0.376	0.111	0.068	Control	II2.34	II2.76
Control	0.316	0.234	0.114	0.069	Control	II2.52	II2.76
Small	0.080	0.248	0.092	0.207	Small	II2.34	II2.52
Small	0.080	0.307	0.093	0.205	Small	II2.34	II2.76
Small	0.265	0.208	0.094	0.206	Small	II2.52	II2.76
Medium	0.046	0.280	0.152	0.223	Medium	II2.34	II2.52
Medium	0.046	0.326	0.152	0.223	Medium	II2.34	II2.76
Medium	0.295	0.248	0.152	0.223	Medium	II2.52	II2.76
Large	0.108	0.320	0.402	0.392	Large	II2.34	II2.52
Large	0.108	0.383	0.402	0.392	Large	II2.34	II2.76
Large	0.352	0.400	0.402	0.392	Large	II2.52	II2.76

The model only takes into account an inversion and two extra markers at once. Thus, I estimated the different combinations of markers with each of the inversions and the control independently (results in Table 29). The results from the model are consistent with the map distances obtained from the germinating tetrads, i.e. the inversions appear to be responsible for the changes seen in recombination rates. Recombination in the interval close to the inversion is reduced in the small and medium inversion and recombination is increased distal from the large inversion. The obtained model parameter for recombination in the interval close to the inversion (***rio*** when ***o*** = II2.34) remains reduced only in the strain with the

medium inversion, when compared to the control (MediumGU = 0.046 vs. ControlGU = 0.083), while it slightly increases in the large inversion (LargeGU = 0.108). For the large inversion, all flanking intervals show increased recombination respect to the control, especially the most distal interval (LargeUR = 0.4 vs. ControlUR = 0.234)

Death due to the inversion was estimated by the model to be ~20% both for the small and medium inversions, while it increased up to ~40% for the large inversion. Some of the genotypes predicted by the model were either missing or overrepresented in our data, showing a significant overall deviation (parametric-bootstrap test, p = 0.019). Moreover, the model suggested an increase in background death with the size of the inversion, which is rejected by the results from the control crosses of each of our inversions in heterozygosis (Figure 33). It is possible that the model allowing two pairwise interactions per interval creates these deviations. In nature, interactions between multiple chromatids might occur at the same time, which can lead to inviability of three or even four spores in a tetrad due to one interval (in our case the inversion). In the model, however, these deaths can only be attributed to background mortality. Additionally, the model does not account for crossover competition or interference, which are known to play a role even in *S.pombe* (Fowler et al. 2018).

The germination rate in the control crosses (crossing two strains with a *natMX* marker truncating *his5* without an associated inversion) shows the lowest germination rates, and it has a significant difference with the germination rate in the largest inversion in homozygosis (Figure 33). This shows an effect of the *natMX* marker on fitness in asexual growth, probably caused by the region where it is inserted, as the other crosses contain the same marker but they do not show any effect on fitness. This effect was already detected and commented on in previous analyses (Figure 34c).

4.3.3 LD decay is neither affected by the presence nor the size of the inversion

For a higher resolution of recombination rates in the regions flanking the inversion, I measured decay of Linkage Disequilibrium (LD). The inversion strains and the control – all containing the nourseothricin resistance marker *natMX* at the right breakpoint of the inversion – were crossed with a heterothallic strain EBC395, derived from natural isolate CBS5557 (Table 6). For each cross, spores were separated in two groups, and DNA was then isolated from all offspring (group 1 – no selection) or from offspring that contained the *natMX* marker, present only in the inversion or control (group 2 – medium with nourseothricin). Next, all DNA was re-sequenced. EBC395 was chosen because it was genetically close enough to the reference strain that they could cross and yield enough offspring. Nevertheless, EBC395 has almost forty thousand variant sites (about three per kb) relative to the reference strain, which give a high

resolution in recombination rates. However, due to partial shared ancestry these are not evenly distributed (Tusso et al. 2019). The strain does not contain major genomic rearrangements on chromosome II but has a large inversion on chromosome I relative to the reference (Tusso et al. 2019). Crosses between diverged natural isolates show low viability in offspring (Jeffares et al. 2015) and test crosses followed by tetrad dissections showed the highest spore survival in this cross compared with other crosses with natural strains.

Under Mendelian segregation and without selection, equal frequencies of alleles from each of the two parents are expected (Figure 36a). Re-sequencing from bulk offspring without artificial selection showed the expected ratios for chromosome II (Figure 36d). Chromosome III was strongly skewed towards EBC395 alleles, probably caused by the large number of *wtf* meiotic drivers that are located on this chromosome (Hu et al. 2017). Chromosome I showed a slightly larger proportion of EBC395 in the region associated with an inversion known to exist on that chromosome (Hu et al. 2015; Tusso et al. 2019), which might be associated with a slight fitness advantage of genes in this region (Figure 36d). Chromosome II shows the expected ratios under no selection. When selection was applied, fixation of the reference strain alleles at the *natMX* marker is expected (selection indicated by coloured dots). All regions linked to this marker are expected to be skewed for the reference genome, while unlinked regions should show similar allele frequencies as in no selection due to recombination or segregation. As expected, Chromosome III showed no difference in allele frequencies between the selected and unselected groups. Also as expected, Chromosome II shows selection of the *natMX* marker and linked regions as expected. Unexpectedly, Chromosome I showed fixation for the reference strain variants in a large part of the chromosome. I will first discuss the observations of chromosome II and then of chromosome I.

To test for LD decay, resequencing was done in bulk after selecting for the presence of the nourseothricin resistance marker, located at *his5* in the control strain, or on the right side of the inversion breakpoint. 100% frequency of the reference alleles were expected at the selected locus and all the regions linked to that locus, with a gradual drop in allele frequencies to levels similar to the non-selected samples for loci unlinked to this locus (Figure 36a). Chromosome II, as explained in the previous paragraph, shows the expected allele frequencies both in the selected and non-selected lines (Figure 36d). The peak in the strains with the inversions encompasses in all cases the totality of the inversion, and does not show signs of high recombination between the two breakpoints. Only in the centre of the largest inversion there are signs of recombination, showed by a drop in allele frequency.

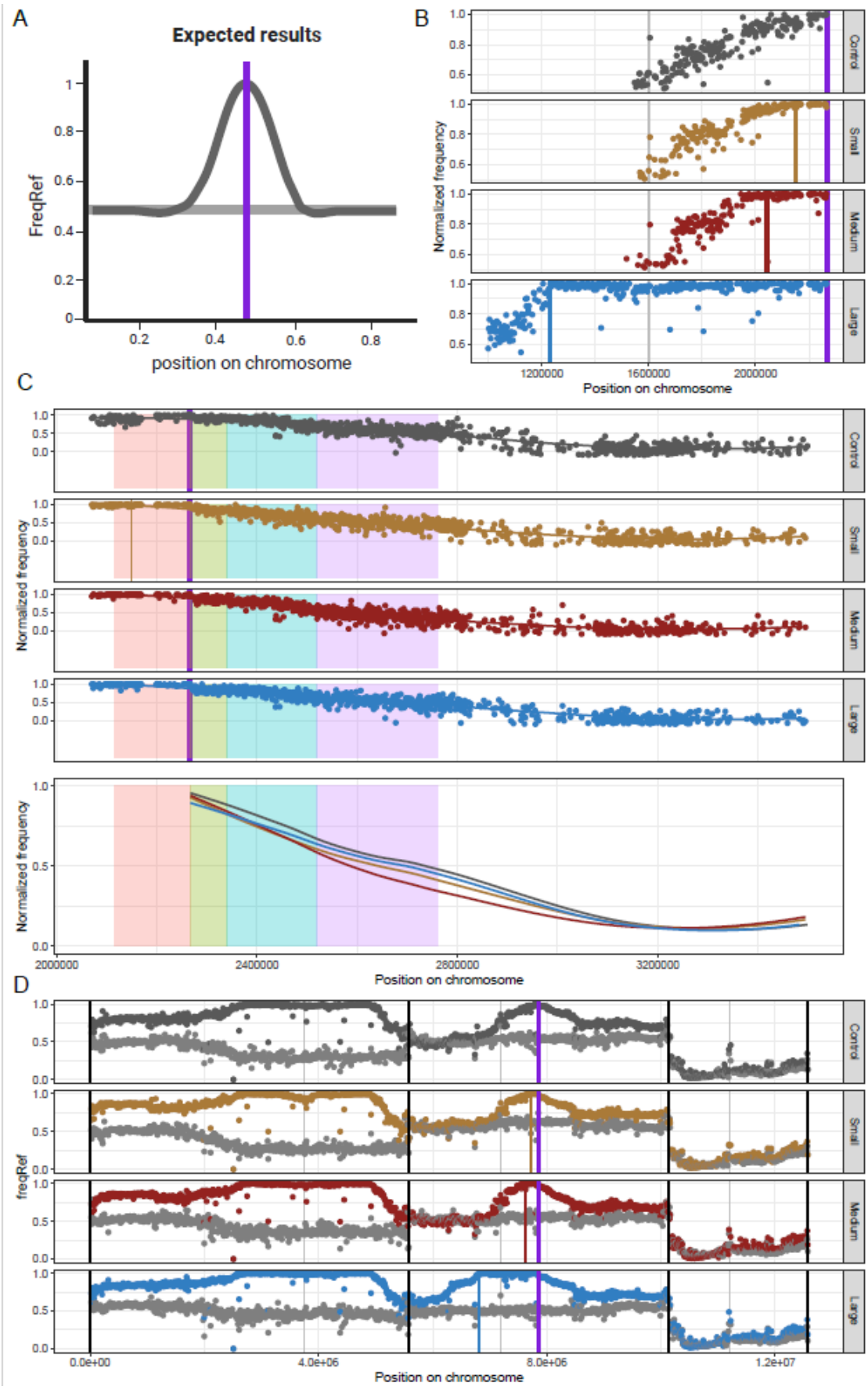
A
Expected results
FreqRef
position on chromosome
B
Normalized frequency
Control
Small
Medium
Large
Position on chromosome
C
Normalized frequency
Position on chromosome
D
freqRef
Position on chromosome

Figure 36. Results from the bulk segregant analysis of crosses to the natural isolate. a) Schematic figure of expected results for allele frequency of the reference strain, containing a nourseothricin resistance marker (*natMX*) at the right inversion breakpoint (indicated by the purple vertical line), when selected with nourseothricin or without in grey or black respectively. b) Relative allele frequencies for the left side of the natMX marker on chromosome II for the nourseothricin selected samples. Vertical lines of the same colour as the SNPs indicate the end of the inversion if present. Frequencies are normalized by dividing by the mean allele frequency of chromosome II in the non-selected strain. c) Allele frequencies per 10kb window normalized per cross after selection for the 1.2Mb region flanking the right side of the inversion. The green, blue and pink vertical lines indicate the location of the markers used in the tetrad dissections. d) Reference strain allele frequencies for all three chromosomes. The allele frequencies are presented in grey for the unselected treatment and in colour for the nourseothricin selection treatment. Vertical lines as indicated for b). In all figures, variant frequencies are binned per 10kb window, black lines delimit chromosomes and grey lines indicate centromeres positions in the reference strain.

Normalisation of the selected and non-selected lines for chromosome II follow the same pattern as previously noticed, and show complete selection for the nourseothricin marker and full linkage of all the alleles within the inversion (Figure 36b). To asses LD decay properly, the allele frequencies around the inversions were scaled setting to zero the main frequency where the right arm of the chromosome levelled off. There does not seem to be a large difference in LD decay among the strains with the inversion (Figure 36c).

Slopes are highly similar in all analysed crosses. However, in the regions more distal to the *natMX* marker, the medium inversion shows a faster decay in LD than the small and large inversions, even though the differences are too small to be significant (Figure 36c, lower panel). When comparing the inversions to the control, they do not reduce the recombination but they rather seem to increase it slightly. Epistasis might also affect LD breakdown, as linkage of regions close to the breakpoint might cause selection that skews frequencies farther away. Epistasis could also explain the differential behaviour between the left and right side of chromosome II in all strains. While allele frequencies on the left side of the inversions return to equal proportions, the allele frequencies on the right side of the *natMX* marker stay skewed towards the reference strain. This trend is visible also in the control. The increase towards alleles in the reference strain could indicate epistasis between the genes linked to the *his5* area – a 60kb region left of *his5* appears tightly linked – and other parts on the right side of the chromosome.

The large region in chromosome I that became fixed for the reference strain alleles after selection, might also be explained by epistasis (Figure 36d). This region coincides exactly with the inversion relative to the reference present in most fission yeast isolates (Brown et al. 2011; Tusso et al. 2019), which arguably occurred in the reference strain, as it is present in almost no other strain found in nature. No resistance marker is present in that region, as was verified by tetrad dissections, and therefore there is no reason why it should have been directly selected. Either this region was i) selected due to genes inducing sensitivity to nourseothricin in the natural isolate strain that cannot be saved by *natMX*, the gene encoding N-acetyl transferase conveying resistance, or ii) one or multiple alleles in this region show lethal epistasis with the

region linked to *his5*. Lethal epistasis could also be the reason why the left flank of chromosome II had a higher frequency of the reference strain in the selected than the non-selected group, rather than reverting to the original frequencies.

5 DISCUSSION

This thesis explores the present variation and forces that affect recombination rates through an evolutionary perspective. I combined analyses of recombination rate variation among natural strains (section nº 4.1) with an evolution experiment (section nº 4.2), and with a study on the role of structural variants on recombination, concretely inversions (section nº 4.3).

Analysing 57 natural isolate strains of fission yeast, showed large differences in recombination rates among all strains, and within each strain between the three chromosomes. These differences ranged, for the same area in every strain, from almost no recombination (~0cM), to the two markers being completely unlinked (50cM). The results could not be explained by any of the tested hypotheses. If recombination were trans-regulated, variation among the strains would be larger than variation within a strain, which was not observed. If recombination variation within the strain were affected by genetic sequence variation, the ancestral variation between the two crossed strains would be correlated to recombination, which was also not found. The high recombination variation found among strains, was not associated with ancestry, suggesting complex underlying mechanisms that need to be further studied for a complete comprehension of recombination rate changes in fission yeast. My results not only confirm the initial hypotheses, but serve also as a base for future research using the experimental setup performed in this thesis by adjusting certain parameters, such as increasing the number of images taken per cross and making sure the same data is obtained for each.

The imaging effort per chromosome differed and as a result, the quality estimate might differ among the chromosomes. Nevertheless, the quality of the cross does not correlate to the recombination rate. The quality did also not correlate with any of the other parameters that could be analysed in this project. Although unlikely, variation in recombination rates might be a highly variable and non-heritable trait. Few replications of recombination rates were performed, and with a higher number of replications this question could be solved. While the genetic yeast map is very consistent and it is unlikely that the recombination rates are non-heritable (Gutz and Doe 1973; Gutz et al. 1974), we cannot exclude this possibility. The lack of variation in the lab strain suggests variation might be globally defined, but my data shows that on the contrary, in natural strains it seems that it might be very locus-dependent. Apart from the already performed analysis of the average recombination per strain, it might be interesting to increase the number of biological replicates per cross, in order to study the variance there might be among strains, a characteristic not usually studied, but that has been increasing its significance in science (de Jong et al. 2019; Wolf et al. 2023). The

large variation observed in recombination rates suggests that recombination is a variable trait that might evolve rapidly, in response to adaptation to different environments.

My evolution experiment in which direct selection for recombinant and non-recombinant lines was performed, showed that recombination rates can change due to direct selection; supporting the idea that recombination rates are evolvable. In two of the four treatments significant changes in recombination rates were detected. The short hotspot showed a significant increase in non-recombinant haplotypes, caused by the repetitive selection for those in the population. This treatment, rather than increase recombination in the first interval, lowered recombination in the second; an effect that, however unexpected, proves that recombination can be directly selected. The long hotspot showed a significant increase in double-recombinant haplotypes, as initially expected.una As double recombinants were less common than single recombinants, selection in the long hotspot treatment was stronger than in any other treatment, which is probably the reason it shows the stronger changes in recombination. Selection for recombination reduction is stronger when there is obligate heterozygosity in the cross, which is what happened in the short hotspot, lowering recombination rates in I2. There is also the possibility of recombination being more malleable in the I2 interval, which might explain why we see more significant changes in that part.

Selection on the offspring must be very high in order to obtain the expected results in the course of the evolution experiment. The significant changes in the two hotspot treatments suggest that a combination of a longer experiment with stronger selection pressures would show significant changes in the coldspot treatments. Performing crosses exclusively between heterozygous haplotypes in ChrI coldspot, and performing the experiment for longer time for the MTA coldspot, might increase the possibility of seeing significant results.

The fluorescent markers seem to have had a small but not negligible fitness effect. Fitness measurements on the individual markers showed no significant effects, but when combined in one haplotype there appears to be an effect. Even though this affected the haplotype frequencies in the control strains over time, their effect over a single generation are likely small, and we expect these will not have had large effects in the selected populations. In these populations always only two haplotypes are maintained, mostly removing competition during the asexual phase. A skew due to variable growth in the measurements after evolution is not expected. The large experiment size (100,000 selected individuals per generation) assured that drift would not affect the results. While this experiment showed that recombination rates can respond to selection, the mechanisms for the regulation of coldspots and hotspots are still largely unknown. The strains generated in this experiment give the opportunity to analyse these mechanisms. Because the ancestral genotypes are known and multiple independent lines were evolved per treatment, phenotypic and genetic comparison can be made for the different strains. In-depth measurements of the recombination rates per

replicate line combined with whole genome resequencing can show how recombination changed, and which mechanisms and pathways might have changed. Changes might be local at the sequence level, global at a regulatory level, or structural – which is most likely in the MTA colspot treatment – through rearrangements or inversions.

To further investigate the factors that affect the evolution of recombination rates, I researched the role of inversions in the recombination landscape. Structural variation in the form of inversions is generally thought to reduce recombination. The results of my experiments prove that not only inversions affect recombination rates, but also their size determines how recombination changes. Moreover, the presence of inversions in heterozygosis significantly affected spore viability. The size of the inversion directly affected the germination rates of the produced spores, by lowering the germination rates with bigger inversion sizes. This is hypothesized to be caused by an odd number of recombination events within the inverted fragment. These recombination events lead to aneuploidy, generating inviable spores. Reduced spore viability was not observed in homozygous inversions, emphasizing the importance of heterozygosity for inversions to have any mechanistic effect. Analysis of recombination rates both within and in the regions flanking the inversions showed changes in both detectable and expected crossover events, indicating that the presence of an inversion in heterozygosis has an effect in recombination rates both within the inversion and beyond its boundaries, and that these effects depend on the size of the inversion.

The findings of all three experiments show existing variability in recombination rates among fission yeast strains, demonstrate that recombination is a heritable trait that respond to direct selection, and prove that inversions affect both recombination rates and spore mortality. These findings not only corroborate earlier studies on the role of recombination in genetic diversity and evolutionary processes but also increased the knowledge in these areas, proving that research in the evolution in recombination rates continues to be an active topic of research, with many potential discoveries. The observed variability in recombination rates and the impact of inversions align with established theories, but also highlight the need for more detailed mechanistic studies (Jaarola et al. 1998; Kirkpatrick 2010; Stevison et al. 2011; Koury 2023). They also emphasize the importance of avoiding the generalization of biological processes after executing studies only in one species (Stapley et al. 2017a). The extreme variability found in only a small analysed portion of the chromosome shows that recombination rates are not always uniform along the chromosomes, as previously affirmed (Lian et al. 2023). In some species, recombination rates are controlled mostly by few genes (Johnston et al. 2016), but there is more complexity than previously thought, and can be used as a beginning for further research. Further investigation into the variation of recombination rates among fission yeast strains can be researched by including a third marker, so that the explored area increases, as now the information obtain includes only a small area of the genome that cannot be extrapolated to the whole

chromosome. Genomic analysis are needed to discover whether the genes responsible for the changes in recombination rates after the evolution experiments are already known genes responsible for recombination rates, or rather new ones. In the area of the effects of inversions in recombination rates, inclusion of further crosses between inverted laboratory strains with natural strains could shed some light to whether they all perform the same way. Moreover, there is still unanswered questions regarding the large area in chromosome I from the laboratory strain that gets selected for when the strains are grown with nourseothricin.

Understanding the variability and evolvability of recombination rates can improve not only the general knowledge in fundamental sciences, where recombination evolution has hold a prominent interest along the years (Morgan 1911; Gutz and Doe 1973; Gutz et al. 1974; Stapley et al. 2017a; Dutheil 2024), but also in commercial breeding efforts. The breeding improvements could be beneficial not only in yeast, but in any other commercial species, as higher knowledge of recombination landscape can enhance the efficiency of breeding programs, and knowing how to manipulate recombination rates can expand the breeding response of certain species to breeding selection (Battagin et al. 2016; Epstein et al. 2023).

In conclusion, the studies performed for this thesis reveals significant variability in recombination rates among fission yeast strains, the impact of direct selection on recombination landscapes and the detrimental effects of inversions on spore variability, as well as their possible effects on recombination. These findings suggest that recombination rates are influenced by complex factors beyond the three main topics studied in this thesis, and encourage further research for the deepening of this fundamental biological mechanism that is meiotic recombination.

6 CONCLUSION

The main objective of this dissertation is to shed light on how recombination rates are determined, from an evolutionary perspective, together with increasing the perspective into how natural populations show such recombination variability in their genomes. To analyse this affect, I studied the relationship between recombination variation, ancestry, direct selection and chromosomal rearrangements. I observed that recombination rates can vary strongly and can evolve over short evolutionary times. The significant variation found among strains, and among chromosomes within the same strain, demonstrates that recombination is not uniformly distributed across the genome. I found that recombination rate does not correlate with genetic background, which suggests that the regulation of recombination rates might happen within very small distances. Strong direct selection for changes in recombination rates demonstrated that recombination rates can evolve under strong selective pressure even over relatively short – 36 sexual generations – evolutionary time. The effective changes in recombination rates, expressed as an increase in double recombinants for the long hotspot and a decrease of recombination in the second analysed interval for the short hotspot, highlight the existing complexity in recombination rates, as well as the selection for recombination rate changes. These significant modifications, though, prove that directed alterations are feasible.

Chromosomal inversions showed to have an effect on recombination rates, both within and on the flanks. Recombination rates mostly decreased in and around inversions in the two smaller sizes, but increased inside and around the largest inversion. Contrary to previous findings in other organisms (Noor et al. 2001; Stevison et al. 2011; Rifkin et al. 2020), this demonstrates that in fission yeast, while inversions affect recombination rates, they do not repress recombination. Inversions significantly affected spore viability in heterozygous conditions, with larger inversions leading to lower germination rates. This finding shows that suppression of recombination in inversions at population levels most likely occurs not due to changes in crossovers, but rather by inviability in the gametes or the offspring caused by aneuploidy.

This dissertation advances our understanding of meiotic recombination by integrating detailed experimental data on recombination variation, direct selection, and the effects of genomic rearrangements in recombination. These studies reveal a high variation in recombination rates in fission yeast, and the high potential of the use of direct selection for their evolution, as well as the effect of inversions on recombination rate changes and cell viability. My findings highlight the intricate interplay between genetic structure, evolutionary processes and recombination mechanisms, offering new perspectives and directions for future research in the field of genetics. These experimental findings on the effects of direct selection

and inversions explain the wide variation in recombination among natural yeast strains, as these show large amounts of structural and genetic variation. This work provides a foundation for further studies aimed at unravelling the complexities and implications of the evolution of recombination.

7 LIST OF ABBREVIATIONS

Centimorgans: cM

Cas9: CRISPR-associated Protein 9

Coldspot: CS

CRISPR: Clustered Regularly Interspaced Short Palindromic Repeats

Fluorescence Activated Cell Sorting: FACS

Hotspot: HS

Homologous Region: HR

Hygromycyn Resistance Marker: hphMX

Kilobases: kb

Linkage Disequilibrium: LD

Mating type associated: MTA

Megabases: Mb

Non-Parental Ditype: NPD

Nourseothricin Resistance Marker: natMX

Parental Ditype: PD

Recombination Interference: RI

Schizosaccharomyces kombucha: Sk

Schizosaccharomyces pombe: Sp

Sinaptonemal Complex: SC

Single guide RNA: sgRNA

Tetra Type: TT

8 REFERENCES

Abbott, J. K., A. K. Nordén, and B. Hansson. 2017. Sex chromosome evolution: historical insights and future perspectives. Proc Biol Sci 284:20162806.

Arcangioli, B., and S. Gangloff. 2023. The Fission Yeast Mating-Type Switching Motto: "One-for-Two" and "Two-for-One." Microbiology and Molecular Biology Reviews 87:e00008-21. American Society for Microbiology.

Asakawa, H., T. Haraguchi, and Y. Hiraoka. 2007. Reconstruction of the kinetochore: a prelude to meiosis. Cell Div 2:17.

Bachtrog, D., M. Kirkpatrick, J. E. Mank, S. F. McDaniel, J. C. Pires, W. Rice, and N. Valenzuela. 2011. Are all sex chromosomes created equal? TRENDS in Genetics 27:350–357.

Battagin, M., G. Gorjanc, A.-M. Faux, S. E. Johnston, and J. M. Hickey. 2016. Effect of manipulating recombination rates on response to selection in livestock breeding programs. Genetics Selection Evolution 48:44.

Baudat, F., J. Buard, C. Grey, A. Fledel-Alon, C. Ober, M. Przeworski, G. Coop, and B. de Massy. 2010. PRDM9 is a major determinant of meiotic recombination hotspots in humans and mice. Science 327:836–840.

Beach, D. H., and A. J. Klar. 1984. Rearrangements of the transposable mating-type cassettes of fission yeast. The EMBO Journal 3:603. Nature Publishing Group.

Berdan, E. L., N. H. Barton, R. Butlin, B. Charlesworth, R. Faria, I. Fragata, K. J. Gilbert, P. Jay, M. Kapun, K. E. Lotterhos, C. Mérot, E. Durmaz Mitchell, M. Pascual, C. L. Peichel, M. Rafajlović, A. M. Westram, S. W. Schaeffer, K. Johannesson, and T. Flatt. 2023. How chromosomal inversions reorient the evolutionary process. Journal of Evolutionary Biology n/a.

Berenguer Millanes, C., and B. P. S. Nieuwenhuis. 2023. Inversions and integrations using CRISPR/Cas9 and a module-based plasmid construction kit for fission yeast. Molecular Biology.

References

Bernstein, H., and C. Bernstein. 2010. Evolutionary Origin of Recombination during Meiosis. BioScience 60:498–505.

Bolger, A. M., M. Lohse, and B. Usadel. 2014. Trimmomatic: a flexible trimmer for Illumina sequence data. Bioinformatics 30:2114–2120.

Boulton, A., R. S. Myers, and R. J. Redfield. 1997. The hotspot conversion paradox and the evolution of meiotic recombination. Proceedings of the National Academy of Sciences 94:8058–8063. Proceedings of the National Academy of Sciences.

Branco, S., F. Carpentier, R. C. R. de la Vega, H. Badouin, A. Snirc, S. L. Prieur, M. A. Coelho, D. M. de Vienne, F. E. Hartmann, D. Begerow, M. E. Hood, and T. Giraud. 2018. Multiple convergent supergene evolution events in mating-type chromosomes. Nature Communications 9:2000.

Brown, W. R. A., G. Liti, C. Rosa, S. James, I. Roberts, V. Robert, N. Jolly, W. Tang, P. Baumann, C. Green, K. Schlegel, J. Young, F. Hirchaud, S. Leek, G. Thomas, A. Blomberg, and J. Warringer. 2011. A Geographically Diverse Collection of Schizosaccharomyces pombe Isolates Shows Limited Phenotypic Variation but Extensive Karyotypic Diversity. G3 Genes|Genomes|Genetics 1:615–626.

Burt, A., and G. Bell. 1987. Mammalian chiasma frequencies as a test of two theories of recombination. Nature 326:803–805. Nature Publishing Group.

Butlin, R. 2002. The costs and benefits of sex: new insights from old asexual lineages. Nat Rev Genet 3:311–317. Nature Publishing Group.

Byrd, R. H., P. Lu, J. Nocedal, and C. Zhu. 1995. A Limited Memory Algorithm for Bound Constrained Optimization. SIAM J. Sci. Comput. 16:1190–1208. Society for Industrial and Applied Mathematics.

Camacho, J. P. M., M. Bakkali, J. M. Corral, J. Cabrero, M. D. López-León, I. Aranda, A. Martín-Alganza, and F. Perfectti. 2002. Host recombination is dependent on the degree of parasitism. Proceedings of the Royal Society of London. Series B: Biological Sciences 269:2173–2177. Royal Society.

Charlesworth, B. 1976. Recombination modification in a fluctuating environment. Genetics 83:181–195. Oxford University Press.

Charlesworth, B. 1989. The evolution of sex and recombination. Trends in Ecology & Evolution 4:264–267.

Charlesworth, B., and D. Charlesworth. 1975. An experiment on recombination load in Drosophila melanogaster. Genetics Research 25:267–273. Cambridge University Press.

Charlesworth, B., and J. D. Jensen. 2021. Effects of Selection at Linked Sites on Patterns of Genetic Variability. Annual Review of Ecology, Evolution, and Systematics 52:177–197. Annual Reviews.

Charlesworth, B., C. Y. Jordan, and D. Charlesworth. 2014. The evolutionary dynamics of sexually antagonistic mutations in pseudoautosomal regions of sex chromosomes. Evolution 68:1339–1350.

Charlesworth, D. 2021. When and how do sex-linked regions become sex chromosomes? Evolution 75:569–581.

Chen, E. S. 2023. Application of the fission yeast *Schizosaccharomyces pombe* in human nutrition. FEMS Yeast Research 23:foac064.

Choi, K., X. Zhao, K. A. Kelly, O. Venn, J. D. Higgins, N. E. Yelina, T. J. Hardcastle, P. A. Ziolkowski, G. P. Copenhaver, F. C. H. Franklin, G. McVean, and I. R. Henderson. 2013. Arabidopsis meiotic crossover hot spots overlap with H2A.Z nucleosomes at gene promoters. Nat Genet 45:1327–1336. Nature Publishing Group.

Claverys, J. P., and S. A. Lacks. 1986. Heteroduplex deoxyribonucleic acid base mismatch repair in bacteria. Microbiol Rev 50:133–165.

Comeron, J. M., A. Williford, and R. M. Kliman. 2008. The Hill–Robertson effect: evolutionary consequences of weak selection and linkage in finite populations. Heredity 100:19–31.

Coop, G., X. Wen, C. Ober, J. K. Pritchard, and M. Przeworski. 2008. High-Resolution Mapping of Crossovers Reveals Extensive Variation in Fine-Scale Recombination Patterns Among Humans. Science 319:1395–1398. American Association for the Advancement of Science.

References

Coyne, J. A., B. C. Moore, J. A. Moore, J. R. Powell, and C. E. Taylor. 1992. Temporal Stability of Third-Chromosome Inversion Frequencies in Drosophila persimilis and D. pseudoobscura. Evolution 46:1558.

Cromie, G., and G. R. Smith. 2008. Meiotic Recombination in Schizosaccharomyces pombe: A Paradigm for Genetic and Molecular Analysis. Genome Dyn Stab 3:195.

Crown, K. N., D. E. Miller, J. Sekelsky, and R. S. Hawley. 2018. Local Inversion Heterozygosity Alters Recombination throughout the Genome. Current Biology 28:2984-2990.e3. Cell Press.

Danecek, P., J. K. Bonfield, J. Liddle, J. Marshall, V. Ohan, M. O. Pollard, A. Whitwham, T. Keane, S. A. McCarthy, R. M. Davies, and H. Li. 2021. Twelve years of SAMtools and BCFtools. GigaScience 10:1–4.

Datta, A., M. Hendrix, M. Lipsitch, and S. Jinks-Robertson. 1997. Dual roles for DNA sequence identity and the mismatch repair system in the regulation of mitotic crossing-over in yeast. Proceedings of the National Academy of Sciences 94:9757–9762. Proceedings of the National Academy of Sciences.

Davis, L., and G. R. Smith. 2001. Meiotic recombination and chromosome segregation in Schizosaccharomyces pombe. Proceedings of the National Academy of Sciences of the United States of America 98:8395–8402.

de Jong, T. V., Y. M. Moshkin, and V. Guryev. 2019. Gene expression variability: the other dimension in transcriptome analysis. Physiological Genomics 51:145–158. American Physiological Society.

Dumont, B. L. 2017. Variation and Evolution of the Meiotic Requirement for Crossing Over in Mammals. Genetics 205:155–168.

Dutheil, J. Y. 2024. On the estimation of genome-average recombination rates. Genetics 227:iyae051.

Efron, B., and R. Tibshirani. 1993. An introduction to the bootstrap. Chapman & Hall, New York.

Egel, R. 1989. Mating-Type Genes, Meiosis, and Sporulation. Pp. 31–73 *in* Molecular Biology of the Fission Yeast. Elsevier.

Epstein, R., N. Sajai, M. Zelkowski, A. Zhou, K. R. Robbins, and W. P. Pawlowski. 2023. Exploring impact of recombination landscapes on breeding outcomes. Proc. Natl. Acad. Sci. U.S.A. 120:e2205785119.

Fantes, P. A., and C. S. Hoffman. 2016. A Brief History of Schizosaccharomyces pombe Research: A Perspective Over the Past 70 Years. Genetics 203:621–629.

Farré, M., D. Micheletti, and A. Ruiz-Herrera. 2012. Recombination Rates and Genomic Shuffling in Human and Chimpanzee—A New Twist in the Chromosomal Speciation Theory. Molecular Biology and Evolution 30:853.

Felsenstein, J. 1974. THE EVOLUTIONARY ADVANTAGE OF RECOMBINATION. Genetics 78:737–756.

Fisher, R. 1930. The Genetical Theory of Natural Selection. Oxford Clarendon Press.

Flor-Parra, I., J. Zhurinsky, M. Bernal, P. Gallardo, and R. R. Daga. 2014. A Lallzyme MMX-based rapid method for fission yeast protoplast preparation. Yeast 31:61–66.

Forsburg, S. L. 2003. Overview of *Schizosaccharomyces pombe*. CP Molecular Biology 64.

Forsburg, S. L. 2005. The yeasts Saccharomyces cerevisiae and Schizosaccharomyces pombe: models for cell biology research. Gravitational and Space Biology 18:3–10. American Society for Gravitational and Space Biology.

Fowler, K. R., R. W. Hyppa, G. A. Cromie, and G. R. Smith. 2018. Physical basis for long-distance communication along meiotic chromosomes. Proc. Natl. Acad. Sci. U.S.A. 115.

Garg, S. G., and W. F. Martin. 2016. Mitochondria, the cell cycle, and the origin of sex via a syncytial eukaryote common ancestor. Genome Biology and Evolution 8:1950–1970.

Girard, C., D. Zwicker, and R. Mercier. 2023. The regulation of meiotic crossover distribution: a coarse solution to a century-old mystery? Biochemical Society Transactions 51:1179–1190.

Gonen, S., M. Battagin, S. E. Johnston, G. Gorjanc, and J. M. Hickey. 2017. The potential of shifting recombination hotspots to increase genetic gain in livestock breeding. Genetics Selection Evolution 49:55.

References

Gong, W. J., K. S. McKim, and R. S. Hawley. 2005. All Paired Up with No Place to Go: Pairing, Synapsis, and DSB Formation in a Balancer Heterozygote. PLOS Genetics 1:e67. Public Library of Science.

Goodenough, U., and J. Heitman. 2014. Origins of Eukaryotic Sexual Reproduction. Cold Spring Harbor Perspectives in Biology 6:a016154.

Gowans, C. S. 1965. Tetra Analysis. Taiwania 11:1–19.

Greig, D., M. Travisano, E. J. Louis, and R. H. Borts. 2003. A role for the mismatch repair system during incipient speciation in Saccharomyces. Journal of Evolutionary Biology 16:429–437.

Gutz, H., and F. J. Doe. 1973. TWO DIFFERENT h - MATING TYPES IN SCHIZOSACCHAROMYCES POMBE. Genetics 74:563–569.

Gutz, H., H. Heslot, U. Leupold, and N. Loprieno. 1974. Schizosaccharomyces pombe. Pp. 395–446 *in* R. C. King, ed. Bacteria, Bacteriophages, and Fungi: Volume 1. Springer US, Boston, MA.

Hagan, I., A. M. Carr, A. Grallert, and P. Nurse. 2016. Fission yeast: a laboratory manual. Cold Spring Harbor Laboratory Press, Cold Spring Harbor, New York.

Hartfield, M. 2016. Evolutionary genetic consequences of facultative sex and outcrossing. Journal of Evolutionary Biology 29:5–22.

Harwood, M. P., I. Alves, H. Edgington, M. Agbessi, V. Bruat, D. Soave, F. C. Lamaze, M.-J. Favé, and P. Awadalla. 2022. Recombination affects allele-specific expression of deleterious variants in human populations.

Hawley, R. S., and B. Ganetzky. 2016. Alfred Sturtevant and George Beadle Untangle Inversions. Genetics 203:1001–1003.

Heim, L. 1990. Construction of an h +Sstrain of Schizosaccharomyces pombe. Curr Genet 13–19.

Hill, W. G., and A. Robertson. 1966. The effect of linkage on limits to artificial selection. Genetics Research 8:269–294.

Hoffman, C. S., V. Wood, and P. A. Fantes. 2015. An Ancient Yeast for Young Geneticists: A Primer on the *Schizosaccharomyces pombe* Model System. Genetics 201:403–423.

Hoffmann, A. A., and L. H. Rieseberg. 2008. Revisiting the impact of inversions in evolution: From population genetic markers to drivers of adaptive shifts and speciation? Annual Review of Ecology, Evolution, and Systematics 39:21–42.

Hu, H., A. Scheben, J. Wang, F. Li, C. Li, D. Edwards, and J. Zhao. 2024. Unravelling inversions: Technological advances, challenges, and potential impact on crop breeding. Plant Biotechnol J 22:544–554.

Hu, W., Z.-D. Jiang, F. Suo, J.-X. Zheng, W.-Z. He, and L.-L. Du. 2017. A large gene family in fission yeast encodes spore killers that subvert Mendel's law. eLife 6:e26057. eLife Sciences Publications, Ltd.

Hu, W., F. Suo, and L. L. Du. 2015. Bulk segregant analysis reveals the genetic basis of anatural trait variation in fission yeast. Genome Biology and Evolution 7:3496–3510.

Hussin, J., M.-H. Roy-Gagnon, R. Gendron, G. Andelfinger, and P. Awadalla. 2011. Age-Dependent Recombination Rates in Human Pedigrees. PLoS Genet 7:e1002251.

Inoue, K., and J. R. Lupski. 2002. Molecular Mechanisms for Genomic Disorders. Annu. Rev. Genom. Hum. Genet. 3:199–242.

Ishii, K., and B. Charlesworth. 1977. Associations between allozyme loci and gene arrangements due to hitch-hiking effects of new inversions. Genetics Research 30:93–106.

Jaarola, M., R. H. Martin, and T. Ashley. 1998. Direct Evidence for Suppression of Recombination within Two Pericentric Inversions in Humans: A New Sperm-FISH Technique.

Jay, P., D. Jeffries, F. E. Hartmann, A. Véber, and T. Giraud. 2024. Why do sex chromosomes progressively lose recombination? Trends in Genetics 40:564–579. Elsevier.

Jay, P., E. Tezenas, A. Véber, and T. Giraud. 2022. Sheltering of deleterious mutations explains the stepwise extension of recombination suppression on sex chromosomes and other supergenes. PLOS Biology 20:e3001698–e3001698.

Jay, P., A. Whibley, L. Frézal, M. Á. R. de Cara, R. W. Nowell, J. Mallet, K. K. Dasmahapatra, and M. Joron. 2018. Supergene Evolution Triggered by the Introgression of a Chromosomal Inversion. Current Biology 0.

Jeffares, D. C., C. Jolly, M. Hoti, D. Speed, L. Shaw, C. Rallis, F. Balloux, C. Dessimoz, J. Bähler, and F. J. Sedlazeck. 2017. Transient structural variations have strong effects on quantitative traits and reproductive isolation in fission yeast. Nat Commun 8:14061. Nature Publishing Group.

Jeffares, D. C., C. Rallis, A. Rieux, D. Speed, M. Převorovský, T. Mourier, F. X. Marsellach, Z. Iqbal, W. Lau, T. M. K. Cheng, R. Pracana, M. Mülleder, J. L. D. Lawson, A. Chessel, S. Bala, G. Hellenthal, B. O'Fallon, T. Keane, J. T. Simpson, L. Bischof, B. Tomiczek, D. A. Bitton, T. Sideri, S. Codlin, J. E. E. U. Hellberg, L. Van Trigt, L. Jeffery, J. J. Li, S. Atkinson, M. Thodberg, M. Febrer, K. McLay, N. Drou, W. Brown, J. Hayles, R. E. C. Salas, M. Ralser, N. Maniatis, D. J. Balding, F. Balloux, R. Durbin, and J. Bähler. 2015a. The genomic and phenotypic diversity of Schizosaccharomyces pombe. Nature Genetics 47:235–241. Nature Publishing Group.

Jeffares, D. C., C. Rallis, A. Rieux, D. Speed, M. Převorovský, T. Mourier, F. X. Marsellach, Z. Iqbal, W. Lau, T. M. K. Cheng, R. Pracana, M. Mülleder, J. L. D. Lawson, A. Chessel, S. Bala, G. Hellenthal, B. O'Fallon, T. Keane, J. T. Simpson, L. Bischof, B. Tomiczek, D. A. Bitton, T. Sideri, S. Codlin, J. E. E. U. Hellberg, L. van Trigt, L. Jeffery, J.-J. Li, S. Atkinson, M. Thodberg, M. Febrer, K. McLay, N. Drou, W. Brown, J. Hayles, R. E. C. Salas, M. Ralser, N. Maniatis, D. J. Balding, F. Balloux, R. Durbin, and J. Bähler. 2015b. The genomic and phenotypic diversity of *Schizosaccharomyces pombe*. Nat Genet 47:235–241.

Jeffries, D. L., J. F. Gerchen, M. Scharmann, and J. R. Pannell. 2021a. A neutral model for the loss of recombination on sex chromosomes. Phil. Trans. R. Soc. B 376:20200096.

Jeffries, D. L., J. F. Gerchen, M. Scharmann, and J. R. Pannell. 2021b. A neutral model for the loss of recombination on sex chromosomes. Philosophical Transactions of the Royal Society B: Biological Sciences 376:20200096. Royal Society.

Johnson, N. A., and J. Lachance. 2012. The genetics of sex chromosomes: evolution and implications for hybrid incompatibility. Ann N Y Acad Sci 1256:E1-22.

Johnston, S. E. 2024. Understanding the Genetic Basis of Variation in Meiotic Recombination: Past, Present, and Future. Molecular Biology and Evolution 41:msae112.

Johnston, S. E., C. Bérénos, J. Slate, and J. M. Pemberton. 2016. Conserved Genetic Architecture Underlying Individual Recombination Rate Variation in a Wild Population of Soay Sheep (Ovis aries). Genetics 203:583–598.

Kapun, M., and T. Flatt. 2019. The adaptive significance of chromosomal inversion polymorphisms in *Drosophila melanogaster*. Molecular Ecology 28:1263–1282.

Kawakami, T., A. Wallberg, A. Olsson, D. Wintermantel, J. R. de Miranda, M. Allsopp, M. Rundlöf, and M. T. Webster. 2019. Substantial Heritable Variation in Recombination Rate on Multiple Scales in Honeybees and Bumblebees. Genetics 212:1101–1119.

Kerstes, N. A., C. Bérénos, P. Schmid-Hempel, and K. M. Wegner. 2012. Antagonistic experimental coevolution with a parasite increases host recombination frequency. BMC Evol Biol 12:18.

Kirkpatrick, M. 2010. How and why chromosome inversions evolve. PLoS Biology 8.

Klar, A. J. S. 2007. Lessons Learned from Studies of Fission Yeast Mating-Type Switching and Silencing.

Klar, A. J. S., and L. M. Miglio. 1986. Initiation of meiotic recombination by double-strand DNA breaks in S. pombe. Cell 46:725–731.

Knaus, B. J., and N. J. Grünwald. 2017. VCFR : a package to manipulate and visualize variant call format data in R. Mol Ecol Resour 17:44–53.

Kong, A., J. Barnard, D. F. Gudbjartsson, G. Thorleifsson, G. Jonsdottir, S. Sigurdardottir, B. Richardsson, J. Jonsdottir, T. Thorgeirsson, M. L. Frigge, N. E. Lamb, S. Sherman, J. R. Gulcher, and K. Stefansson. 2004. Recombination rate and reproductive success in humans. Nat Genet 36:1203–1206. Nature Publishing Group.

Korunes, K. L., C. A. Machado, and M. A. F. Noor. 2021. Inversions shape the divergence of Drosophila pseudoobscura and Drosophila persimilis on multiple timescales. Evolution 75:1820–1834.

Koury, S. A. 2023. Predicting recombination suppression outside chromosomal inversions in Drosophila melanogaster using crossover interference theory. Heredity, doi: 10.1038/s41437-023-00593-x. Springer Nature.

Kulathinal, R. J., L. S. Stevison, and M. A. F. Noor. 2009. The genomics of speciation in Drosophila: Diversity, divergence, and introgression estimated using low-coverage genome sequencing. PLoS Genetics 5.

Küpper, C., M. Stocks, J. E. Risse, N. Dos Remedios, L. L. Farrell, S. B. McRae, T. C. Morgan, N. Karlionova, P. Pinchuk, Y. I. Verkuil, A. S. Kitaysky, J. C. Wingfield, T. Piersma, K. Zeng, J. Slate, M. Blaxter, D. B. Lank, and T. Burke. 2015. A supergene determines highly divergent male reproductive morphs in the ruff. Nature Genetics 48:79–83. Nature Publishing Group.

Lam, T. H., M. Shen, J.-M. Chia, S. H. Chan, and E. C. Ren. 2013. Population-specific recombination sites within the human MHC region. Heredity (Edinb) 111:131–138.

Lane, N., and W. F. Martin. 2012. The Origin of Membrane Bioenergetics. Cell 151:1406–1416. Elsevier.

Lenormand, T., and J. Dutheil. 2005. Recombination Difference between Sexes: A Role for Haploid Selection. PLOS Biology 3:e63. Public Library of Science.

Lenormand, T., and D. Roze. 2022. Y recombination arrest and degeneration in the absence of sexual dimorphism. Science 375:663–666.

Li, D., M. Roca, R. Yuecel, and A. Lorenz. 2019. Immediate visualization of recombination events and chromosome segregation defects in fission yeast meiosis. Chromosoma 128:385–396.

Li, H. 2013. Aligning sequence reads, clone sequences and assembly contigs with BWA-MEM. arXiv.

Li, H., E. Berent, S. Hadjipanteli, M. Galey, N. Muhammad-Lahbabi, D. E. Miller, and K. N. Crown. 2023. Heterozygous inversion breakpoints suppress meiotic crossovers by altering recombination repair outcomes. PLoS Genetics 19. Public Library of Science.

Lian, Q., L. Maestroni, M. Gaudin, B. Llorente, and R. Mercier. 2023. Meiotic recombination is confirmed to be unusually high in the fission yeast Schizosaccharomyces pombe. iScience 26:107614.

Lichten, M., and A. S. H. Goldman. 1995. MEIOTIC RECOMBINATION HOTSPOTS. 29:423–444.

Lisachov, A., K. Tishakova, S. Romanenko, L. Lisachova, G. Davletshina, D. Prokopov, L. Kratochvíl, P. O`Brien, M. Ferguson-Smith, P. Borodin, and V. Trifonov. 2023. Robertsonian fusion triggers recombination suppression on sex chromosomes in Coleonyx geckos. Sci Rep 13:15502. Nature Publishing Group.

Liu, H., C. J. Maclean, and J. Zhang. 2019. Evolution of the Yeast Recombination Landscape. Molecular Biology and Evolution 36:412–422.

Livernois, A. M., J. a. M. Graves, and P. D. Waters. 2012. The origin and evolution of vertebrate sex chromosomes and dosage compensation. Heredity 108:50–58. Nature Publishing Group.

Lowry, D. B., and J. H. Willis. 2010. A Widespread Chromosomal Inversion Polymorphism Contributes to a Major Life-History Transition, Local Adaptation, and Reproductive Isolation. PLoS Biol 8:e1000500.

Lucchesi, J. C., and D. T. Suzuki. 1968. The Interchromosomal Control of Recombination. Annual Review of Genetics 2:53–86. Annual Reviews.

Ma, C., and R. K. Mortimer. 1983. Empirical equation that can be used to determine genetic map distances from tetrad data. Mol Cell Biol 3:1886–1887.

Manoukis, N. C., J. R. Powell, M. B. Touré, A. Sacko, F. E. Edillo, M. B. Coulibaly, S. F. Traoré, C. E. Taylor, and N. J. Besansky. 2008. A test of the chromosomal theory of ecotypic speciation in Anopheles gambiae. Proceedings of the National Academy of Sciences 105:2940–2945. Proceedings of the National Academy of Sciences.

Marillonnet, S., and R. Grützner. 2020. Synthetic DNA Assembly Using Golden Gate Cloning and the Hierarchical Modular Cloning Pipeline. Current Protocols in Molecular Biology 130:e115.

Michel, A. P., S. Sim, T. H. Q. Powell, M. S. Taylor, P. Nosil, and J. L. Feder. 2010. Widespread genomic divergence during sympatric speciation. Proceedings of the National Academy of Sciences 107:9724–9729. Proceedings of the National Academy of Sciences.

Morgan, T. H. 1911. Random Segregation Versus Coupling in Mendelian Inheritance. Science 34:384–384. American Association for the Advancement of Science.

Morin, S. J., J. Eccles, A. Iturriaga, and R. S. Zimmerman. 2017. Translocations, inversions and other chromosome rearrangements. Fertility and Sterility 107:19–26.

Muller, H. J. 1932. Some Genetic Aspects of Sex. The American Naturalist 66:118–138. The University of Chicago Press.

Muller, H. J. 1964. The relation of recombination to mutational advance. Mutation Research/Fundamental and Molecular Mechanisms of Mutagenesis 1:2–9.

Muñoz-Fuentes, V., M. Marcet-Ortega, G. Alkorta-Aranburu, C. Linde Forsberg, J. M. Morrell, E. Manzano-Piedras, A. Söderberg, K. Daniel, A. Villalba, A. Toth, A. Di Rienzo, I. Roig, and C. Vilà. 2015. Strong Artificial Selection in Domestic Mammals Did Not Result in an Increased Recombination Rate. Molecular Biology and Evolution 32:510–523.

Murata, C., Y. Kuroki, I. Imoto, M. Tsukahara, N. Ikejiri, and A. Kuroiwa. 2015. Initiation of recombination suppression and PAR formation during the early stages of neo-sex chromosome differentiation in the Okinawa spiny rat, Tokudaia muenninki. BMC Evolutionary Biology 15:234.

Nasim, A., P. Young, and B. F. Johnson (eds). 1989. Molecular Biology of the Fission Yeast. Elsevier.

Nieuwenhuis, B. P. S., R. Shraim, and H. Al Ghaithi. 2023. Self-compatibility in yeast is selected for reproductive assurance not population-level compatibility. Evolution 77:1647–1658.

Nieuwenhuis, B. P. S., S. Tusso, P. Bjerling, J. Stångberg, J. B. W. Wolf, and S. Immler. 2018. Repeated evolution of self-compatibility for reproductive assurance. Nat Commun 9:1639.

Noor, M. A. F., K. L. Grams, L. A. Bertucci, and J. Reiland. 2001. Chromosomal inversions and the reproductive isolation of species.

Ohtsuka, H., K. Imada, T. Shimasaki, and H. Aiba. 2022. Sporulation: A response to starvation in the fission yeast *Schizosaccharomyces pombe*. MicrobiologyOpen 11.

Olito, C., and J. K. Abbott. 2023. The evolution of suppressed recombination between sex chromosomes and the lengths of evolutionary strata. Evolution 77:1077–1090.

Olito, C., S. Ponnikas, B. Hansson, and J. K. Abbott. 2024. Consequences of partially recessive deleterious genetic variation for the evolution of inversions suppressing recombination between sex chromosomes1. Evolution qpae060.

Opperman, R., E. Emmanuel, and A. A. Levy. 2004. The Effect of Sequence Divergence on Recombination Between Direct Repeats in Arabidopsis. Genetics 168:2207–2215.

Otto, S. P. 2009. The Evolutionary Enigma of Sex. The American Naturalist 174:S1–S14. The University of Chicago Press.

Otto, S. P., and N. H. Barton. 2001. SELECTION FOR RECOMBINATION IN SMALL POPULATIONS. Evolution 55:1921–1931.

Otto, S. P., and T. Lenormand. 2002. Resolving the paradox of sex and recombination. Nature Reviews Genetics 3:252–261. Nat Rev Genet.

Paigen, K., and P. M. Petkov. 2018. PRDM9 and its role in genetic recombination. Trends Genet 34:291–300.

Parsons, P. A. 1988. Evolutionary rates: effects of stress upon recombination. Biological Journal of the Linnean Society 35:49–68.

Parvanov, E. D., P. M. Petkov, and K. Paigen. 2010. Prdm9 Controls Activation of Mammalian Recombination Hotspots. Science 327:835–835. American Association for the Advancement of Science.

Peck, J. R. 1994. A ruby in the rubbish: beneficial mutations, deleterious mutations and the evolution of sex. Genetics 137:597–606.

Peñalba, J. V., and J. B. W. Wolf. 2020. From molecules to populations: appreciating and estimating recombination rate variation. Nature Reviews Genetics 21:476–492. Springer US.

Perkins, D. D. 1949. BIOCHEMICAL MUTANTS IN THE SMUT FUNGUS USTILAGO MAYDIS. Genetics 34:607–626.

Plough, H. H. 1917. The effect of temperature on crossingover in Drosophila. J. Exp. Zool. 24:147–209.

Ponnikas, S., H. Sigeman, J. K. Abbott, and B. Hansson. 2018. Why Do Sex Chromosomes Stop Recombining? Trends in Genetics 34:492–503. Elsevier Ltd.

Prakash, S., and R. C. Lewontin. 1971. A Molecular Approach to the Study of Genic Heterozygosity in Natural Populations. V. Further Direct Evidence of Coadaptation in Inversions of Drosophila. Genetics 69:405–408.

Pryce, D. W., and R. J. McFarlane. 2009. The Meiotic Recombination Hotspots of Schizosaccharomyces pombe. Pp. 1–13 *in* R. Benavente and J.-N. Volff, eds. Genome Dynamics. KARGER, Basel.

R Core Team. 2023. R: A language and environment for statistical computing. R Foundation for Statistical Computing, Vienna, Austria.

Rhind, N., Z. Chen, M. Yassour, D. A. Thompson, B. J. Haas, N. Habib, I. Wapinski, S. Roy, M. F. Lin, D. I. Heiman, S. K. Young, K. Furuya, Y. Guo, A. Pidoux, H. M. Chen, B. Robbertse, J. M. Goldberg, K. Aoki, E. H. Bayne, A. M. Berlin, C. A. Desjardins, E. Dobbs, L. Dukaj, L. Fan, M. G. FitzGerald, C. French, S. Gujja, K. Hansen, D. Keifenheim, J. Z. Levin, R. A. Mosher, C. A. Müller, J. Pfiffner, M. Priest, C. Russ, A. Smialowska, P. Swoboda, S. M. Sykes, M. Vaughn, S. Vengrova, R. Yoder, Q. Zeng, R. Allshire, D. Baulcombe, B. W. Birren, W. Brown, K. Ekwall, M. Kellis, J. Leatherwood, H. Levin, H. Margalit, R. Martienssen, C. A. Nieduszynski, J. W. Spatafora, N. Friedman, J. Z. Dalgaard, P. Baumann, H. Niki, A. Regev, and C. Nusbaum. 2011. Comparative functional genomics of the fission yeasts. Science 332:930–936.

Rifkin, J. L., F. E. G. Beaudry, Z. Humphries, B. I. Choudhury, S. C. H. Barrett, and S. I. Wright. 2020. Widespread Recombination Suppression Facilitates Plant Sex Chromosome Evolution. Mol Biol Evol 38:1018–1030.

Ritz, K. R., M. A. F. Noor, and N. D. Singh. 2017. Variation in Recombination Rate: Adaptive or Not? Trends in Genetics 33:364–374. Elsevier Ltd.

Rodríguez-López, M., C. Cotobal, O. Fernández-Sánchez, N. Borbarán Bravo, R. Oktriani, H. Abendroth, D. Uka, M. Hoti, J. Wang, M. Zaratiegui, and J. Bähler. 2017. A CRISPR/Cas9-based method and

primer design tool for seamless genome editing in fission yeast. Wellcome Open Research 1:19–19. F1000 Research Ltd.

Rosas-Murrieta, N. H., G. Rojas-Sánchez, S. R.Reyes-Carmona, R. D. Martínez-Contreras, N. Martínez-Montiel, L. Millán-Pérez-Peña, I. P. Herrera-Camacho, N. H. Rosas-Murrieta, G. Rojas-Sánchez, S. R.Reyes-Carmona, R. D. Martínez-Contreras, N. Martínez-Montiel, L. Millán-Pérez-Peña, and I. P. Herrera-Camacho. 2015. Study of Cellular Processes in Higher Eukaryotes Using the Yeast Schizosaccharomyces pombe as a Model. P. *in* Microbiology in Agriculture and Human Health. IntechOpen.

Ross-Ibarra, J. 2004. The Evolution of Recombination under Domestication: A Test of Two Hypotheses. The American Naturalist 163:105–112.

Roze, D. 2014. Selection for sex in finite populations. Journal of Evolutionary Biology 27:1304–1322. Blackwell Publishing Ltd.

Sambrook, J., E. F. Fritsch, and T. Maniatis. 1989. Molecular Cloning: A Laboratory Manual. Cold Spring Harbor, N.Y.: Cold Spring Harbor Laboratory.

Sandor, C., W. Li, W. Coppieters, T. Druet, C. Charlier, and M. Georges. 2012. Genetic Variants in REC8, RNF212, and PRDM9 Influence Male Recombination in Cattle. PLOS Genetics 8:e1002854. Public Library of Science.

Schultz, J., and H. Redfield. 1951. INTERCHROMOSOMAL EFFECTS ON CROSSING OVER IN DROSOPHILA.

Schwarzkopf, E. J., and O. E. Cornejo. 2021. PRDM9 directs recombination hotspots to prevent competition with meiotic transcription. bioRxiv.

Schwarzkopf, E. J., J. C. Motamayor, and O. E. Cornejo. 2020. Genetic differentiation and intrinsic genomic features explain variation in recombination hotspots among cocoa tree populations. BMC Genomics 21:332.

Ségurel, L., E. M. Leffler, and M. Przeworski. 2011. The case of the fickle fingers: How the PRDM9 zinc finger protein specifies meiotic recombination hotspots in humans. PLoS Biology 9.

Seike, T., and H. Niki. 2022. Pheromone Response and Mating Behavior in Fission Yeast. Microbiol Mol Biol Rev 86:e00130-22.

Sigeman, H., P. A. Downing, H. Zhang, and B. Hansson. 2024. The rate of W chromosome degeneration across multiple avian neo-sex chromosomes. Sci Rep 14:16548. Nature Publishing Group.

Singh, G., and A. J. S. Klar. 2002. The 2.1-kb inverted repeat DNA sequences flank the mat2,3 silent region in two species of Schizosaccharomyces and are involved in epigenetic silencing in Schizosaccharomyces pombe. Genetics 162:591–602.

Smith, G. R. 2009. Genetic Analysis of Meiotic Recombination in Schizosaccharomyces pombe. Methods Mol Biol 557:65–76.

Smith, J. M., and J. Maynard-Smith. 1978. The evolution of sex. Cambridge University Press Cambridge.

Smukowski, C. S., and M. A. F. Noor. 2011. Recombination rate variation in closely related species. Heredity 107:496–508.

Spassky, B., N. Spassky, H. Levene, and T. Dobzhansky. 1958. RELEASE OF GENETIC VARIABILITY THROUGH RECOMBINATION. I. DROSOPHILA PSEUDOOBSCURA. Genetics 43:844–867.

Speijer, D., J. Lukeš, and M. Eliáš. 2015. Sex is a ubiquitous, ancient, and inherent attribute of eukaryotic life. Proceedings of the National Academy of Sciences 112:8827–8834. Proceedings of the National Academy of Sciences.

Spiess, E. B. 1958. Effects of Recombination on Viability in Drosophila. Cold Spring Harb Symp Quant Biol 23:239–250. Cold Spring Harbor Laboratory Press.

Spiess, E. B. 1959. RELEASE OF GENETIC VARIABILITY THROUGH RECOMBINATION. II. DROSOPHILA PERSIMILIS. Genetics 44:43–58.

Stapley, J., P. G. D. Feulner, S. E. Johnston, A. W. Santure, and C. M. Smadja. 2017a. Recombination: The good, the bad and the variable. Philosophical Transactions of the Royal Society B: Biological Sciences 372:1–5.

Stapley, J., P. G. D. Feulner, S. E. Johnston, A. W. Santure, and C. M. Smadja. 2017b. Variation in recombination frequency and distribution across eukaryotes: patterns and processes. Phil. Trans. R. Soc. B 372:20160455.

Stebbins, G. L. 1957. Self Fertilization and Population Variability in the Higher Plants. The American Naturalist 91:337–354.

Stetsenko, R., and D. Roze. 2022. The evolution of recombination in self-fertilizing organisms. Genetics, doi: 10.1093/genetics/iyac114.

Stevison, L. S., K. B. Hoehn, and M. A. F. Noor. 2011. Effects of Inversions on Within- and Between-Species Recombination and Divergence. Genome Biology and Evolution 3:830–841.

Stolle, E., R. Pracana, P. Howard, C. I. Paris, S. J. Brown, C. Castillo-Carrillo, S. J. Rossiter, and Y. Wurm. 2019. Degenerative Expansion of a Young Supergene. Molecular Biology and Evolution 36:553–561.

Stone, W. S. 1955. Genetic and Chromosomal Variability in Drosophila. Cold Spring Harb Symp Quant Biol 20:256–270. Cold Spring Harbor Laboratory Press.

Sturtevant, A. H., and G. W. Beadle. 1936. The Relations of Inversions in the X Chromosome of Drosophila Melanogaster to Crossing Over and Disjunction. Genetics 21:554–604.

Styrkársdóttir, U., R. Egel, and O. Nielsen. 1993. The smt-O mutation which abolishes mating-type switching in fission yeast is a deletion. Curr Genet 23:184–186.

Thon, G., A. Cohen, and A. J. Klar. 1994. Three additional linkage groups that repress transcription and meiotic recombination in the mating-type region of Schizosaccharomyces pombe. Genetics 138:29–38.

Tock, A. J., and I. R. Henderson. 2018. Hotspots for Initiation of Meiotic Recombination. Frontiers in Genetics 9. Frontiers Media S.A.

Torres-garcia, S., L. D. Pompeo, L. Eivers, B. Gaborieau, S. A. White, A. L. Pidoux, P. Kanigowska, I. Yaseen, Y. Cai, R. C. Allshire, A. Carr, and T. V. Emden. 2021. SpEDIT : A fast and efficient CRISPR / Cas9 method for fission yeast [version 1 ; peer review : 3 approved]. 1–24.

Tsubouchi, H., B. Argunhan, and H. Iwasaki. 2021. Biochemical properties of fission yeast homologous recombination enzymes. Curr Opin Genet Dev 71:19–26.

Tusso, S., B. P. S. Nieuwenhuis, F. J. Sedlazeck, J. W. Davey, D. C. Jeffares, J. B. W. Wolf, and R. Nielsen. 2019. Ancestral Admixture Is the Main Determinant of Global Biodiversity in Fission Yeast. Molecular Biology and Evolution 36:1975–1989. Oxford University Press.

Vyas, A., A. V. Freitas, Z. A. Ralston, and Z. Tang. 2021. Fission Yeast *Schizosaccharomyces pombe* : A Unicellular "Micromammal" Model Organism. Current Protocols 1:e151.

Wahls, W. P. 1998. Meiotic Recombination Hotspots: Shaping the Genome and Insights into Hypervariable Minisatellite DNA Change. Curr Top Dev Biol 37:37–75.

Weismann, A. 1891. Essays upon heredity and kindred biological problems. Clarendon press.

Weng, Z., A. Wolc, H. Su, R. L. Fernando, J. C. M. Dekkers, J. Arango, P. Settar, J. E. Fulton, N. P. O'Sullivan, and D. J. Garrick. 2019. Identification of recombination hotspots and quantitative trait loci for recombination rate in layer chickens. J Animal Sci Biotechnol 10:20.

Wolf, S., D. Melo, K. M. Garske, L. F. Pallares, A. J. Lea, and J. F. Ayroles. 2023. Characterizing the landscape of gene expression variance in humans. PLoS Genet 19:e1010833.

Wood, V., R. Gwilliam, M.-A. Rajandream, M. Lyne, R. Lyne, A. Stewart, J. Sgouros, N. Peat, J. Hayles, S. Baker, D. Basham, S. Bowman, K. Brooks, D. Brown, S. Brown, T. Chillingworth, C. Churcher, M. Collins, R. Connor, A. Cronin, P. Davis, T. Feltwell, A. Fraser, S. Gentles, A. Goble, N. Hamlin, D. Harris, J. Hidalgo, G. Hodgson, S. Holroyd, T. Hornsby, S. Howarth, E. J. Huckle, S. Hunt, K. Jagels, K. James, L. Jones, M. Jones, S. Leather, S. McDonald, J. McLean, P. Mooney, S. Moule, K. Mungall, L. Murphy, D. Niblett, C. Odell, K. Oliver, S. O'Neil, D. Pearson, M. A. Quail, E. Rabbinowitsch, K. Rutherford, S. Rutter, D. Saunders, K. Seeger, S. Sharp, J. Skelton, M. Simmonds, R. Squares, S. Squares, K. Stevens, K. Taylor, R. G. Taylor, A. Tivey, S. Walsh, T. Warren, S. Whitehead, J. Woodward, G. Volckaert, R. Aert, J. Robben, B. Grymonprez, I. Weltjens, E. Vanstreels, M. Rieger, M. Schäfer, S. Müller-Auer, C. Gabel, M. Fuchs, C. Fritzc, E. Holzer, D. Moestl, H. Hilbert, K. Borzym, I. Langer, A. Beck, H. Lehrach, R. Reinhardt, T. M.

Pohl, P. Eger, W. Zimmermann, H. Wedler, R. Wambutt, B. Purnelle, A. Goffeau, E. Cadieu, S. Dréano, S. Gloux, V. Lelaure, S. Mottier, F. Galibert, S. J. Aves, Z. Xiang, C. Hunt, K. Moore, S. M. Hurst, M. Lucas, M. Rochet, C. Gaillardin, V. A. Tallada, A. Garzon, G. Thode, R. R. Daga, L. Cruzado, J. Jimenez, M. Sánchez, F. del Rey, J. Benito, A. Domínguez, J. L. Revuelta, S. Moreno, J. Armstrong, S. L. Forsburg, L. Cerrutti, T. Lowe, W. R. McCombie, I. Paulsen, J. Potashkin, G. V. Shpakovski, D. Ussery, B. G. Barrell, and P. Nurse. 2002. The genome sequence of *Schizosaccharomyces pombe*. Nature 415:871–880.

Wright, A. E., R. Dean, F. Zimmer, and J. E. Mank. 2016. How to make a sex chromosome. Nature Communications 7. Nature Publishing Group.

Yadav, V., S. Sun, and J. Heitman. 2023. On the evolution of variation in sexual reproduction through the prism of eukaryotic microbes. Proceedings of the National Academy of Sciences of the United States of America 120:e2219120120.

Zanders, S. E., M. T. Eickbush, J. S. Yu, J.-W. Kang, K. R. Fowler, G. R. Smith, and H. S. Malik. 2014. Genome rearrangements and pervasive meiotic drive cause hybrid infertility in fission yeast. eLife 3:e02630. eLife Sciences Publications, Ltd.

Zanders, S. E., and R. L. Unckless. 2019. Fertility Costs of Meiotic Drivers. Current Biology 29:R512–R520. Cell Press.

Zhong, W., and N. K. Priest. 2011. Stress-induced recombination and the mechanism of evolvability. Behav Ecol Sociobiol 65:493–502.

Zickler, D., and N. Kleckner. 2015. Recombination, Pairing, and Synapsis of Homologs during Meiosis. Cold Spring Harb Perspect Biol 7:a016626.

9 ACKNOWLEDGEMENTS

This is going to be long. For some people this will be the most interesting part of the thesis, or even the only part they can understand if they don't speak English. If you reached this point, it means that you successfully read the whole thesis (and for that you already deserve a drink) or you skipped everything to get here (then you owe me a drink). Regardless of how you got here, I want you to know that I cried during half the time I was writing this. While most of the work has been done by me, and for that I thank **myself** first of all, this piece of art could have never been achieved without the help of many people, both in and out of the department. Therefore, it would make no sense to finish without writing a way-too-long letter thanking everyone who showed support during this period, in no special order but what comes to mind.

First of all, I am deeply thankful to **Bart**. Thank you for choosing me to be your first doctoral student and for your wonderful supervision. It has been both amazing and horrible to learn everything I now know about fission yeast, fungi, evolution, and whatnot. But especially thank you for all the support you have given me as a mentor and a friend. Thanks for all the 1-on-1 meetings that we have had where you had patience and hope for my experiments when I already had none left. Thank you for always making me feel like my ideas mattered, and like I had a space in research. You always had a calming impression on me, with your (scary to some) directness, and your extremely logical sentences such as "don't get stressed it is useless".

Thank you to all my members of the TAC, **Bart**, **Jochen**, **Alexander** and **Christof**. I know my experiments and explanations were complicated to understand, but I know your help was invaluable to get different points of view, and I hope – if you get to read the thesis – that your points of view have ultimately been implemented. Thank you also to all the people who agreed to be part of my committee, apart from Jochen and Cristof. **Julia, Korbinian and Silke**. I hope you enjoyed this thesis at least a little bit.

One of the first people I met here was **Lucie**, when I saw her in our shared office. For sure in the beginning I did not realize how lucky I was to share an office with you. Thank you for being my first friend in Germany, thank you for always being there for me, from the first mental breakdown where we barely knew each other. Meeting you gave me hope in a time and place (Covid pandemic, Munich) where I never thought I would feel at home.

Thank you **Pranshu**, for living with me and making every day a little bit better, and a little bit funnier. We practically became family in our crazy flat, and you have been a constant in my life since we both moved there. You have helped me always remember that I have to be proud of who I am, and to have the soon-to-

be doctor title. And also thanks for all the food you have cooked for me, and all the Indian culture you have taught me.

Thank you to all the people in the university. Concretely to the girls that somehow started all together in the department and, still now, can't believe how lucky I was to meet. **Linda**, **Jessica**, come back please. **Dörte**, aún no me puedo creer que tardé meses en darme cuenta de que hablabas muy bien español porqué eras de Ecuador, ojalá habernos hecho amigas antes y que volviera el tiempo perdido. **Júlia**, obrigada por ter sempre a alma mais jovem do grupo. To both of you, thank you for always being there, for the coffee breaks, for all the advice, for getting drunk together, for making the department better. **Sarah**, as I have told you a million times, I don't know how I find my best friend in the whole world in this city. You make it feel like a home (like a literal home, as I spend as much time as I can in your house). I wish I could say more, but I have no words to express how much it means to have you as a friend. **Rodaria,** thank you for being quite literally crazy, the fresh air that you always bring to the room, for being my other best friend in the whole world. I cannot understand how you are so Greek and yet so German, and what a good combination it makes.

Chantal, Murphy and **Dmytro**, my dearest yeasty boys, my first true group of friends here in Munich, I simply don't know what I would do if you had never decided to be students in our lab.

Gonzalo, muchas gracias a ti también, por aceptar que llegue a tu casa la mitad de las veces sin avisar, gracias por tu amistad, por explicarme cosas de pedales de guitarra, y por ser un rinconcito de Aragón que no creía encontrar fuera de mi casa. **Edu** por las risas, las tonterías y las fiestas, y por demostrarme que si se quiere, se puede. **Luca,** un pezzo del mio cuore, per farmi sentire sempre stupenda e per insegnarmi l'italiano senza rendermene conto.

Ara en català, la meva llengua estimada. **Enric,** sembla que no però ens coneixem des de fa més de deu anys, gràcies per tots els viatges espontanis que hem organitzat, que m'han demostrat que només cal tenir les ganes. Per totes les trucades de telèfon per posar-nos al dia i per respondre totes les preguntes de la tesi que et preguntava, fins i tot les que no tenien sentit. Junt amb la **Fàtima**, gràcies pel trio rauwrauw que ens vam muntar durant el màster, i que espero reviure ben aviat.

I finalment, moltíssimes gràcies per tot el suport rebut de **la familia – els meus pares i els meus germans**. Sé que no sabeu ben bé què he fet i per què he tardat tant, però que ha valgut la pena. Sé que hi sereu sempre, passi el que passi, i sé que esteu orgullosos de mi. Vosaltres m'heu ensenyat a tenir paciencia i a ser treballadora, i m'heu fet la persona que sóc. Espero veure-us a tots a la defensa de la tesi, el Tato ja sé segur que hi serà. Us estimo moltíssim.